

**SURFACE ENHANCED RAMAN SPECTROSCOPY OF VEGETATIVE
CELLS AND ENDOSPORES OF *Bacillus thuringiensis* AS A MODEL
FOR DETECTION OF BIOTHREATS**

By

Hilsamar Félix-Rivera

A dissertation submitted in partial fulfillment of the requirements for the degree of

DOCTOR OF PHILOSOPHY

**in
Applied Chemistry**

UNIVERSITY OF PUERTO RICO
MAYAGÜEZ CAMPUS
MAY 2012

Approved by:

Samuel P. Hernández-Rivera, PhD
President, Graduate Committee

Date

Carlos Ríos-Velázquez, PhD
Member Graduate Committee

Date

Nilka M. Rivera-Portalatín, PhD
Member Graduate Committee

Date

Julio G. Briano-Peralta, PhD
Member Graduate Committee

Date

Jaime Ramírez-Vick, PhD
Representative of Graduate Studies

Date

René S. Vieta, PhD
Chairperson of the Department

Date

ABSTRACT

The development of rapid and efficient techniques for biological detection, identification and classification has a positive impact in fields ranging from medical, environmental and industrial microbiology to biological warfare agents countermeasures and national security. Traditional and standoff Raman spectroscopy can be used at near or long distances from the sample to obtain information of the chemical fingerprint of microorganisms. In this research, biochemical components of the bacterial cell wall and endospores of *Bacillus thuringiensis* (*Bt*) in aqueous suspensions and as well as aerosol particles were identified by surface enhanced Raman spectroscopy (SERS) using small silver (Ag) nanospheres (NS) excited by a 532 nm laser source. These nanoparticles were chemically reduced by hydroxylamine and borohydride and capped with citrate. Volume ratio of bacteria to NS, activation of “hot spots”, aggregation, and surface charge modification of the NS were studied and optimized to obtain good *Bt* signal enhancements by a simple SERS protocol of detection. A volume ratio of 0.125 using a bacterial concentration at the specific OD₆₀₀ of 1 ± 0.1 and NaCl 0.1 M as blank was used to analyze the vegetative cells and endospores samples. Slight aggregation of the NS using NaCl 0.1M as well as surface charge modification to a more acidic ambient (pH range 5 to 7) was induced using small size (19±3 nm) borohydride reduced NS in the form of metallic suspensions aimed at increasing the Ag NS-*Bt* interactions. Principal component analyses (PCA) and partial least squares (PLS) regressions of SERS spectra coupled to discriminant analysis were used to classify and discriminate between vegetative cells and endospores components of bacterial samples growth at 5 and 24 h at a 95% confidence level and at different stages of bacterial growth. Bioaerosol detection was the largest challenge in this research. Results show that the optimization was successfully used observing and assigning the characteristic peaks of aerosolized *Bt*. In this study, the bacterial detection range used was 10^4 cells. In terms of concentration, it is important because it is considered as pathogenic.

RESUMEN

El desarrollo de técnicas rápidas y eficientes para la detección, identificación y caracterización de muestras biológicas tiene un impacto positivo desde varios campos de la medicina, medio ambiente y la microbiología industrial hasta campos como contramedidas de agentes de guerra biológica y la seguridad nacional. Espectroscopía Raman tradicional y a distancia puede ser utilizado a cortas o largas distancias de la muestra para obtener información de la huella química de los microorganismos. En esta investigación, los componentes bioquímicos de la pared celular y endosporas de *Bacillus thuringiensis* (*Bt*) en suspensiones acuosas y en forma de aerosoles fueron identificados por Espectroscopía Raman con aumento de señal por superficie (SERS) utilizando nanoesferas (NS) de plata (Ag) utilizando 532 nm de longitud de onda del láser de excitación. Estas nanopartículas fueron reducidas por hidroxilamina y por borohidruro estabilizadas con citrato. La relación de volumen de las bacterias a NS, la activación de "puntos calientes", la agregación, y la modificación de la carga superficial de las NS fueron los parámetros estudiados y optimizados para obtener buenos aumentos en las señales de *Bt* mediante un protocolo simple de detección de SERS. Una relación volumen de 0.125 con una concentración de bacterias a una medida de OD₆₀₀ de 1 ± 0.1 con NaCl 0.1 M como blanco fue utilizado para las muestras de células vegetativas y endosporas. Agregación ligera de las NS utilizando NaCl 0.1 M, así como la modificación de la carga superficial a un ambiente más ácido (intervalo de pH 5 a 7) inducido a las pequeñas NS (19 ± 3 nm) reducidas con borohidruro en forma de suspensiones metálicas fue utilizado con el propósito de aumentar las interacciones Ag-NS-*Bt*. Un análisis de componentes principales (PCA) y de regresión de cuadrados mínimos parciales (PLS) de los espectros SERS, junto con análisis discriminante fueron utilizados para clasificar y discriminar entre componentes de las células vegetativas y endosporas en las muestras de 5 y 24 horas de crecimiento bacterial a un nivel de confianza de 95%, incluso pudo diferenciarse a diferentes etapas de crecimiento de *Bt*. La detección de los bioaerosoles fue el mayor reto en esta investigación. Los resultados mostraron que la optimización se utilizó con éxito para observar y asignar los picos característicos de aerosol de *Bt*. En este estudio, el rango de detección bacterial usado fue de 10^4 células, esta concentración es importante porque es considerado como patógeno.

Copyright ©2012

By
Hilsamar Félix-Rivera

Dedication

To:

God

Héctor, Hilda & Tito

Luis Angel

ACKNOWLEDGMENTS

Thank you God for always been my protector and my guide in the right direction, helping me finish this stage of my life. I would like to express my gratitude to my advisor Dr. Samuel P. Hernández for accepting me in his high standard research group and trusting me many task and responsibilities. To my graduate committee members, who help me with direction, suggestions and corrections in this research work, please receive all my thanks: Dr. Carlos Ríos-Velázquez, Dr. Nilka M. Rivera and Dr. Julio Briano. Thanks to the Chemistry Department at UPR-Mayagüez: Professors and administrative personal. Thanks to Lockheed Martin, Co., MFC Orlando, FL, to Mr. Frey and Dr. Comstock for the opportunity to complete the internship requirement and let me experience real life industry research work. Also to ALERT for giving me the opportunity to be part of the research students of Dr. Peter Chen's Lab at Spelman College Atlanta, GA.

Sincerely, I would like to thank two angels who help me in 500%: Oliva and Michael!!!. Without the push to continue in the program I don't know where or who would I be today. Thanks for all suggestions to the surrogate sister and brother with all my heart. To my friends and colleagues: Joann, Leo, Jenny, William, Manuel, Pedro, Celia, Marce, Natalia, Jose, Eduardo, John, Jorge R., Nelson, Cacimar, Yarely, Raymond, Héctor A., ... thanks for being as a family to me. Special thanks to the undergraduate students who help in the research experiments and motivate the focus of this research: Roxannie, Gabriela, Rosa and Yami. Thanks to the family of the Microbial Biotechnology and Bioprospecting Lab., Department of Biology UPRM, and especially to Kristina Soto-Feliciano for initial collaboration and dedication with sample preparation. Thanks to Dr. Rong Zhang from Jackson State University for facilitating the TEM images, Nelson Granda and Dr. Wilfredo Otaño from UPR-Cayey for facilitating the SEM images, and to Celia Osorio from The NANOMaterials Processing Laboratory, Department of Engineering Science & Materials for facilitating some measurements.

Finally and not less important, thanks to my family Félix-Rivera: Mami Hilda, Papi Héctor and my brother Tito for all the unconditional support and emotional motivation. To my love Luis Angel, baby thanks for all your patience, support, motivation and love.

Support from ALERT/DoD from the U.S. Department of Homeland Security under Award Number 2008-ST-061-ED0001 is also acknowledged.

TABLE OF CONTENTS

TABLE LIST	IX
FIGURE LIST	X
SYMBOLS LIST.....	XV
1. INTRODUCTION	1
1.1 MOTIVATION	1
1.2 LITERATURE REVIEW	3
1.2.1 RAMAN SPECTROSCOPY AND SURFACE ENHANCED RAMAN SPECTROSCOPY.....	3
1.2.2 <i>BACILLUS THURINGIENSIS</i>	8
1.2.3 BACTERIA DETECTION TECHNIQUES.....	11
1.2.3.1 CURRENT BIOLOGICAL TECHNIQUES.....	11
1.2.3.2 NORMAL RAMAN AND SURFACE ENHANCED RAMAN SPECTROSCOPIES.....	11
1.2.3.2.1 NORMAL RAMAN SPECTROSCOPY (RS).....	11
1.2.3.2.2 SURFACE ENHANCED RAMAN SPECTROSCOPY.....	13
1.2.4 OPTIMAL CONTROLS IN SERS ANALYSIS.....	15
1.2.5 DATA ANALYSIS.....	19
1.2.6 SUMMARY AND JUSTIFICATION.....	20
2. <i>BACILLUS THURINGIENSIS</i>: GROWTH, PREPARATION AND CHARACTERIZATION OF VEGETATIVE CELLS AND ENDOSPORES	22
2.1 MATERIALS	22
2.2 INSTRUMENTATION.....	22
2.3 BACTERIAL CULTURE PREPARATION	23
2.3.1 PREPARATION OF BACTERIAL SAMPLE.....	23
2.3.2 BACTERIAL GROWTH CURVE	23
2.3.3 BACTERIAL SAMPLE CENTRIFUGATION.....	25
2.4 BACTERIAL SAMPLE CHARACTERIZATION.....	25
2.4.1 GRAM AND ENDOSPORE STAINING	25
2.4.2 COLONY FORMING UNIT (CFU).....	27
2.5 SUMMARY	27
3. NORMAL OR SPONTANEOUS RAMAN (NR) SPECTROSCOPY EXPERIMENTS.....	29
3.1 INSTRUMENTATION.....	29
3.2 SAMPLE PREPARATION.....	29
3.3 RESULTS AND DISCUSSION.....	30
3.4 SUMMARY	32
4. SERS EXPERIMENTS: SYNTHESIS, CHARACTERIZATION, AGGLOMERATION AND MODIFICATIONS TO THE SURFACE CHARGE OF THE NANOPARTICLES (NP).....	33
4.1 MATERIALS	33
4.2 INSTRUMENTATION.....	34
4.3 SYNTHESIS OF NANOPARTICLES.....	34
4.3.1 HYDROXYLAMINE REDUCED AG COLLOIDS	34
4.3.2 BOROHYDRIDE REDUCED AG-NP	35

4.3.3	INDUCING NP AGGREGATION	36
4.3.4	SURFACE CHARGE MODIFICATIONS	37
4.4	RESULTS AND DISCUSSION	37
4.4.1	CHARACTERIZATION BY UV-VIS AND TEM	37
4.4.1.1	HYDROXYLAMINE NANOPARTICLES	37
4.4.1.2	CITRATE-CAPPED BOROHYDRIDE REDUCED NANOPARTICLES	37
4.4.2	UV-VIS ABSORPTION AT SEVERAL pH VALUES AND RAMAN SPECTROSCOPY EXPERIMENTS OF NP ...	39
4.4.2.1	HYDROXYLAMINE REDUCED NP	39
4.4.2.1.1	SURFACE CHARGE MODIFICATION AND INDUCING AGGLOMERATION TO NP	39
4.4.2.2	BOROHYDRIDE REDUCED NP	43
4.4.2.2.1	INDUCING NANOPARTICLES AGGREGATION	43
4.4.2.2.2	SURFACE CHARGE MODIFICATIONS TO THE NP	45
4.5	SUMMARY AND CONCLUSIONS	47
5.	OPTIMIZATION PROCEDURES FOR DETECTION OF VEGETATIVE CELLS AND	
	ENDOSPORES OF <i>BT</i> BY SERS	48
5.1	SAMPLE PREPARATION	48
5.2	RESULTS AND DISCUSSION	49
5.2.1	SURFACE ENHANCED RAMAN SPECTROSCOPY (SERS) OF <i>BT</i>	49
5.2.2	PARAMETERS TO BE OPTIMIZED IN THE SERS EXPERIMENTS	50
5.2.2.1	VOLUME RATIO EXPERIMENTS	51
5.2.2.2	INDUCING AGGLOMERATION OF NP	55
5.2.2.3	SURFACE CHARGE MODIFICATION OF THE NANOPARTICLES	60
5.2.3	BACTERIAL CELLS ANALYZED BY SERS	67
5.2.4	AMINO ACIDS SERS EXPERIMENTS	68
5.2.5	CONCLUSION	74
6.	APPLICATIONS IN DETECTION OF <i>BT</i> SAMPLES: MONITORING, DISCRIMINATION AND	
	BIOAEROSOL DETECTION.....	76
6.1	METHODOLOGY FOR DATA ANALYSIS	76
6.2	MONITORING AND DISCRIMINATION OF BACTERIAL SAMPLES	78
6.2.1.1	SPECTRAL DIFFERENCES BETWEEN VEGETATIVE CELLS AND ENDOSPORES	78
6.2.1.2	SERS ASSISTED MONITORING OF THE <i>BT</i> GROWTH STAGES	82
6.3	BIOAEROSOL DETECTION OF <i>BT</i> ENDOSPORES.....	89
6.3.1	MATERIALS AND INSTRUMENTATION FOR BIOAEROSOL GENERATION	89
6.3.1.1	SERS FOR DETECTION OF ENDOSPORES OF <i>BT</i> AS BIOAEROSOL PARTICLES	90
6.3.1.1.1	USING COLLOIDAL SUSPENSION SOLUTION	91
6.3.1.1.2	USING A SOLID SUBSTRATE	94
6.3.1.1.2.1	PREPARATION OF THE Ag/PDMS POLYMER SOLID SUBSTRATE	95
6.3.1.1.2.2	SERS RESULTS OF <i>BT</i> ENDOSPORES DETECTION USING A Ag/PDMS SOLID SUBSTRATE	96
6.4	CONCLUSION.....	98
7.	RESEARCH CONTRIBUTIONS.....	100
	REFERENCES	101

Table List

Tables	Page
Table 1. Assignment of bands frequently found in Raman spectra of biological specimens [29].	14
Table 2. Sequential dilutions of <i>Bt</i> to obtain the colony forming unit.....	27
Table 3. Hydrodynamic radii (nm) values for NP aggregated at different concentrations of NaCl.....	44
Table 4. Hydrodynamic radii (nm) values of surface charge modified Ag NP by adjusting the pH.....	46
Table 5. An approximately bacterial cells number analyzed in this study.....	68
Table 6. Chemical structures of the aminoacids analyzed by SERS, is included the final concentration of detection and the pKa and pI values used in the experiments.....	70
Table 7. SERS vibrational assignments of selected components analyzed present in vegetative cells samples and endospores samples of <i>Bt</i> . [30,63-65,49].....	73
Table 8. Summary of the optimization parameters obtained from the simple protocol established for SERS detection of vegetative cells and endospores of <i>Bt</i>	75
Table 9. Tentative assignment for vibrational bands of vegetative cells and endospores samples of suspension solution of <i>Bt</i> [29,40,66]	79
Table 10. Band assignment of the areas with the variation captured by PC1 for vegetative cells and endospores <i>Bt</i> samples.....	80
Table 11. Spectral regions analyzed in SERS spectra of the samples at different growth stages.....	83
Table 12. Sum squared captured information from PLS analysis.....	87
Table 13. Tentatively Raman band assignments of the SERS spectra obtained from the mixture of aerosolized bacterial sample solution of endospores (24 h of bacterial growth) at different bacteria concentration.....	94
Table 14. Tentative Raman band assignments of the SERS spectra obtained from aerosolized bacterial sample solution of <i>Bt</i> endospores (24 h of bacterial growth) to the Ag/PDMS solid substrate.....	97

Figure List

Figures	Page
Figure 1. A study from The Center for Disease Control Analysis demonstrated that bioaerosols have a significant influence of health problems. (http://www.cdc.gov/nceh/ehs/)	2
Figure 2. (a) Representation of collision phenomena in which photons with frequency ν_0 interact with the electron cloud of a molecule of the sample. The photon-molecule collision events result in scattering of the incident radiation with photons with the same frequency (Rayleigh radiation) and photons with shifted frequencies ($+\nu$ and $-\nu$) producing the Raman radiation. (b) Energy level diagram showing the states involves in photon scattering. Excitation energies: light green lines; Rayleigh scattering (no energy/frequency change): dark green lines; inelastic (energy loss) Stokes scattering: red line; superelastic scattering (energy/frequency gain): blue line.	4
Figure 3. General schematic diagram of normal or spontaneous Raman spectroscopy (RS) conventional detection geometry (90° scattering). This arrangement is typically used as one of the simplest experimental setups to implement.	5
Figure 4. Signal enhancement effect of metallic nanoparticles in SERS is produced by closely spaced interacting particles generated at the location of adsorbed molecules on (a) the metal surface and (b) in colloidal suspension. So-called “hot spots” seem to provide extra electromagnetic field signal amplification.	7
Figure 5. <i>Bt</i> cell wall composition: (a) Gram positive cell wall and (b) chemical structure of the repeating unit in peptidoglycan. [13]	9
Figure 6. <i>Bt</i> endospores wall contain the several layers from internal to external location. (http://www.tutorvista.com/content/biology/biology-iii/kingdoms-living-world/reproduction-bacteria.php)	10
Figure 7. Effect of colloid volume on SERS signal-to-noise ratio (S/N). It is important to optimize for maximum S/N as a function of colloid volume for increasing the scattered radiation collected and decreasing contributions from interferences.	16
Figure 8. (a) Experimental growth curve of <i>Bt</i> . (b) Sporulation in <i>Bacillus thuringiensis</i> (FAO AGRICULTURAL SERVICES BULLETIN No. 96).	24
Figure 9. White light micrographs of <i>Bt</i> characterization at 5 (a, c) and 24 (b, d) h of bacterial growth: (a, b) Gram staining (purple: Gram +); (c, d) endospores staining with high magnification image of stained endospores.	26
Figure 10. Characterization of <i>Bt</i> by SEM images at 5 and 24 h of bacterial growth. (a) vegetative cells; (b) endospores forming bacteria.	26
Figure 11. Normal Raman experimental set up for biological sample detection.	30
Figure 12. Raman spectra of (a) concentrated and (b) diluted sample of <i>Bt</i> suspended in 0.1 M NaCl at 5 h and 24 h of bacterial growth. As can be observed, a highly fluorescence due to the bacterial components presents in the sample limits the chemical information.	31
Figure 13. Experimental setup and procedure summary for the preparation of Ag-NP reduced by hydroxylamine to obtain a final concentration of 10^{-3} M of Ag.	35
Figure 14. Experimental setup and procedure summary for the preparation of Ag-NP	36

reduced by borohydride capped with sodium citrate to obtain a final concentration of 10^{-4} M of Ag.	
Figure 15. UV-Vis spectra (top), final yellowish color of freshly prepared sols (center) and TEM images (bottom) of: (a) borohydride reduced-citrate capped Ag NPs and (b) hydroxylamine reduced Ag-NPs used in the experiments described.	39
Figure 16. UV-Vis spectra of hydroxylamine NP at different pH's values. As can clearly seen the UV max absorbance of hydroxylamine NP at different pH is insignificant from the range 3 to 11.	40
Figure 17. Raman spectra of the NP reduced by hydroxylamine at different pH values. The surface charge modification induced by change the pH of the sols contains anomalous bands that can interfere in the identification of bacterial composition.	42
Figure 18. UV-Vis spectrum showing the decrease of the plasmon band when hydroxylamine reduced Ag-NP were aggregated with NaCl 1.0 M.	42
Figure 19. Raman spectra of hydroxylamine reduced NP and the NP aggregated with NaCl. The vibrational bands observed can mask the vibrational bands of the biosample.	43
Figure 20. (a) UV-Vis spectrum showing the decrease of the plasmon band when borohydride reduced Ag-NP were aggregated with NaCl 1.0 M; (b) grayish color of NP suspensions evidencing oxidation of the borohydride reduced Ag NP.	44
Figure 21. No anomalous bands can be observed in the Raman spectrum of agglomerated NP effect obtained with NaCl at concentrations of 0.1 and 1.0 M.	45
Figure 22. UV-Vis spectra of borohydride NP at different pH values. As can be clearly observed, the UV-Vis max absorbance of borohydride NP at different pH is significant in the 5 to 7 range.	45
Figure 23. No anomalous bands were observed in the Raman spectra by the effect of modifications to the surface charge of NP in 3 to 9 pH range.	46
Figure 24. Experimental set up for bacterial identification by SERS using a laser excitation line of 532 nm with a 10x objective of radius spot of 25 μm and a glass capillary tube of 0.9 mm of inner diameter.	49
Figure 25. Principal cases can be involved in the volume ratio of colloidal NP suspension to bacterial sample in SERS. To obtain a maximum signal-to-noise ratio is important to optimize the colloid volume and the bacterial sample concentration. From these cases can be observed (a, b) high concentration of NP and bacteria, respectively and (c) good proportion of NP and bacteria.	53
Figure 26. (a) SERS spectra range of Bt sample at 24 h of bacterial growth at different bacterial concentrations suspended in NaCl 0.1 M. (b) The results obtained were used for the optimization until achieve a maximum intensity in the 730 cm^{-1} peak indicating an increasing in the scattered radiation collected and decreasing contributions from interferences at 10^4 bacterial cells. Higher (10^5 bacterial cells) or lower concentrations (10^3 bacterial cells) resulted in a decrease of the SERS signal intensity.	54
Figure 27. Effect observed when the agglomeration of nanoparticles is induced by the addition of a salt increasing in ionic strength.	55
Figure 28. Changes in colors observed due to aggregation induced by adding different concentrations of NaCl to the mixtures of colloidal suspension and bacterial solution for 5 and 24 h of bacterial growth (above for 5 h and below for 24 h of bacterial growth).	57
Figure 29. SERS results for the aggregation effect using different concentration of NaCl in mixtures of colloidal suspension and bacterial solution for (a) 5 (right axis) and (b) 24 h of	

bacterial growth (left axis); (c) aggregation promoted to nanoparticles using low concentration of this aggregation agent resulted in good SERS signals as shows the 730 cm^{-1} peak intensity graph for the spectra of 5 and 24 h of bacterial growth.	59
Figure 30. TEM images of the mixtures colloidal suspension and bacterial solution using different concentrations of the aggregating agent for (a) 5 and (b) 24 h. As can be clearly observed, lower concentrations of the aggregating agent resulted in an increasing of the affinity nanoparticles to bacterial cell wall. Higher concentrations resulted in a high agglomeration of the NP and a decrease in the close contact of the small NP to the analyte..	60
Figure 31. Effect observed on the formation of a double-charge layer to the slight negatively charged induced by the citrate capping agent, it becomes slightly more positive with the H^+ ions added.	61
Figure 32: Zeta potential measurements of silver nanoparticles as a function of pH [59].	63
Figure 33. (a) Changes in colors observed due to surface charge modification induced by adjusting the pH of the sols. The colloidal suspension mixtures at different pH values (3, 5, 7 and 9) with the bacterial solution for (b) 5 and (c) 24 h of bacterial growth.	64
Figure 34. SERS results for the surface charge modification to the NP in mixtures of colloidal suspension and bacterial solution for (a) 5 (right axis) and (b) 24 (left axis) h of bacterial growth. (c) The interaction of the NP to bacterial cell wall promoted by modifications to the surface charge of the NP resulted better in a range to 5 to 7 in which the charge of the NP is turned to a slightly positive one in good agreement to a best interaction, it is showed on the SERS results for the 730 cm^{-1} peak intensity graph for the spectra of 5 and 24 h of bacterial growth.	65
Figure 35. TEM images of the mixtures colloidal suspension and bacterial solution with modifications to the surface charge of the NP for (a) 5 and (b) 24 h of bacterial growth sample. As can be clearly observed, pH in range 5 to 7 resulted in an increasing the affinity of nanoparticles to bacterial cell wall. Lower pH value (~ 3) resulted in a high oxidation and precipitation of the nanoparticles and a decrease in the close contact of the small NP to the analyte.	66
Figure 36. SERS of aminoacids such as (a) calcium dipicolinate complex, (b) L-lysine, (c) L-glutamic acid, (d) L-cysteine, (e) methionine and (f) NAG using 532 nm, 10x objective, 10s, 47.5 mW.	72
Figure 37. SERS of vegetative cells (5 h) and endospores (24 h) of <i>Bt</i> sample solutions using the optimization procedure discussed previously.....	79
Figure 38. (a) The PCA scores plot allowed a comparison between the vegetative cells and endospores SERS spectra. (b) Loadings plot presenting the spectral regions contributing to the spectral differences between samples.	81
Figure 39. PLS-based discriminant analysis of <i>Bt</i> samples at two different bacterial content. A positive value (~ 1) implies presence of vegetative cells and zero value (~ 0) implies not considered vegetative cells samples (suggesting in this case the endospores.).....	82
Figure 40. Example of a SERS spectrum of <i>Bt</i> to show the regions in which the peaks area were analyzed according Table 10.	84
Figure 41. SERS results of <i>Bt</i> at different growth stages: (a) SERS spectra of <i>Bt</i> at different h of bacterial growth. As can be seen while <i>Bt</i> grows. (b, c) The peak area of several spectral regions presents an increasing behavior.	86
Figure 42. PLS regression of time in the growth of <i>Bt</i> . Spectra was preprocessed with first derivate and mean centering. With 6 variables the error is estimated in 1.59 h (RMSECV)	88

and the correlation is 0.98.	
Figure 43. Scores plot per sample showing three stages during the growth of <i>Bt</i>	89
Figure 44. Experimental set up system for SERS experiments to aerosolized samples used by Sengupta [30] in the bioaerosol experiments published.	91
Figure 45. Experimental setup used to aerosolize the bacterial sample to the nanoparticles for SERS experiments. The parameters used were 50 mL/h, 1.5 atm at 0.10 of broadband speed.	92
Figure 46. Results obtained from the bioaerosol experiments: (a) the change in color of the nanoparticles and bacteria mixture (bacterial sample suspension non aerosolized at left and aerosolized at right) and (b) the SERS results obtained from the aerosolized bacterial sample at two different concentrations (<i>i</i> OD ₆₀₀ at 1 and <i>ii</i> 0.5).	93
Figure 47. (a) View of the bacterial sample aerosolized to the solid substrate from Raman microscopy using a 10x objective. (b) The bacterial sample was spread 1” x 1” to the solid substrate using the same experimental parameters of NP suspension solution experiments to generate the aerosol.	96
Figure 48. SERS spectra of endospores of <i>Bt</i> aerosolized for 10s to the Ag/PDMS solid substrate, it shows a good SERS detection and identification of the vibrational band assigned to bacterial content.	97

Abbreviations List

RS	Normal Raman Spectroscopy
SERS	Surface Enhanced Raman Spectroscopy
NS	Nanosphere
<i>Bt</i>	<i>Bacillus thuringiensis</i>
NP	Nanoparticle
h	hour
VR	Volume ratio
HR	hydrodynamic radii
SEF	Surface enhancement factor
PCA	Principal components analysis
PLS	Partial least square
PDMS	Polydimethyl siloxane

Symbols List

λ_{exc}

Wavelength excitation

1. INTRODUCTION

1.1 Motivation

As a student of chemistry with great concern in environmental problems, I have a particular interest in biological matter that can be present at airborne state. Bioaerosols are extremely small living organisms or fragments of living things suspended in the air. The broad class of microorganisms includes dust mites, molds, fungi, spores, pollen, bacteria, viruses, amoebas, fragments of plant materials, and human and pet dander. When they are disrupted or release their spores into the air, this results in bioaerosol formation [1,2].

These biological influences are relevant issues of environmental and health problems. The Center for Disease Control Analysis determined that 34% of allergies are caused by living organisms, such as molds, fungi, spores and bacteria (Figure 1). These cause infections and allergic reactions on the skin and/or in the respiratory tract. Specifically, bacteria also can be present in food causing food poisoning and water contamination; and recently pathogenic microorganism are been used for bioterrorism threats.

Because of above mentioned problems, the development of techniques that could be useful in fields other than biological warfare agents countermeasures such as medical diagnostics, industrial microbiology, environmental applications, among others have become a very important subject of research. The time required for identification of pathogens is a determinant factor of infection related sickness; therefore research in this area is very important and demanding.

The Center for Disease Control Analysis of What Causes Allergies

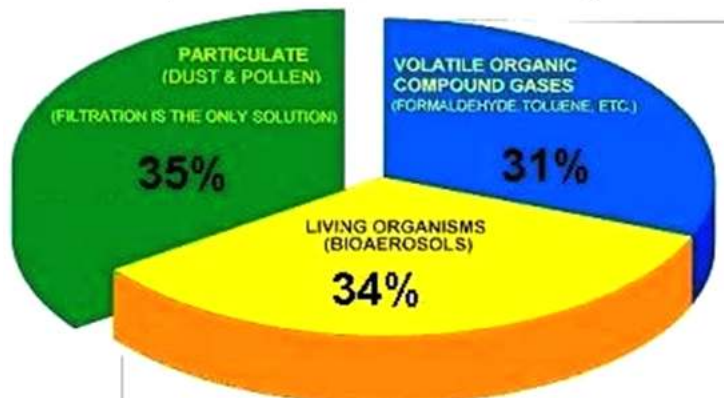


Figure 1. A study from The Center for Disease Control Analysis demonstrated that bioaerosols have a significant influence of health problems. (<http://www.cdc.gov/nceh/ehs/>)

Spectroscopic methods have been successfully applied to the detection, identification, and characterization of chemical and biological threats. Raman spectroscopy (RS) has a wide range of applications in these fields [3-5]. Chemical agents that are commonly used as liquids and highly energetic materials can be successfully detected and identified by RS. The remote detection of highly energetic [6,7] and biological materials [8] have been successfully achieved at low limits of detection, which can be useful for defense and security applications and for monitoring environmental pollution. RS and several of its variations have been applied in the detection and spectroscopic analysis of microorganisms and other airborne biological matter. All of these organisms have Raman active constituents. Biological particles, specifically bacteria, are of particular interest in this research. The biological particles of interest in the aerosol-sized range usually have characteristic dimensions (e.g., diameter for spheres and long axis lengths for rods) between $0.002\ \mu\text{m}$ (2 nm) and $100\ \mu\text{m}$ in size. These bioaerosols can be detected in air or collected on a solid or liquid support and are analyzed in bulk or as single particles. Although bioaerosol particles are considered some of the most complex aerosol dispersed particles and

biomolecules in a suspension, they can be detected and successfully characterized by Raman spectroscopy techniques. RS is also called normal or spontaneous Raman scattering and some of its variations or modalities can be used for vibrational spectroscopy detection of biosamples. As an analytical method, RS is a fast, specific, and noninvasive technique, through which fingerprinting information on the chemical composition of samples can be obtained with high reliability.

Based on this, a particular interest in establishing easy detection protocols using RS, specifically surface enhanced Raman spectroscopy (SERS), have focused the main research objective to detect and identify components of vegetative cells and endospores of bacteria in suspension solution and as aerosol particles.

1.2 Literature review

Several information collected and presented below describing the Raman spectroscopy technique for the detection biological samples in suspensions and as aerosol particles by Raman has been already published in a review by the author and the mentor [9].

1.2.1 Raman Spectroscopy and Surface enhanced Raman spectroscopy

Raman scattering is the name given to the inelastic (energy loss/gain, i.e. superelastic) processes that occur when photons interact with matter transferring part of their energy and changing frequency in the event. When a sample is illuminated with a monochromatic light beam of frequency ν_0 , photons in the beam interact with the electron density surrounding the bonds of the molecules under investigation (Figure 2a). Most of the radiation is elastically scattered (Rayleigh scattering) and the emerging photons have the same frequency as the incident photons.

This type of scattering event does not provide information about the sample composition, but it can be used, for example, to determine the average molecular size in a collection of high molecular weight polymers in a technique called dynamic light scattering. The Rayleigh scattering event is at least 10 million times more probable than the Raman scattering phenomenon. A small fraction of the incident photons (as low as 1 in 10^7) are inelastically scattered in discrete amounts of lower and higher frequencies (Raman scattering). Thus, in order to observe the Raman scattering a high power source that generates large quantities of photons is typically required.

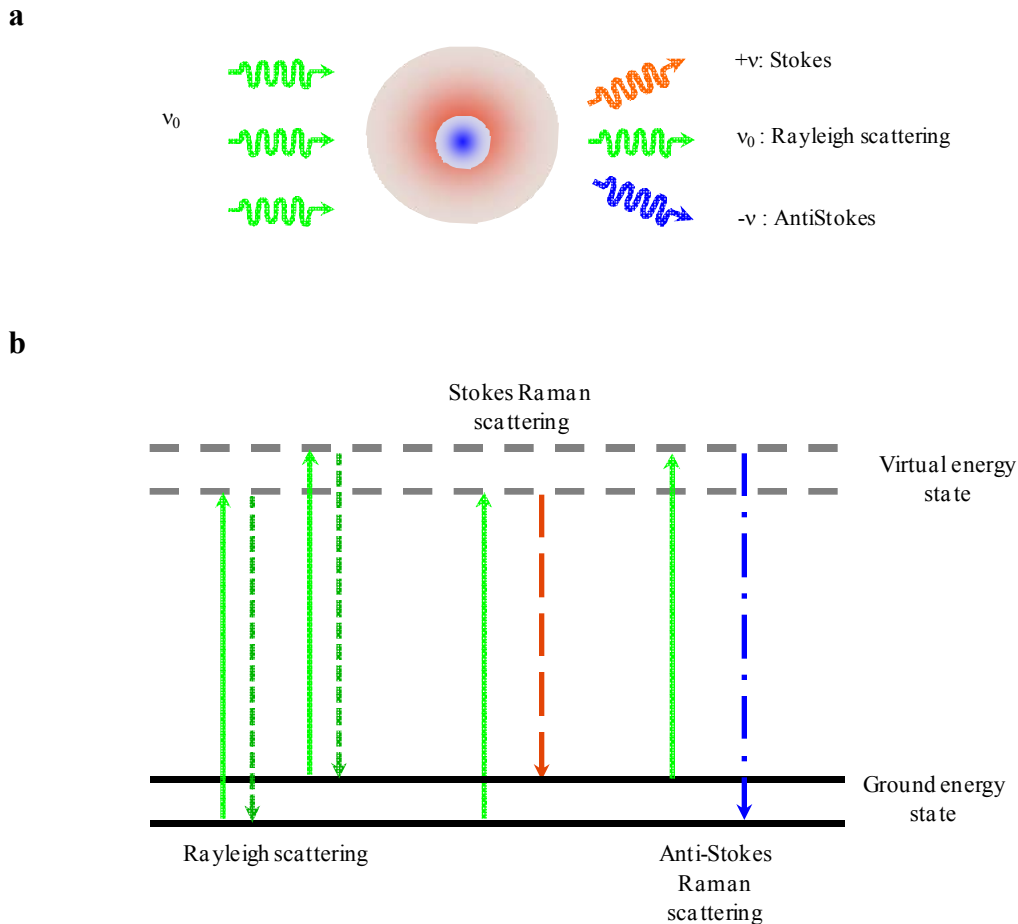


Figure 2. (a) Representation of collision phenomena in which photons with frequency ν_0 interact with the electron cloud of a molecule of the sample. The photon-molecule collision events result

in scattering of the incident radiation with photons with the same frequency (Rayleigh radiation) and photons with shifted frequencies ($+\nu$ and $-\nu$) producing the Raman radiation. **(b)** Energy level diagram showing the states involved in photon scattering. Excitation energies: light green lines; Rayleigh scattering (no energy/frequency change): dark green lines; inelastic (energy loss) Stokes scattering: red line; superelastic scattering (energy/frequency gain): blue line.

If the incident photons excite one of the electrons into a virtual electronic state, the molecule will spontaneously decay to an allowed vibrationally excited state of the ground electronic state of the molecule, resulting in a fast emission of photons having different energies than those of the exciting photons. This produces the inelastic event called the spontaneous or normal Raman Effect. Energy losses are called Stokes events, while energy gains are classified as anti-Stokes (Figure 2b). A general spectroscopic system for normal RS detection is shown in Figure 3. This traditional sampling system shows a conventional 90° scattering geometry. The monochromatic laser source arrives at the sample, and the scattered Raman signal is directed towards the detector. This is one of the simplest experimental setups to implement. Biosamples in aerosol suspensions and in liquid suspensions have been directly detected by normal RS in time sensitive situations.

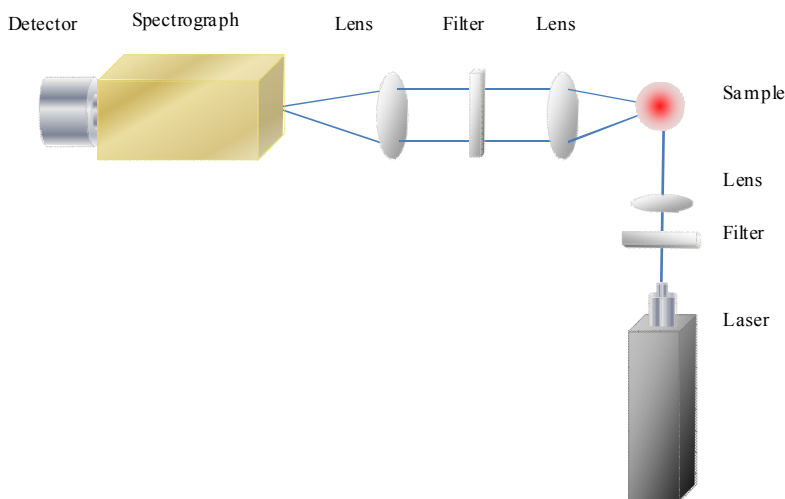
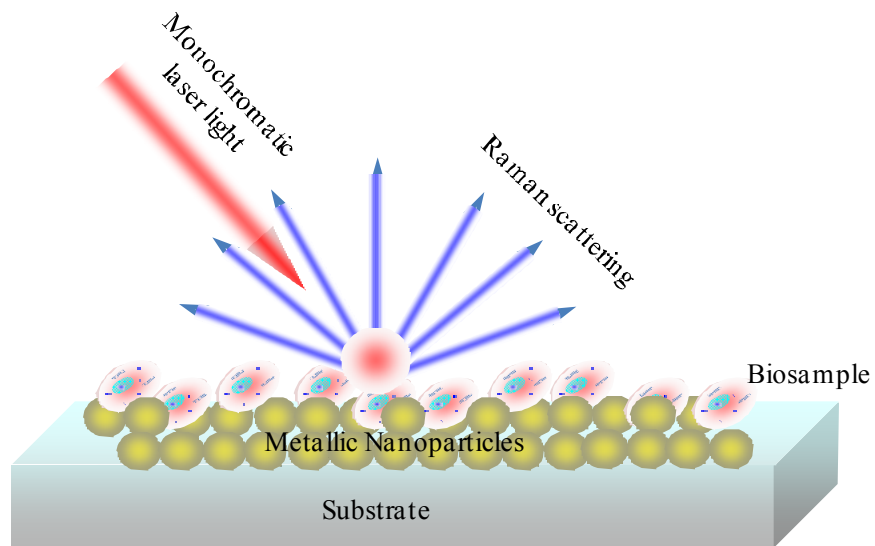


Figure 3. General schematic diagram of normal or spontaneous Raman spectroscopy (RS) conventional detection geometry (90° scattering). This arrangement is typically used as one of the simplest experimental setups to implement.

Surface enhanced Raman spectroscopy (SERS) has been more successful in the detection of biocompounds compared with RS. SERS is a powerful spectroscopic technique that is routinely used to detect analytes at very low concentrations. The intensity of vibrational signatures using SERS can be enhanced by factors of 10^6 to 10^{11} or even higher under well-controlled conditions. The enhancement in Raman scattering due to the presence of suspended metallic nanoparticles or a rough metal surface has been explained using two complementary theories: electromagnetic field enhancement and chemical field enhancement. The electromagnetic field theory is based on a change in the electric field of the laser light in the vicinity of a rough or discontinuous metal surface (or clusters of metallic nanoparticles) leading to an interaction between the analyte and the surface plasmon of the discontinuous metallic surface. The chemical enhancement theory is based on the chemical bonds that can be produced by the transfer of electron density between the analyte and the surface or by the formation of strong covalent bonds with the metal [10]. Figure 4 illustrates a schematic diagram of the SERS effect for biological cell detection using (Figure 4a) metallic nanoparticles in a solid substrate and (Figure 4b) in suspension colloids solution.

a



b

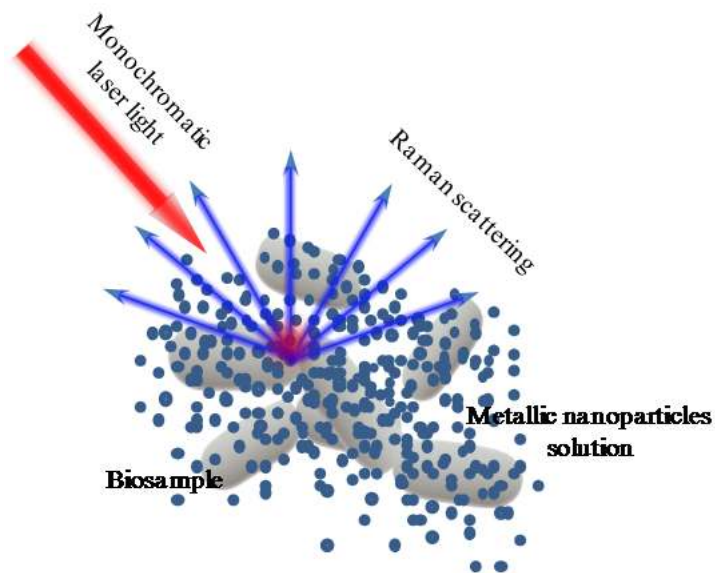


Figure 4. Signal enhancement effect of metallic nanoparticles in SERS is produced by closely spaced interacting particles generated at the location of adsorbed molecules on **(a)** the metal surface and **(b)** in colloidal suspension. So-called “hot spots” seem to provide extra electromagnetic field signal amplification.

The complete elucidation of the strong electromagnetic field enhancement produced at the vicinity of a rough metal surface or a cluster of metallic nanostructures is still a matter of intense research and interpretation. Highly active areas on the substrate (“hot spots”) contribute to the large vibrational signal enhancement and are generated at the location of adsorbed molecules on the metal surface, where the local electric field is large because of the collective excitation of conducting electrons within the small metallic structure (i.e., the surface plasmon) [11,10]. Substrates such as zero valence gold, silver, and copper nanoparticles are most commonly used for SERS experiments. These metals absorb visible light between 400 and 700 nm, which make them excellent substrates for the light scattering phenomenon. The preparation method of silver nanoparticles reported by Lee and Meisel is most widely used for preparing the so called “queen” of SERS: Ag nanospheres [12]. The dynamic charge transfer between the molecule and the metallic nanoparticle allows for the enhancement of the detected signal.

1.2.2 *Bacillus thuringiensis*

Bacillus thuringiensis (*Bt*), a Gram-positive bacterium that lives within the soil and is widely renowned for its toxicity on insect larvae. It produces intracellular protein crystals that are toxic to a wide number of insect larvae, as a result it is commercially used as insecticide. *Bt*, as a *bacillus* species, has a bacterial life cycle in which it grows as vegetative cells forming endospores as a defense mechanism. The bacterial cell wall contains a peptidoglycan layer responsible for strengthening the wall. This rigid layer in a Gram-positive cell wall is typically much thicker. The peptidoglycan layer contains alternating repeats of N-acetylglucosamine (NAG) and N-acetylmuramic (NAM) acid. It encloses a group of molecules called teichoic and lipoteichoic acids which are unique to Gram-positive bacteria cell wall (Figure 5).

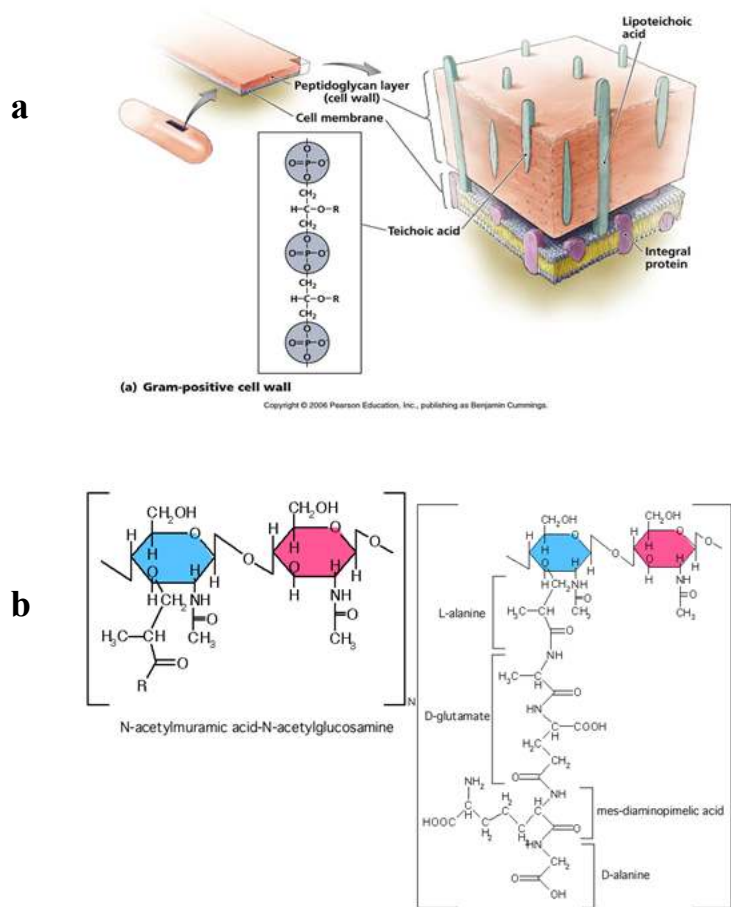


Figure 5. *Bt* cell wall composition: **(a)** Gram positive cell wall and **(b)** chemical structure of the repeating unit in peptidoglycan. [13]

Bt produces a crystalline protein during sporulation called parasporal body that is converted to a toxin by proteolytic cleavage in the larval gut. Endospores are highly resistant to environmental stresses such as high temperature, irradiation, strong acids, disinfectants, etc. They are able to tolerate extreme environments thus making them suitable for transporting before or during a biological attack. The bacterial endospores contain several well-known layers (Figure 6), from internal to external location. Among these are the cortex, the core wall, the spore coat and the exosporium. Biochemical components of these layers include sugar chains, short

peptides of peptidoglycan, polypeptides, fatty acids (lipids), carbohydrates and proteins. In the core, thick layer of proteins, dipicolinic acid and calcium ions normally exist in the form of a calcium-dipicolinate complex that stabilize and protect the genetic material of the endospores [5-7].

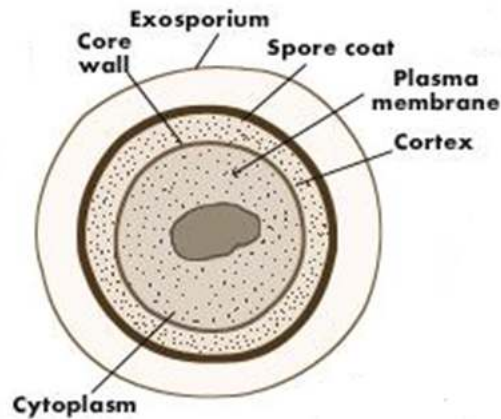


Figure 6. *Bt* endospores wall contain the several layers from internal to external location. (<http://www.tutorvista.com/content/biology/biology-iii/kingdoms-living-world/reproduction-bacteria.php>)

Bt, an is a non-harmful microorganism to humans, is a *bacillus* group member with *Bacillus cereus* and *Bacillus anthracis*, has been chosen as a model because of its similarities with *Bacillus anthracis* which has a great potential of being used for terrorist attacks. *Bacillus cereus* and *Bacillus anthracis* are important pathogens of mammals, including humans. They, as closely related species, can be distinguished functionally by the mostly genes carried on plasmids. The three species have the same cellular size and morphology and form oval spores located centrally in a nonswollen sporangium. [14]

The vegetative *Bacillus anthracis* cells are Gram-positive; therefore they contain an extensive peptidoglycan layer, lipoteichoic acids, and crystalline cell surface proteins (S-layer proteins). *Bacillus anthracis*, differing from other Gram-positive bacteria, is capable of capsule formation and the production of toxins that lead to carbuncles in animals and in humans, causing the disease known as anthrax. It does not contain teichoic acids and the S-layer proteins are not glycosylated. Cell wall polysaccharides function in anchoring the protective S-layer to the cell wall [15].

1.2.3 Bacteria detection techniques

1.2.3.1 Current biological techniques

There are several biological standard detection techniques to identify bacteria, such as polymerase chain reaction, ELISA and flow cytometry. These techniques are time consuming and expensive [16,17]. In addition, the fluorescence analysis is not generally adequate because of the similarity in the biological samples spectra; and the ultraviolet spectra reveal the bands related to chromophore groups in the structure of the molecule [18]. Among new methods under development, vibrational Raman Spectroscopy and SERS provide the basis for reagentless procedures in which there is no need to add chemical dyes or labels for identification.

1.2.3.2 Normal Raman and surface enhanced Raman spectroscopies

1.2.3.2.1 Normal Raman Spectroscopy (RS)

Essential components of bacteria and bacterial endospores including dipicolinic acid (DPA) and other components of biological samples have been detected by RS. The solid phase and liquid suspension spectra allow for the identification of characteristic vibrational modes of

the biosample content. Raman microspectroscopy has enabled the detection and characterization of individual bacterial endospores, such as those of *Bacillus cereus*, *Bacillus megaterium*, *Bacillus subtilis*, and *Bacillus thuringiensis* [19,20] as well as complex samples containing mixtures of microorganisms [21]. Vibrational bands can be compared with those detected by other spectroscopic techniques with the caveat that Raman bands in these systems are almost always observed at low to very low intensity levels [22,23]. Raman spectroscopy can also be used to obtain images of biological samples as a detection and characterization technique providing a full spectrum assessment of bioaerosol samples [24]. The fluorescent compounds found in biological samples, such as some proteins and amino acids, present problems in obtaining their corresponding RS spectra because of endogenous fluorescence. Many of these compounds resonantly absorb at the incident Raman excitation frequency leaving the molecule in an upper electronic state rather than in a virtual state. Because of this absorbance, Raman spectra of the target microorganisms present a broad fluorescence emission that overlaps the Raman signals [11].

The Raman spectrum can be efficiently used to identify and characterize some types of biosamples. However, the spectral definition is generally poor except for a few RS molecular signatures. Spontaneous Raman imaging is also possible and very attractive because, contrary to other imaging techniques sample images are free of additives (i.e., only the sample is present). The limitation of this technique is the time required to obtain the complete Raman image and the restriction to live cell applications. Modifying the scanning mode and detection approaches can reduce this limiting factor.

1.2.3.2.2 Surface Enhanced Raman Spectroscopy

SERS is able to suppress the high fluorescence that biological samples exhibit virtue of the interaction with a metal surface or collection of metallic nanoparticles (NP) [25,26]. The SERS spectrum can be efficiently used to identify and characterize biosamples. The enhanced intensity signals can be differentiated from the signals observed in the normal RS spectrum. The SERS spectrum allows identification and characterization of the peaks detected in suspended solutions and bioaerosol samples more efficiently than RS. High intensity peaks can be observed in the SERS spectrum when compared with the normal RS spectrum. The Raman spectra of the biosamples can be different or slightly different depending on the components of the biosample that are in closer contact with SERS-active substrate. The chemical constituents of the bacteria interacting with the nanoparticles can be selectively controlled in the SERS bacterial spectrum. The colloid and the bacteria can be simply mixed to achieve the SERS detection of the external cell wall composition. Also, the colloids can be directly produced within the presence of the bacteria to observe the inner side components of the cell wall membrane [27,28]. Most Raman measurements identify biosamples using the exterior membrane components for detection.

The spectral data obtained by Raman spectroscopy measurements show the vibrational modes of the biosample constituents. The vibrational signals allow for the detection of biosamples and the subsequent identification and characterization of the biological matter according to frequency ranges and vibrational mode assignments. Tentative band assignments obtained can be compared with those reported in the literature to assure correct identification. In addition to this, the presence of more peaks or the lack of peaks in the spectra indicates the formation or breakdown of chemical bonds in the sample under scrutiny. Table 1 includes the

vibrational assignments of signals frequently found in Raman spectra of biological specimens [29].

The detection of aerosol and suspension samples by SERS can be influenced by the colloidal substrate and the laser radiation of the source used. Specific procedures must be used to obtain the best SERS signal.

Table 1. Assignment of bands frequently found in Raman spectra of biological specimens [29].

Assignment	Frequency (cm⁻¹)
(C=C-H) aromatic str	3059
CH ₃ str	2975
CH ₃ & CH ₂ str	2935
CH ₂ str	2870-2890
C=O ester str	1735
Amide I	1650-1680
Tyrosine	1614
Phenylalanine	1606
Guanine, Adenine ring str	1575
C-H ₂ def	1440-1460
CH ₂ def	1295
Amide III	1230-1295
C-N and C-C str	1129
PO ₂ ⁻ sym str	1102
CC skeletal and COC str from glycosidic link	1098
C-O str	1085
C-N and C-C str	1061
Phenylalanine	1004
COC str	897
CC str, COC 1,4-glycosidic link	858
Tyrosine “buried”	852
Tyrosine “exposed”	829
Cytosine and Uracil ring str	785
Adenine	720
Guanine	665
Tyrosine skeletal	640
Phenylalanine skeletal	620
COC glycosidic ring def	540
S-S str	520-540

str: stretching; def: deformation; sym: symmetric

SERS has some restrictions on analyte properties to ensure highly enhanced Raman signals and consequently, low limits of detection. A particular bioaerosol sampling system was prepared by Sengupta et al. [30], in which the biological matter was transferred to a Raman spectrometer by deposition onto a surface to maintain an aqueous suspension for the analysis. Another way to generate aerosols for SERS experiments in an aqueous suspension was presented by Ayora et al. [31]. Important assessments based on the requirements for handling sample devices for bioaerosol generation including dry powder bioaerosols have been summarized in the review by Griffiths et al. [32]. SERS has also been used for kinetic process monitoring of endospore germination in real time. The electromagnetic enhancement provided by the metallic NP allowed for the identification of endospores at different concentrations [33] and temperatures [34]. Fluorescence quenching or suppression of fluorescence is caused by absorption of the stimulating radiation by biosample chromophores when using SERS metallic NP because of the independence of the energy transfer process [11]. Quenching of the endogenous fluorescence is necessary to obtain a good signal with Raman detection.

1.2.4 Optimal controls in SERS analysis

Raman analysis requires optimal control of the experimental setups for the particular Raman technique used. This control depends markedly on the type of Raman experiment performed: incoherent or coherent; spontaneous or stimulated processes. SERS, which is an incoherent technique, has become one of the most used Raman spectroscopy modalities for obtaining large signal enhancements and attaining low limits of detection in a very wide variety of samples. Suspension and aerosol sample detection of biosamples by SERS have certain parameters that need be optimized to obtain optimum signal enhancement without masking the

Raman signals. Selectivity, sensitivity, reproducibility, intensification of signal, response, and the analysis time in SERS experiments depend on the following:

- **Ratio of biosample to metallic NP concentration:** The amount of sample used for detection must be controlled in order to obtain a good Raman signal. Low and high concentrations of the biosample in the mixture affect SERS experiments because of very weak Raman signals or strong scattering from the background (background can also be Raman enhanced). Figure 7 shows the general behavior for the scenario, in which the optimum volume of the colloid increases the scattered radiation, reaches a maximum intensity, and then decreases the detected SERS signal.

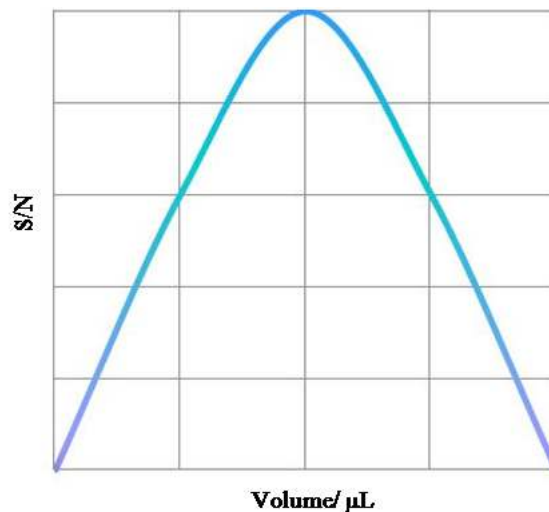


Figure 7. Effect of colloid volume on SERS signal-to-noise ratio (S/N). It is important to optimize for maximum S/N as a function of colloid volume for increasing the scattered radiation collected and decreasing contributions from interferences.

For high metal NP concentrations, the vibrational SERS signals cannot be clearly observed, and there is a decrease in the intensity that is inversely proportional to the NP concentration. In the case of SERS experiments for the detection of bacterial samples,

concentrations of 10^2 cfu/mL and 10^6 cfu/mL (cfu: colony forming units) are considered low and high concentrations, respectively [35]. Determining the optimum volume of NP used is also important for increasing the scattered radiation collected, [31] but a minimum amount of sample is required [36].

- **Thermodynamics and kinetics of the analyte adsorption to the surface of interest:**

This property is related to both time required to obtain the effective binding of the analyte and metallic NP as well as the type and strength of the adsorbate-substrate bond. It also depends on the effective binding to Raman active sites involved in the signal enhancement (“hot spots”). The binding kinetics can be fast (i.e., seconds to a few minutes) or slow (i.e., several minutes to hours) depending on the interaction between the analyzed system and the NP surface [37]. It has been clearly demonstrated that factors such as pH, density of bacteria in solution, and type of bacteria greatly influence the time-dependent behavior of colloidal/bacterial suspensions or the adsorption rate of the metallic colloidal NP and the bacteria analyzed [18,25,38]. The electrostatic interaction between the NP surfaces and the bacterial cell wall can be increased by modifying the surface charge of the NP. This in turn depends on the reducing agent of the metallic ions solutions [39]. Ag-borohydride NP surface charges were modified by changing the pH of the colloid to obtain a more intimate interaction with the bacterial cell wall in which at low and high pH values (3.25 and 9.74), but did not result in improved detection of *Escherichia coli* [18,33]. Improved SERS signals at pH 5 and higher were obtained for *Bacillus* Gram-positive species with citrate reduced NP [16] and for biological molecules with amine groups using hydroxylamine hydrochloride reduced NP [25]. The changes in NP surfaces increase the formation of hot spots and consequently further augment SERS

effect observed. To induce aggregation, pH changes as well as adding halide anions to the NP can also be used. The use of aggregation agents in SERS of bacterial samples was studied to allow the NP induced aggregation and to generate highly SERS-active inter-particle spaces [38]. *Bacillus thuringiensis* detection has been studied by SERS using silver oxide films [37], Au NP covered by SiO₂ [11], Ag colloids reduced by citrate [40] and by hydroxylamine hydrochloride [3].

- **Shape and size of the biosample:** Raman light scattering in SERS analysis results in intensity variations that depend on the morphological properties of the biosample. The biological samples have a wide range of particle shapes and sizes, and the dependence on the Raman scattered light has been theoretically and experimentally studied. For example, Vehing *et al.* [41] studied the size dependence of homogeneous spheres. The shape, size, and orientation of metallic NP affect the selection of the optimal excitation wavelength. Heterogeneously roughened surfaces limit the surface enhancement, but it is difficult to obtain reproducible SERS-active substrates because the density and location of “hot spots” are very hard to control.

Kahraman *et al.* has studied the SERS sensitivity in bacterial detection [42]. The study included comparisons between types of colloid and excitation wavelengths in two types of bacteria, for reproducibility purposes. The reproducibility and consistency of enhancement of vibrational signatures of microorganisms and their stability and dependence on morphology of SERS active substrates has also been studied in depth [11]. It is well known that the electromagnetic and chemical mechanisms of SERS produced by NP upon interaction with analytes is in general determined by the intimacy of the interaction of the molecules to the

surface plasmon field and the charge transfer at the “hot spots” sites. The optimization procedure for achieving maximum signals plays an important role in the attainment of high Raman enhancements for *Bt*. Several previous reports concentrated on the experimental parameters that had to be optimized when studies focused on biological samples detection and discrimination was carried on.

1.2.5 Data analysis

Chemometrics statistical routines, such as partial least squares (PLS), principal components analysis (PCA), discriminant analysis (DA), partial least squares-discriminant analysis (PLS-DA), discriminant factor analysis (DFA), hierarchical cluster analysis (HCA), linear discriminant analysis (LDA), quadratic discriminant analysis (QDA), K-nearest neighbor classifier (kNN), support vector machines (SVMs), Gaussian mixture discriminant analysis (MDA), and spectral angle mapping are some of the currently used methods to find patterns in spectral data. These routines have been used to identify microbial cells from the single cell level to the bulk analysis level, discriminating between bacterial strains in mixtures of aerosol particles, different cultivation parameters, and taxonomic discrimination between microorganisms, among others. Spectral angle mapping can be used under the microscope objective to compare an experimental spectrum with a library spectrum. The accurate interpretation of models can provide robustness and reliability to the correlative analysis of Raman data [20,21,43-45,40,46,47].

Data analysis has been used to validate the applicability of qualitative SERS spectroscopy for analysis of bacterial species by utilizing PCA to show discrimination of biological threat stimulants. Different types of bacteria have been detected and discriminated after important

optimization experiments to obtain good SERS results. For example, PCA of extracted SERS spectra from single bacterial cells coated with silver NP, such as *Bacillus cereus* vegetative cells, *Bacillus anthracis* spore and *Bacillus thuringiensis* vegetative cells, were sufficient to allow for discrimination between the three single bacteria [48]. Also, SERS spectra have been used to discriminate between different species and the possible differentiation of strains of *bacillus* spores [40]. Gram-negative and Gram-positive species as well as spores and vegetative cells of *Bacillus globiggi* were discriminated by PCA with spectral differences mainly attributed to lipid layer component of the cell walls and membranes and C-C skeletal in proteins at endospores samples. However, SERS spectral results that contain fluorescence can limit the chemical information obtained and the reliability of the sample identification. A multivariate analysis was performed on multiple sets of measurements, wavelength, samples and data sets [49].

This research work has been focused on analyzing the SERS spectra by PCA to reveal several spectroscopic characteristic features enabling vegetative cells and endospores species differentiation. PLS analysis was also used to model and predict information for future samples.

1.2.6 Summary and justification

Suspension solution and/or aerosol of bacteria detection, identification, and characterization can be achieved using Raman spectroscopy techniques. These techniques can generate Raman scattered signals from bio-suspensions and bioaerosols with high sensitivity, selectivity, and reproducibility providing fast, real-time detection schemes. Several Raman technique modalities have numerous advantages over conventional methods of bioaerosol detection with significant improvements in sensitivity and selectivity, but they also all have limitations.

This is an important area of investigation. Research in bioaerosol detection using Raman spectroscopy has great potential for various applications, but currently, there are many limitations and problems. The standoff detection of bioaerosol using Raman spectroscopy represents a great technological challenge that is continuously being improved. The coupling of Raman spectroscopy with others detection and characterization analytical tools can be used to overcome many of the challenges that current detection boundaries pose and will undoubtedly contribute to reach the goals of improved selectivity, sensitivity, lower duty cycles, lower biosample concentrations, and real-time analysis.

Also, Kahraman [42] and Sengupta [18] proposed that a standard protocol must be developed depending on the goal of the study in order to optimize the SERS detection system by controlling interaction parameters. Since no specific studies addressing these important issues of *Bt* using these sensing platforms were found, it was decided to study them. This research has a special interest in identification of biochemical components of the cell wall and endospores of *Bacillus thuringiensis* (*Bt*) by surface enhanced Raman scattering (SERS) spectroscopy using Ag NP reduced by hydroxylamine and borohydride capped with sodium citrate. Activation of “hot spots”, aggregation and surface charge modification of the NP would be studied and optimized to obtain signal enhancements from *Bt* samples as suspension. Part of the work was aimed at detection of *Bt* endospores as aerosol particles using metal rough surfaces in colloidal suspension and solid substrate by SERS. Multivariate analysis was used to discriminate between samples at different growth stages in suspension and the monitoring the grown process of the bacterial life cycle using PCA, PLS and PLS-DA.

2. *Bacillus thuringiensis*: growth, preparation and characterization of vegetative cells and endospores

This chapter focuses on the incubation, growth, preparation and characterization of the *Bacillus thuringiensis* (*Bt*) samples used on this research. Standard Biosafety Level 2 procedures were employed to handle, process and discard the samples.

2.1 Materials

Bt strain (ATCC #35646) was provided by the Microbial Biotechnology and Bioprospecting Lab, Biology Department, UPRM. It was grown using Miller modified Luria-Bertani (LB) agar and broth (Fisher Scientific International; Thermo Fisher Scientific, Waltham, MA).

2.2 Instrumentation

A storage freezer maintained at -80°C was used to preserve the pure bacterial culture. An orbital shaker operated at 32°C was used to incubate the bacterial sample. To obtain the optical density measurements at 600 nm (OD_{600}) an Eppendorf Biophotometer was used. The samples were centrifuged using an Eppendorf centrifuge, model 54150D. White light microscopy images of samples were acquired in order to determine the content of the sample. An Olympus America, Inc. (Center Valley, PA) model BH2-UMA high resolution optical microscope designed for mineralogy studies and equipped with objectives of 10-250 \times magnification and a 6.0 MB PAX-Cam image capturing CCD camera controlled by PAX-it!TM Software (Midwest Information Systems, Inc., Villa Park, IL) were used to capture the white light micrographs of the bacterial

samples. Most of the images captured were taken with 10× and 100× ultra-long working distance objectives. SEM images were recorded by using a JEOL model 5800LV Scanning Electron Microscope (Peabody, MA) using an accelerating voltage of 15-25 keV at University of Puerto Rico-Cayey.

2.3 Bacterial culture preparation

2.3.1 Preparation of bacterial sample

Pure culture of *Bt* stored at -80°C in 20% glycerol was inoculated in LB agar plates and incubated at 32°C overnight. After transferring pure culture sample to 5.0 mL LB broth in a culture tube, it was placed in an orbital shaker at 32°C (~120 rpm) during 24 h. An Erlenmeyer flask (250 mL) was prepared with nutrient media and microorganism culture to a final volume of 25 mL to obtain an initial optical density at 600 nm (OD_{600}) of 0.025.

2.3.2 Bacterial growth curve

The *Bt* life cycle, has two main phases, the vegetative growth phase where bacteria are duplicated by bipartition every 30-90 min depending on the culture medium and the sporulation phase, which is a differentiation program of bacteria to spores [50]. In order to obtain detailed information on the microorganism growth behavior and bacterial life cycle, OD_{600} measurements were collected every two hours during a period of twenty four (24) hours using 100 μ L of the growing bacterial suspension. A bacterial growth curve was constructed in terms of absorbance vs. time, and then the bacterial growth measurement was normalized to represent the percentage growth as shows Figure 8a. The results were compared with the growth behavior reported on literature as shown in Figure 8b. It was very helpful to select the two growth stages (hours) to be

worked on this study, in which the bacterial content is mostly vegetative cells or endospores. The samples were chosen at 5 h and at 24 h as representative samples of bacterial content for vegetative cells and endospores, respectively.

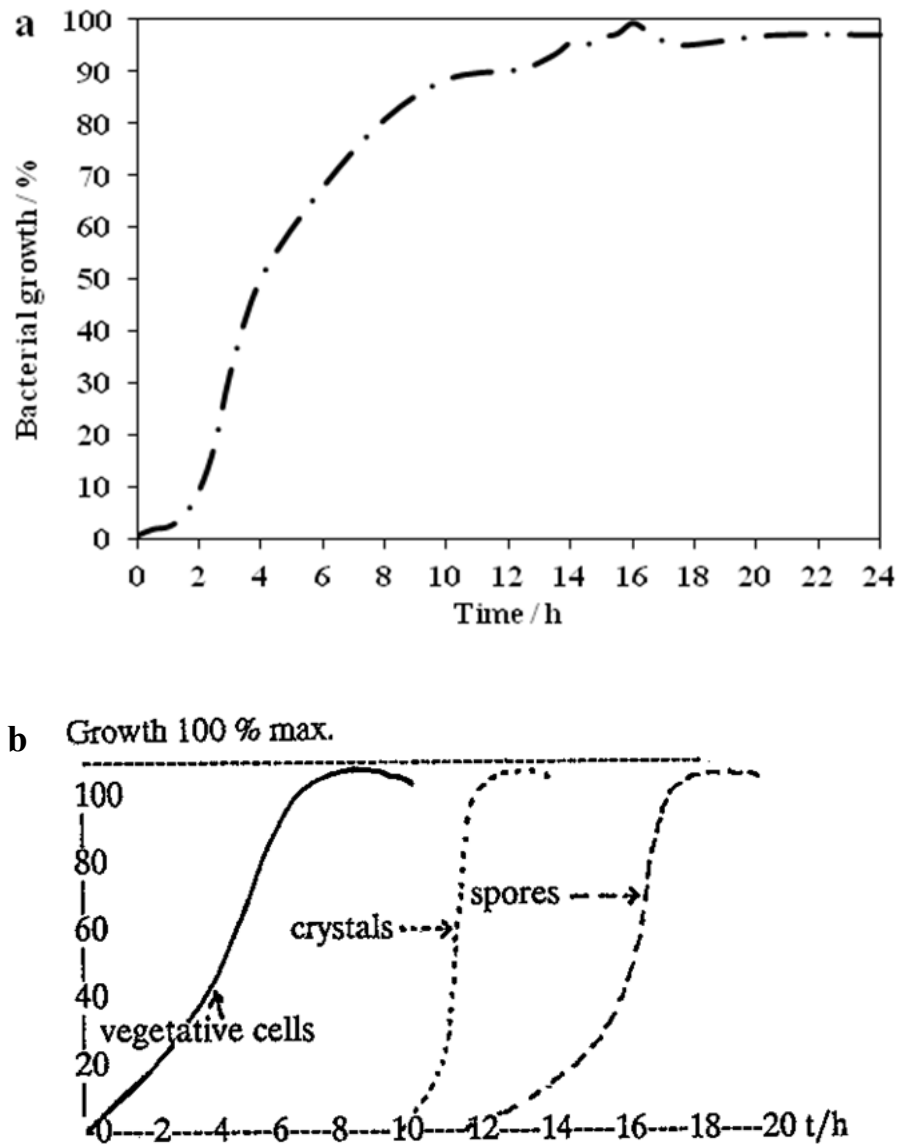


Figure 8. (a) Experimental growth curve of *Bt.* (b) Sporulation in *Bacillus thuringiensis* (FAO AGRICULTURAL SERVICES BULLETIN No. 96)

2.3.3 Bacterial sample centrifugation

Samples were collected after bacteria were cultured for 5 h and 24 h, then centrifuged for 4 to 6 min at 4000 rpm and the supernatant was discarded. The pellet obtained was washed twice with 5 mL of 0.1 M NaCl and finally resuspended in 0.1 M NaCl until obtaining an absorbance of 1.0 ± 0.1 for 5 h and 24 h of bacterial growth. The bacterial samples were stored at 4°C until experiments were performed.

2.4 Bacterial sample characterization

2.4.1 Gram and endospore staining

Bt was characterized using Gram and Fulton-Schaeffer spore staining techniques. The Gram staining technique confirmed the presence of Gram-positive bacillus strain (Figure 9a and Figure 9b). Endospore staining was performed to establish the presence of vegetative cells and endospores in several samples. Figure 9c and Figure 9d consist of micrographs taken under a white light microscope, showing vegetative cells or/and endospores content of *Bt* strain. Bacterial samples growth at 5 h and 24 h were chosen and used in the experiments as these samples contain mainly vegetative cells and endospores, respectively. SEM images were also used to confirm the presence of vegetative cells and endospores (Figure 10). The size of the bacterial cell is about 4 μm length and 1.3 μm width.

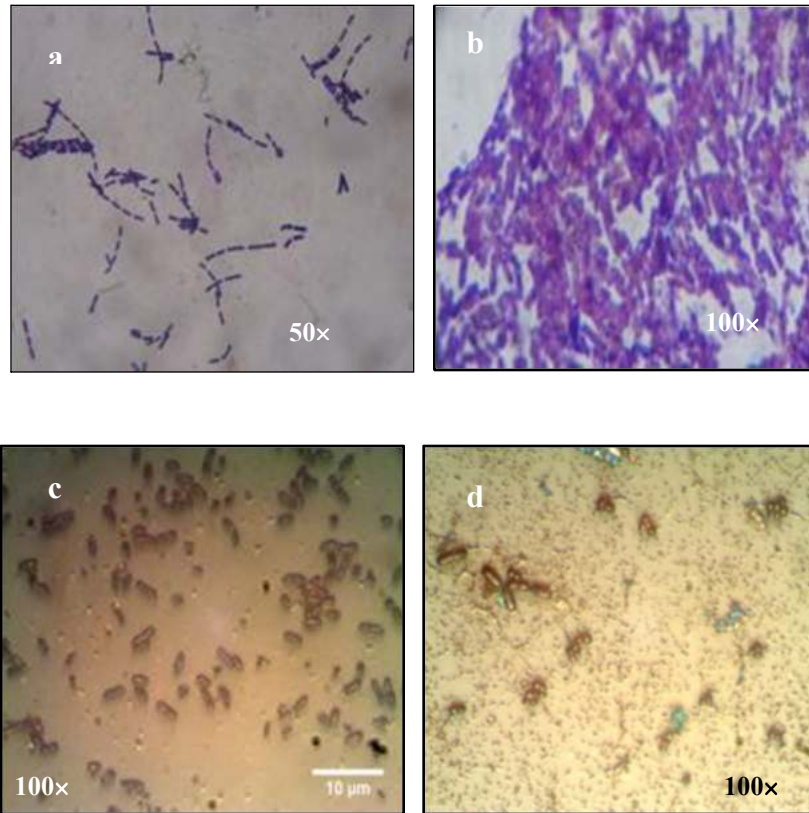


Figure 9. White light micrographs of *Bt* characterization at 5 (**a, c**) and 24 (**b, d**) h of bacterial growth: (**a, b**) Gram staining (purple: Gram +); (**c, d**) endospores staining with high magnification image of stained endospores.

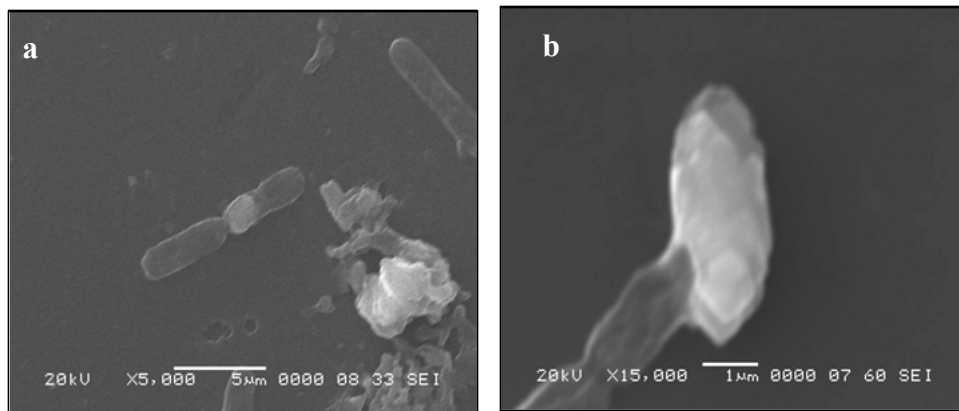


Figure 10. Characterization of *Bt* by SEM images at 5 and 24 h of bacterial growth. (**a**) vegetative cells; (**b**) endospores forming bacteria.

2.4.2 Colony forming unit (CFU)

The bacterial concentration was obtained by several low concentration dilutions of the bacteria growing in LB broth. Bacterial solutions with concentrations in the range of 10^{-3} to 10^{-10} M were prepared from a 5 mL culture tube of *Bt* growth. Following the colony forming unit formula (plate count*dilution factor) [1], the bacterial sample had 1×10^8 cells per milliliter CFU. The calculations of the sequential inoculations to obtain the bacterial concentration at 24 h of bacterial growth are presented in Table 2.

Table 2. Sequential dilutions of *Bt* to obtain the colony forming unit

24 h	Dilution 1	Dilution 2	Dilution 3	To plate (mL)
Vt (mL)	7	10	10	
Vad <i>Bt</i> (mL)	0.007	0.1	1	
Vad broth (mL)	6.993	9.9	9	
<i>Bt</i> tube concentration (M)	0.001	0.01	0.1	
Dilution factor tube (M)	1.00E-03	1.00E-05	1.00E-06	
Plate count T2: 24 h	TNTC	50	TFTC	0.05
CFU (cfu/mL): 24 h	TNTC	1.00E+08	TFTC	0.05
CFU (cfu/mL) ave		1.10E+08		

TNTC: too numerous to count; TFTC: too few to count

2.5 Summary

In this chapter discussed all the *Bt* samples procedures such as incubation, growth, preparation and characterization the bacterial samples used on the experiments detailed below. To achieve the research objectives, two bacterial samples were chosen in which the main bacterial content present were vegetative cells and endospores, respectively for the samples growth of 5 h and 24 h. All efforts are intended to obtain mainly this kind of biosample in each sample, but some vegetative cells-forming endospores could be present in the 24 h of bacterial

growth sample. It is insignificant with respect to the amount of endospores present in this sample. *Bt* sample used for the experiments have 1×10^8 cells per milliliter of original sample. Once the bacterial sample is obtained, it is suspended in NaCl 0.1 M to preserve the bacterial sample refrigerated until experiments were conducted. The bacterial dilution required for the experiments are well explained in the next chapters, and the bacterial concentration for analysis is also presented in Chapter 3 and 4.

3. NORMAL OR SPONTANEOUS RAMAN (NR) SPECTROSCOPY EXPERIMENTS

This chapter contains all the results obtained from the Normal or Spontaneous Raman spectroscopy experiments of bulk and diluted suspension samples at 5 h and 24 h of bacterial growth. Normal Raman experiments can bring information to identify and characterize biosamples, but the spectral definition is generally poor except for a few RS molecular signatures.

3.1 Instrumentation

Raman experiments were done using a Raman Microspectrometer, model RM-2000 (Renishaw Inc., Hoffman Estates, IL, USA). The spectroscopic system also contained a spectroscopic grade CCD camera, Leica LX microscope, 532 nm diode pumped-solid state (DPSS) laser (Newport-Spectra Physics, Mountain View, CA), 10-50 s exposure time, 3 accumulations and a 10× objective lens in a spectral range of 100-3000 cm^{-1} .

3.2 Sample preparation

Bacterial samples were transferred to glass capillary tubes (0.9 x 90 mm) using sterile, disposable needles and syringes in order to process the Raman spectra. A small amount of the bacterial solution dissolved in 0.1 M NaCl was used for Raman experiments. The capillary tube was placed in the stainless steel holder under the Raman microscope for Raman experiments. Figure 11 illustrates a schematic diagram of the experimental set up used for the experiments.

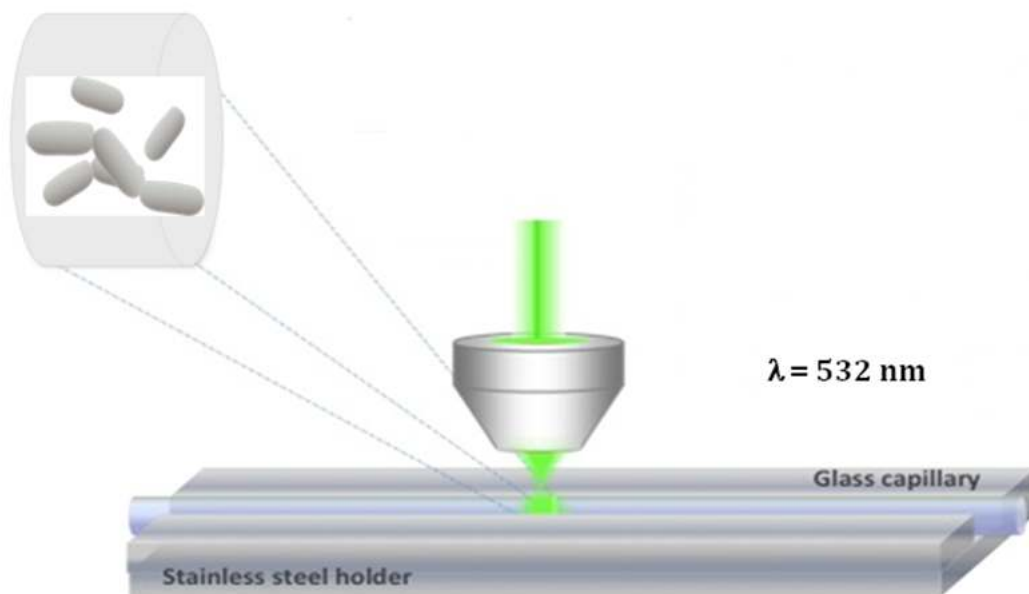
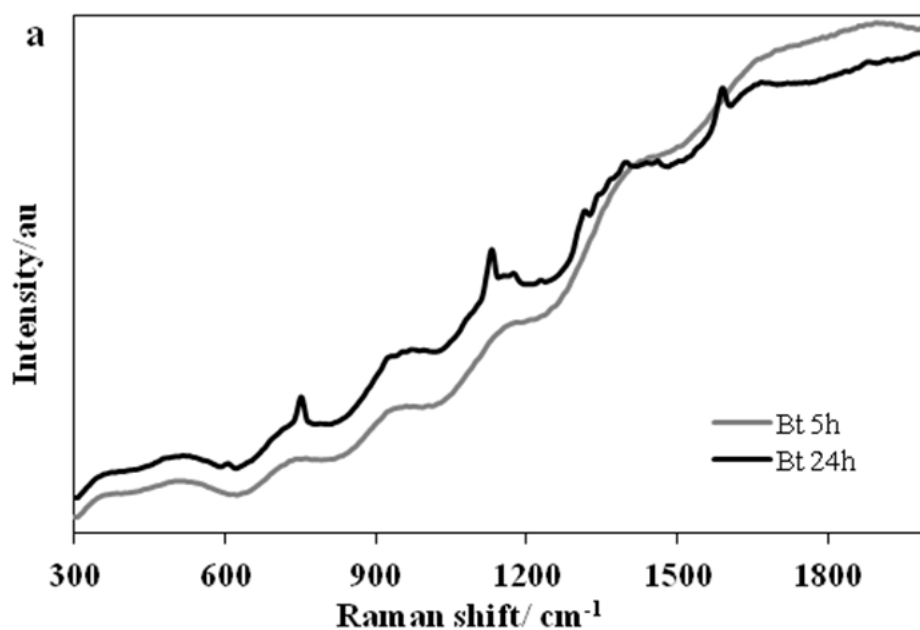


Figure 11. Normal Raman experimental set up for biological sample detection.

3.3 Results and discussion

The Normal Raman spectra of *Bt* bulk at 5 h and 24 h of bacterial growth was contaminated with fluorescence from the presence of fluorophores commonly found in many biological compounds (Figure 12).



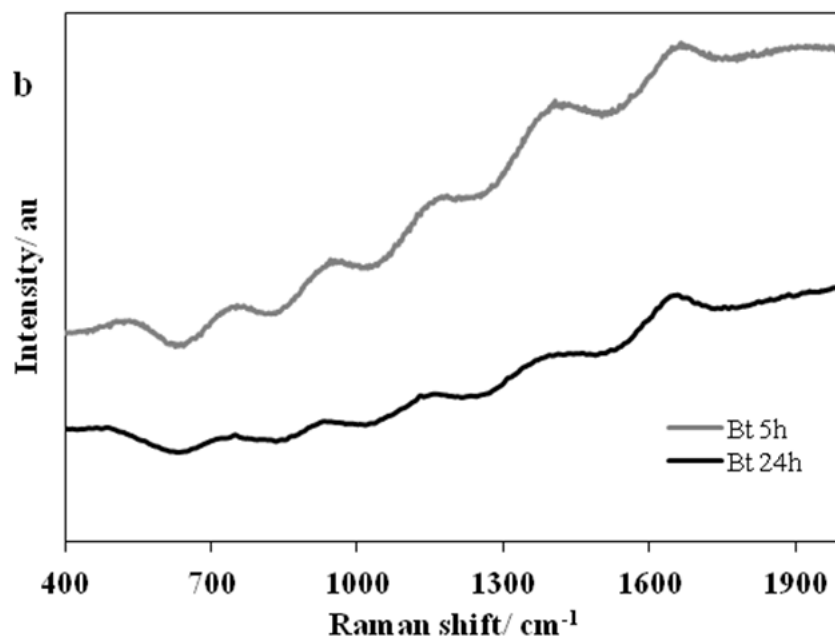


Figure 12. Raman spectra of (a) concentrated and (b) diluted sample of *Bt* suspended in 0.1 M NaCl at 5 h and 24 h of bacterial growth. As can be observed, a highly fluorescence due to the bacterial components presents in the sample limits the chemical information.

However, important signals could be tentatively assigned from the spectra obtained of a highly concentrated bacterial suspension (Figure 12a), even though many of them appeared as low intensity bands in a highly congested background. Several of the bands observed were from: glycosidic ring of NAG and NAM at 753 cm⁻¹; C-N and C-C stretching at 1130 cm⁻¹; signals from lipid content, =C-C= at 1144 cm⁻¹ and C=C at 1588 cm⁻¹. Most of the signals observed are related to calcium dipicolinate (CaDPA), which is the main component of the protective layers of the central core cell, the endospores [51]. The Raman spectrum of a diluted sample of *Bt*, at 5 h and 24 h of bacterial growth, was covered with high fluorescence from the presence of fluorophores commonly found in many biological compounds. These bacterial sample dilution spectra were (Figure 12b) obtained with low intensity bands in a highly congested background, and, as can be observed, the spectrum at 5 h of bulk *Bt* solution did not showed vibrational bands

that can be tentatively assigned. This system under study can be optimized to suppress the fluorescence and obtain good signals for identification of the biological content.

3.4 Summary

To enhance the signal identification of the biological content and decrease the fluorescence of the bacterial content, several aspects of the biomolecular system under study have to be taken into account. To begin with, SERS spectra in these systems result from the interaction of the metal NP surface with the outer coating content of the cells. Due to poor signal definition and limited chemical information in the Raman spectra of *Bt*, aspects like the volume and concentration of the NP colloidal suspensions used, the sample amount and concentration of the biological system under study analyzed, the charge of the layer of NP, and the aggregation induction effects of the colloidal NP need to be optimized. The affinity of the biomolecular sample (*Bt*) to Ag-NP was improved resulting in an enhancement of the signal to noise ratio of the SERS spectra obtained. Also, a significant decrease in fluorescence present in the Raman spectra of this *bacillus* sample was observed. Details of these effects dealing with Ag-NP reduced by borohydride and hydroxylamine are clearly discussed in the next chapter.

4. SERS EXPERIMENTS: SYNTHESIS, CHARACTERIZATION, AGGLOMERATION AND MODIFICATIONS TO THE SURFACE CHARGE OF THE NANOPARTICLES (NP)

This chapter shows in detail the synthesis and characterization of two types of silver nanoparticles that were used to compare the SERS results of the bacterial samples. In SERS, the effect of Ag or Au metallic colloids to optimize procedures for detection, identification and classification is commonly used with biological samples. The potential of the reducing agent was evaluated according to the necessities in order to obtain several manipulations of the NP until the best interaction NP and biosample components for the detection were achieved. Citrate capped borohydride reduced NP and hydroxylamine reduced NP were chosen as the nanoparticles to induce the SERS effect for this study.

4.1 Materials

Silver nitrate (AgNO_3 , 99+%), sodium borohydride (NaBH_4 , 98%), hydroxylamine hydrochloride ($\text{NH}_2\text{OH}\cdot\text{HCl}$), trisodium citrate dihydrate ($\text{Na}_3\text{C}_6\text{H}_5\text{O}_7\cdot 2\text{H}_2\text{O}$), sodium chloride (NaCl , 99.9+%) and sodium hydroxide (NaOH) were acquired from Sigma-Aldrich Chemical Co. (Milwaukee, WI). Nanopure deionized ultra-high purity water (UHP; $18.2\text{ M}\Omega\text{-cm}$) was used for the preparation of aqueous metal ions solutions. Glassware was cleaned by soaking in *aqua regia* and finally washing with distilled and deionized water several times.

4.2 Instrumentation

Ag-NP were characterized by UV-VIS spectrophotometry and by transmission electron microscopy (TEM). Absorption spectra of the solutions were acquired using a Cary 5000 UV-VIS-NIR spectrophotometer (Varian, Palo Alto, CA). TEM images were recorded by a JEOL Transmission Electron Microscope (TEM), model 1011, providing a resolution of 0.2 nm lattice with magnification of 50 to 10^6 under the accelerating voltage of 40 to 100 kV (JEOL, Peabody, MA). Samples were prepared by placing 1.0 μL of the Ag-NP solution in ultrathin carbon film/holey carbon 400 mesh copper TEM grids (CF300-Cu, Electron Microscopy Sciences, Hatfield, PA) and allowing the solvent to evaporate at room temperature. The grids were kept in a desiccator to provide a dust free environment. Hydrodynamic radius (HR) measurements were obtained using a Zetasizer™ Nano Series (Malvern Instruments Ltd. manufacturer, Worcestershire, U.K). Raman experiments were done using a Raman Microspectrometer, model RM-2000, CCD camera, Leica LX microscope, 532nm laser line, 10-50 s exposure time, 3 accumulations and a 10x objective lens in a spectra range of 100-3000 cm^{-1} (Renishaw Inc., Hoffman Estates, Ill, USA).

4.3 Synthesis of nanoparticles

4.3.1 Hydroxylamine reduced Ag colloids

The synthesis of the hydroxylamine reduced nanoparticles follows the next following redox reaction [52]:



Hydroxylamine reduced Ag colloids were prepared by the method of Leopold and Lendl [53] by dissolving 10.44 mg of hydroxylamine in UHP water (1.67×10^{-3} M) and 11.98 mg of NaOH 3.33×10^{-3} M in UHP water and 90 mL of pure degasified water for 15 min while stirring with a magnetic bar. Then, 10 mL of 1.0×10^{-2} M silver nitrate solution were added dropwise with constant nitrogen bubbling. Figure 13 shows a summary of the experimental setup used for NP preparation.

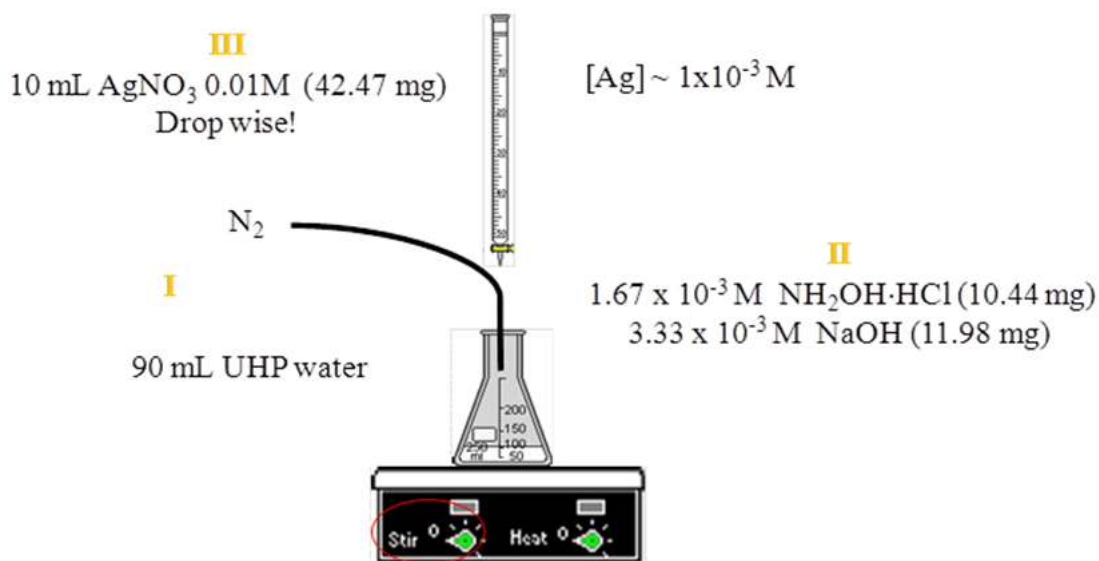
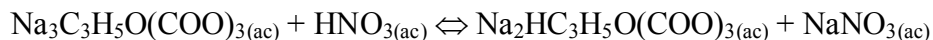
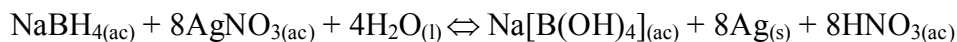


Figure 13. Experimental setup and procedure summary for the preparation of Ag-NP reduced by hydroxylamine to obtain a final concentration of 10^{-3} M of Ag.

4.3.2 Borohydride reduced Ag-NP

The synthesis of the borohydride reduced NP follows the next redox reactions:



Borohydride reduced Ag-NP were prepared using the method of Keir, Sadler and Smith [54] using 1 mL of 1% sodium citrate. The method was modified by using citrate as capping agent to avoid colloidal precipitation over time. A typical synthesis consisted of dissolving 3.4 mg of

NaBH₄ in 75 mL of UHP water that had been previously degassed with N₂ and cooled at 4°C under vigorous stirring using rotating magnetic bar. Then, 1 mL of trisodium citrate 1% was added to the flask. Finally, 9 mL of AgNO₃ 0.0022 M was added at a rate of 20.5 μL/s and stirred for 45 min at 4°C. Figure 14 shows a summary of the experimental setup used for NP preparation.

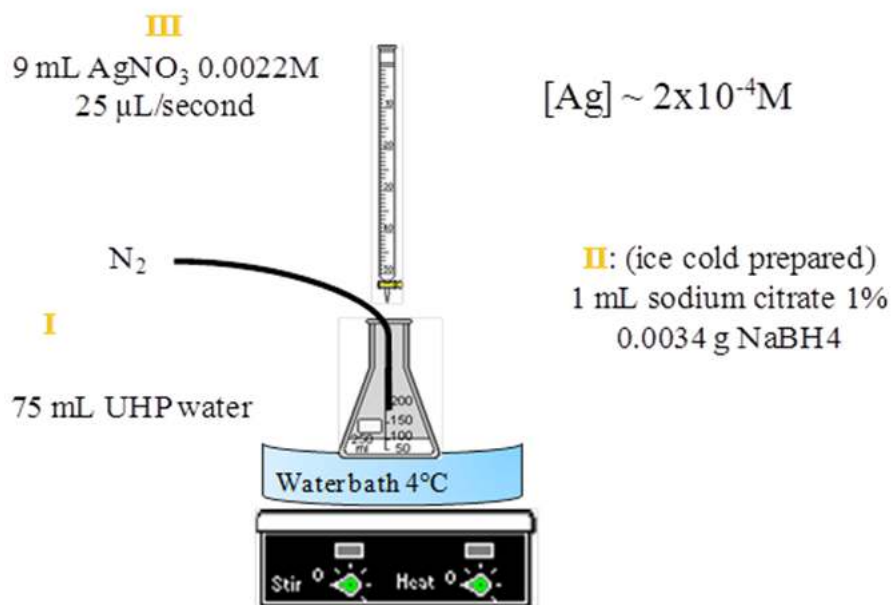


Figure 14. Experimental setup and procedure summary for the preparation of Ag-NP reduced by borohydride capped with sodium citrate to obtain a final concentration of 10⁻⁴ M of Ag.

4.3.3 Inducing NP aggregation

NP clustering (aggregation) was promoted by the addition of Cl⁻ ions through NaCl solution to the colloidal suspensions to increase Raman signals by stimulating the formation of hot spots on aggregation of NP. Several concentrations (0.1, 0.3, 0.5 and 1.0 M) of this aggregating agent was used to observe the distribution of the NP in the bacterial sample. For SERS experiments, 200 μL of colloidal NP suspensions (as prepared) were mixed with 25 μL of aggregating agent in a microcentrifuge tube and vigorously shaken in a mini vortex for 10 s. [55]

4.3.4 Surface charge modifications

The surface charge modifications of the silver NP were induced adjusting the pH values of colloidal suspensions with small amounts of HCl and NaOH. Several amounts of HCl and NaOH at concentration of 0.01 or 0.1 M were added until obtaining the desired pH (1 to 11). For SERS experiments, 200 μL of colloidal NP suspensions (pH modified) were mixed with 25 μL of aggregating agent in a microcentrifuge tube and vigorously shaken in a mini vortex for 10 s. The Raman spectra were collected following the same experimental procedure described for NR experiments.

4.4 Results and discussion

4.4.1 Characterization by UV-VIS and TEM

4.4.1.1 Hydroxylamine nanoparticles

Ag-NP reduced with hydroxylamine were obtained after a few seconds and had a grayish-brown color with an atomic Ag final concentration of $\sim 10^{-3}$ M. The freshly synthesized NP colloidal suspensions obtained by hydroxylamine reduction were acid with pH of 5.7 and an absorption maximum at 437 nm. Average particle diameter was 28 ± 10 nm.

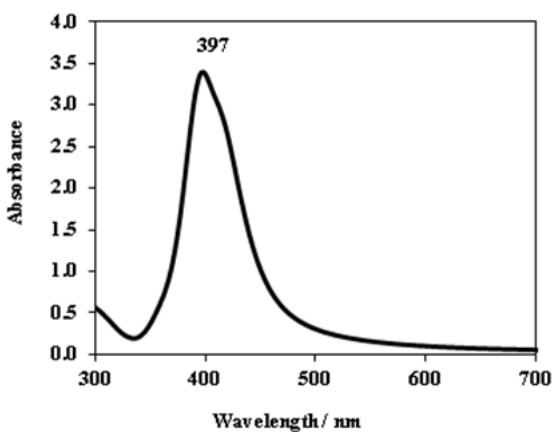
4.4.1.2 Citrate-capped borohydride reduced nanoparticles

Borohydride reduced-citrate capped Ag NP suspensions had a yellowish color when present in an atomic silver concentration of $\sim 10^{-4}$ M. The freshly prepared suspensions were slightly alkaline with a pH of 8.9 and an absorption maximum at 397 nm. The average diameter obtained from many TEM measurements was 19 ± 3 nm. The use of citrate as the capping agent

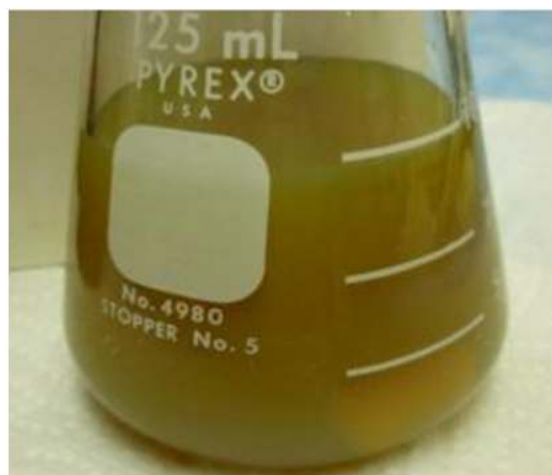
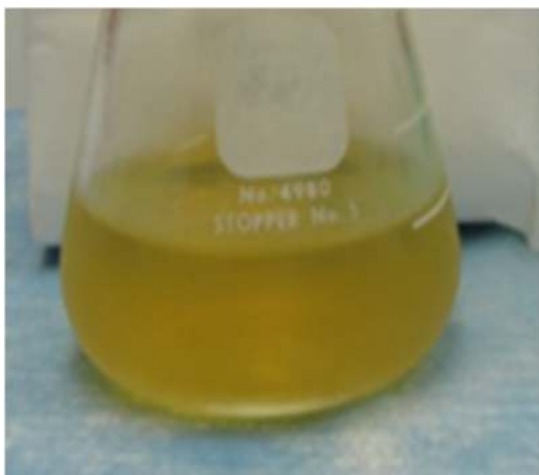
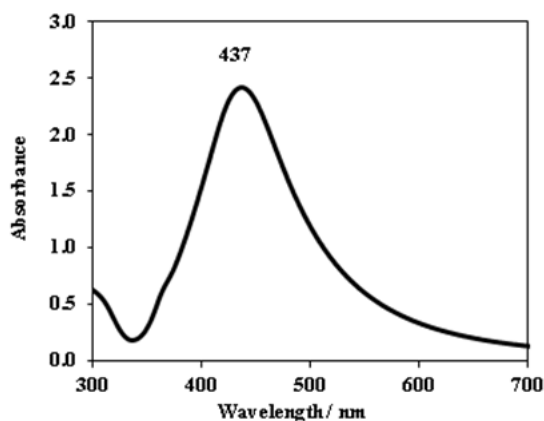
brings an advantage as a stabilizer agent covering with negative charges the nanoparticles surface; it makes NP more stable without being an additional variable in the experiment. In this synthesis the NP obtained are regularly monodisperse, the borohydride as the reducing agent allows that faster cores are formed at the same time.

Figures 15a and Figure 15b show the UV-Vis spectra of the prepared Ag-NP. The colors of freshly prepared sols and corresponding TEM images of the borohydride and hydroxylamine reduced NP are also shown.

a



b



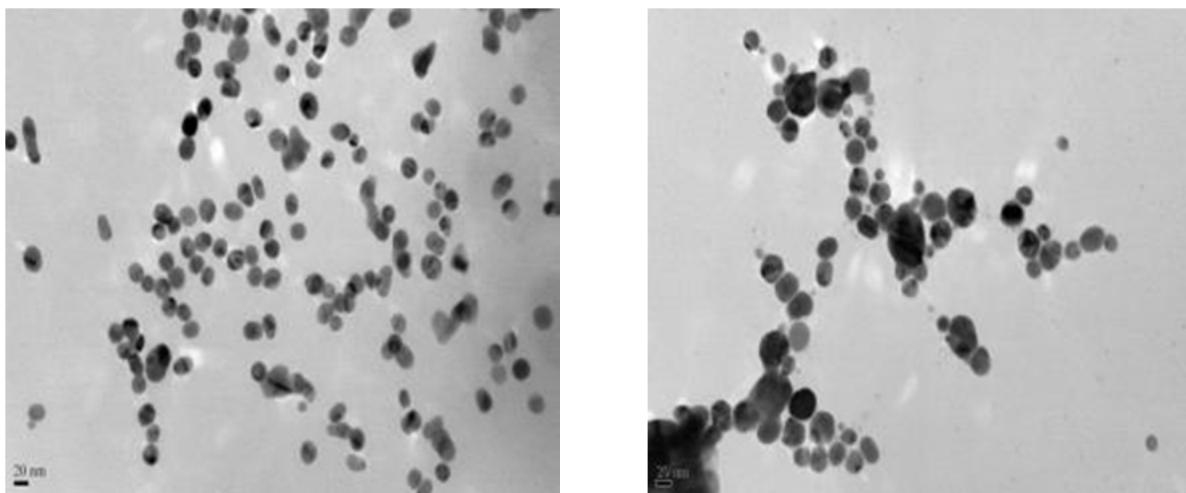


Figure 15. UV-Vis spectra (top), final yellowish color of freshly prepared sols (center) and TEM images (bottom) of: **(a)** borohydride reduced-citrate capped Ag NPs and **(b)** hydroxylamine reduced Ag-NPs used in the experiments described.

4.4.2 UV-VIS absorption at several pH values and Raman Spectroscopy experiments of NP

4.4.2.1 Hydroxylamine reduced NP

4.4.2.1.1 Surface charge modification and inducing agglomeration to NP

Just to have brief idea of the NP behavior when they are exposed to agglomeration and surface charge modifications, the hydroxylamine nanoparticles were analyzed at those two effects. The UV-Vis absorption spectra of the NP reduced by hydroxylamine hydrochloride at different pH values are depicted in Figure 16. It can be clearly observed the maximum in absorbance plasmon is in the range of 3 to 11.

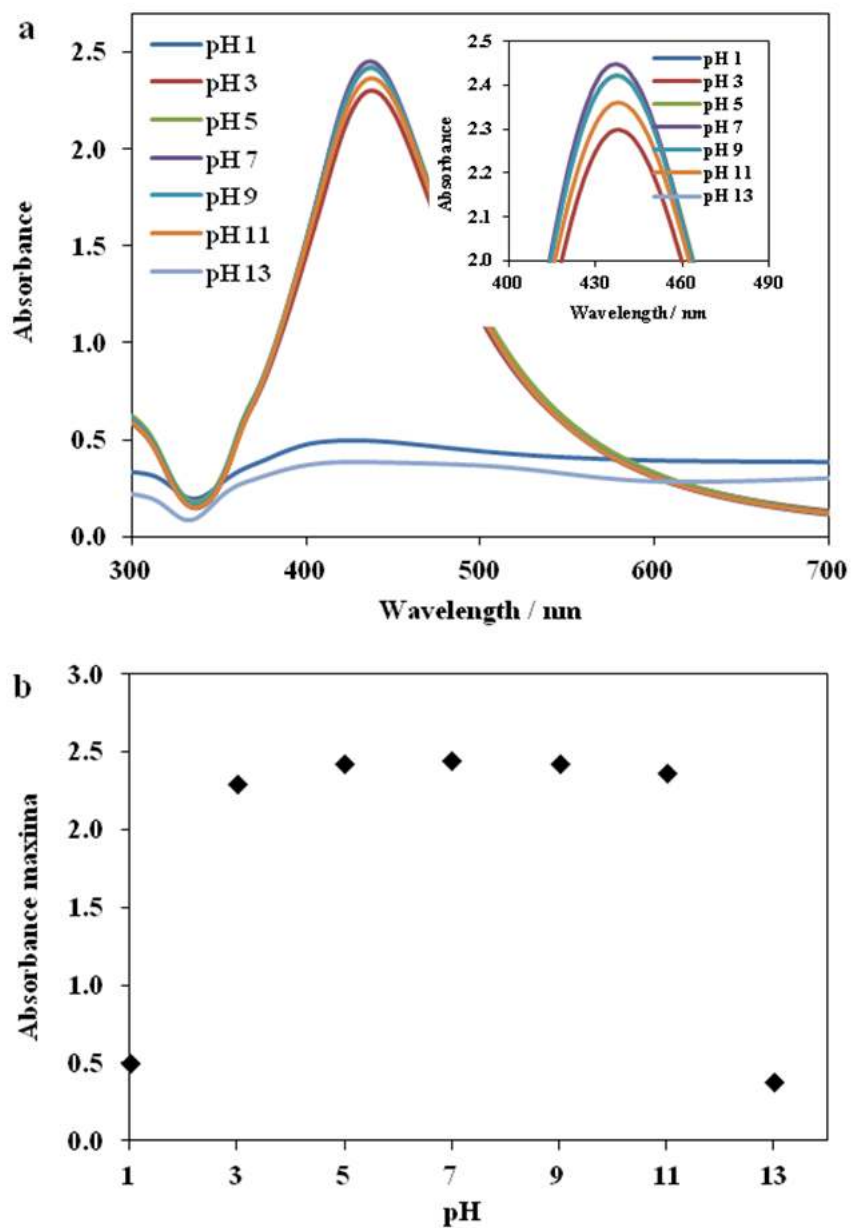


Figure 16. UV-Vis spectra of hydroxylamine NP at different pH's values. As can clearly seen the UV max absorbance of hydroxylamine NP at different pH is insignificant from the range 3 to 11.

The modifications to the surface charge of the NP were obtained by a reduction of the charge on the colloid by the addition of HCl or NaOH. The Raman spectrum of the hydroxylamine reduced NP at pH obtained as prepared from synthesis is free from anomalous

bands (Figure 17). However, high intensity anomalous bands were found when adding H^+ or OH^- for surface charge modifications to the NP. This is due by the pH-dependent ionizable functional groups that can undergo dissociation and protonation, depending on bulk solution pH values, for hydroxylamine-reduced silver colloids as it was previously explained by Yaffe *et al.* [56] and by Kazanzi *et al.* [25].

The agglomeration effect obtained by adding Cl^- ions was also studied for the hydroxylamine NP. The agglomeration induction effects of the colloidal NP can be increased by increasing the ionic strength by the addition of a salt. NaCl was used in these experiments. Several concentrations such as, 0.1, 0.3, 0.5 and 1.0 M were used to analyze the best agglomeration effect. High concentrations of the aggregation agent as 1.0 M resulted in a decrease of the plasmon band of the nanoparticles as shown in Figure 18. This evidences the oxidation of the NP, decreasing the SERS activity. Attempts of adding high concentrations of chloride ions as an aggregator agent failed. The Raman spectrum of the NP aggregated by chloride anions (Figure 19) is too rich in spectroscopic information above 1160 cm^{-1} to use it as background Raman spectrum for the microorganism studied.

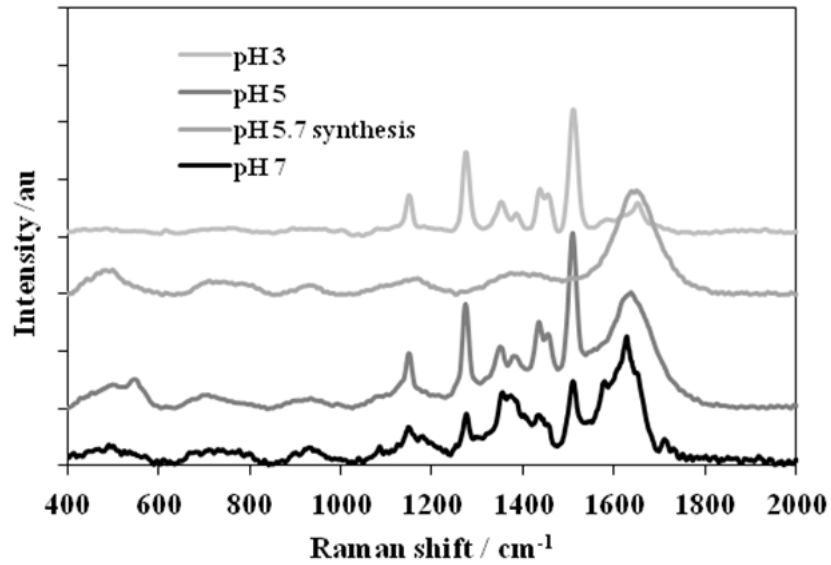


Figure 17. Raman spectra of the NP reduced by hydroxylamine at different pH values. The surface charge modification induced by change the pH of the sols contains anomalous bands that can interfere in the identification of bacterial composition.

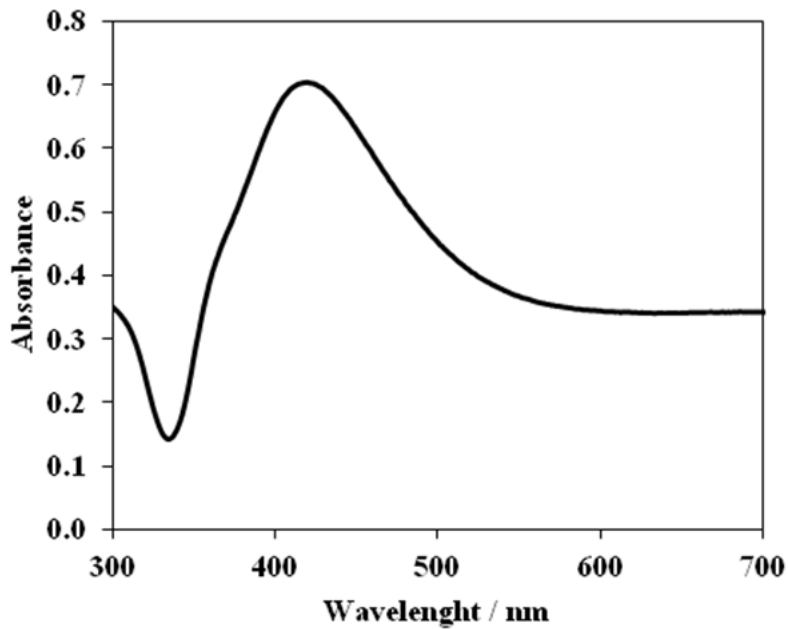


Figure 18. UV-Vis spectrum showing the decrease of the plasmon band when hydroxylamine reduced Ag-NP were aggregated with NaCl 1.0 M.

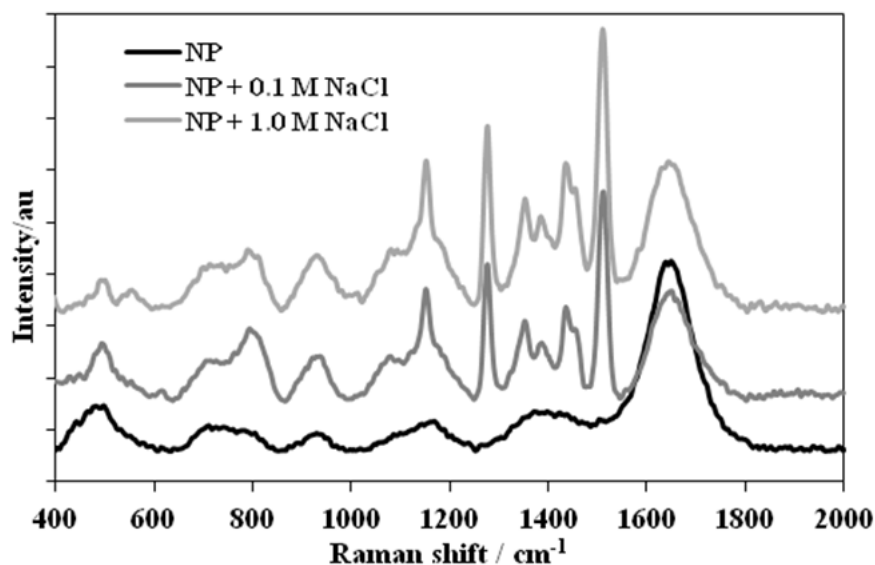


Figure 19. Raman spectra of hydroxylamine reduced NP and the NP aggregated with NaCl. The vibrational bands observed can mask the vibrational bands of the biosample.

The results indicate that the hydroxylamine NP required slight aggregation and no pH modifications in order to obtain high spectral quality results in bringing out SERS signatures.

4.4.2.2 Borohydride reduced NP

In order to have brief idea of the borohydride citrate-capped Ag-NP behavior, they were also exposed to agglomeration and surface charge modifications. Discussion of the most relevant results obtains follows.

4.4.2.2.1 Inducing nanoparticles aggregation

NP agglomeration effects of borohydride Ag-NP induced by NaCl was confirmed by the values of hydrodynamic radii (HR: nm) of the colloidal suspension. Table 3 summarizes the results obtained.

Table 3. Hydrodynamic radii (nm) values for NP aggregated at different concentrations of NaCl.

[NaCl]	HR NP / nm
0.1	14.51
0.3	15.00
0.5	122.1
1.0	191.0

Because the concentration used for aggregating the NP is a critical parameter, high concentrations of the aggregation agent (1.0 M) resulted in a decrease of the plasmon band of the NP as shown in Figure 20a and the appearance of a grayish color in the NP suspensions (Figure 20b), indicating possible oxidation of the NP. Attempts of adding high concentrations of chloride ions as aggregator agent failed.

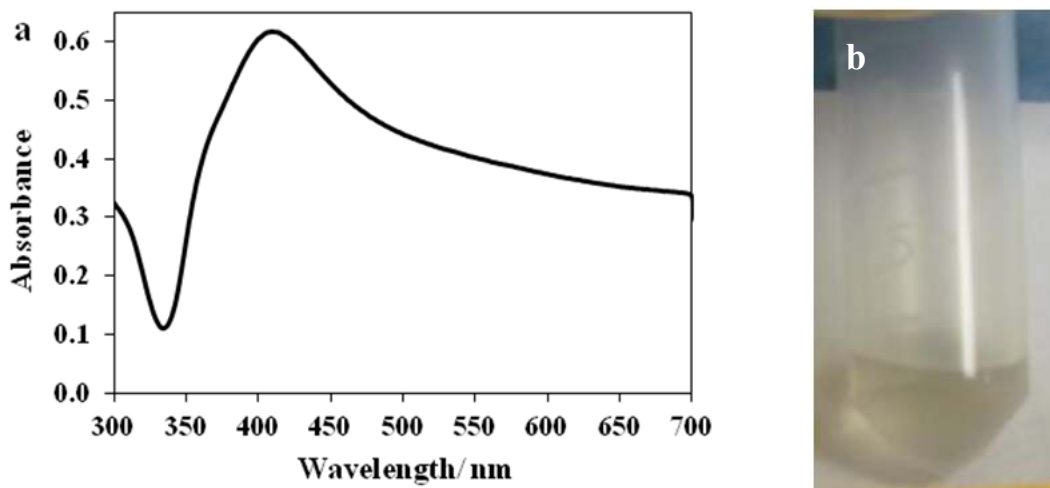


Figure 20. (a) UV-Vis spectrum showing the decrease of the plasmon band when borohydride reduced Ag-NP were aggregated with NaCl 1.0 M; (b) grayish color of NP suspensions evidencing oxidation of the borohydride reduced Ag NP.

However, no Raman anomalous bands are present in the Raman spectrum of agglomerated borohydride reduced Ag NP at 0.1 and 1.0 M of NaCl (Figure 21). This is the desired situation because there will not be any interference from background enhancement and only the vibrational Raman bands of the analyte (*Bt*) will be enhanced.

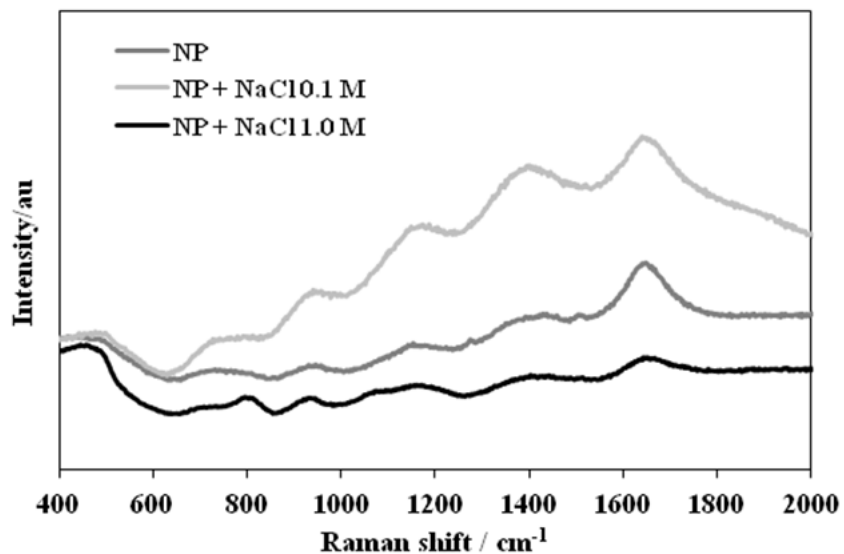


Figure 21. No anomalous bands can be observed in the Raman spectrum of agglomerated NP effect obtained with NaCl at concentrations of 0.1 and 1.0 M.

4.4.2.2.2 Surface charge modifications to the NP

UV-VIS absorption of NP reduced by borohydride at different pH is shown in Figure 22.

As can be clearly observed, the maximum in absorbance plasmon is in the range of 5 to 7.

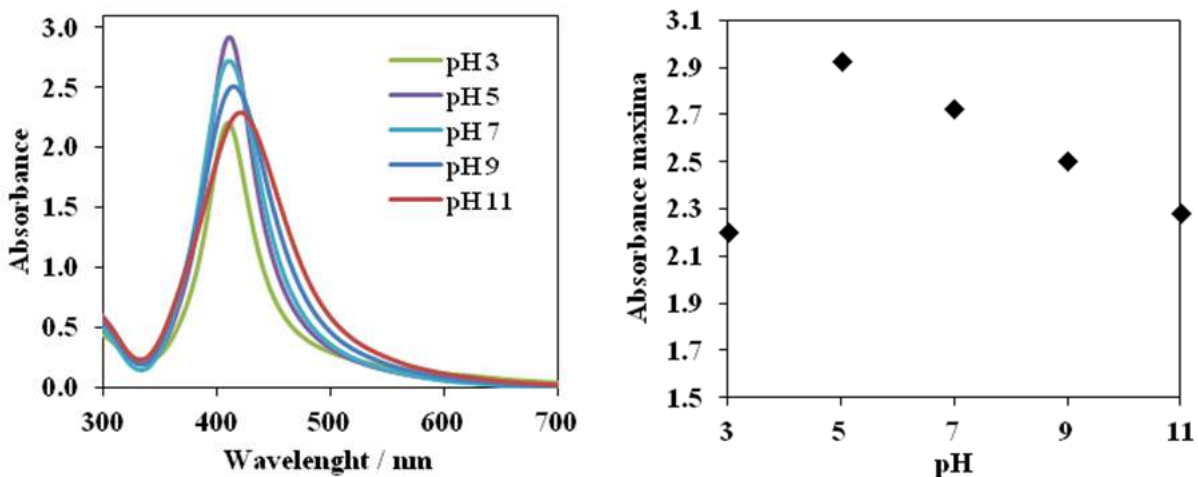


Figure 22. UV-Vis spectra of borohydride NP at different pH values. As can be clearly observed, the UV-Vis max absorbance of borohydride NP at different pH is significant in the 5 to 7 range.

No Raman anomalous bands were observed in the Raman spectra for the modified NP surface charge at 3 to 9 pH range (Figure 23). It is important to have a clean spectroscopic window fingerprint region: 400-2000 cm^{-1} in order to observe the biosample vibrational bands without interfering with the identification of bacterial composition.

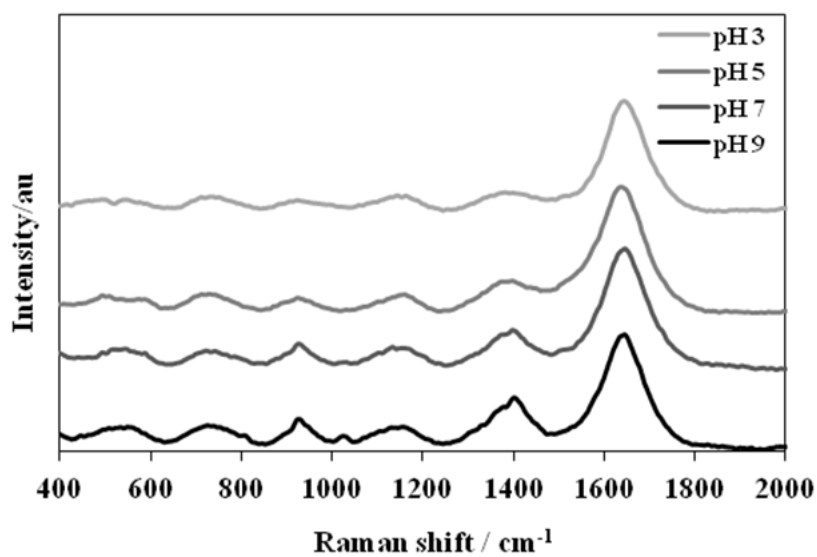


Figure 23. No anomalous bands were observed in the Raman spectra by the effect of modifications to the surface charge of NP in 3 to 9 pH range.

Table 4 present the values of hydrodynamic radii (nm) of the NP at different pH values. Small aggregation of NP in the pH range from 5 to 9 is observed, however at pH 3 it is slightly different indicating aggregation of NP that results in precipitation after approximately two hours [25].

Table 4. Hydrodynamic radii (nm) values of surface charge modified Ag NP by adjusting the pH

pH	HR NP/ nm
3.3	90.3
4.9	52.8
7.1	31.2
8.6	17.6
9.4	21.0

4.5 Summary and conclusions

Borohydride reduced-citrate capped silver NP were chosen as the rough metal surface to enhance the Raman scattering of the adsorbed biological components in SERS experiments. These borohydride NP were stable at different pH changes in the range 3 to 9 with small changes in their hydrodynamic radius. These NP do not interfere with the identification of bacterial composition by inducing agglomeration of the nanoparticles and modifications to the surface charge of the nanoparticles. This makes them ideal for the desired SERS applications. Therefore, borohydride-citrate capped Ag-NP were selected as the metal rough surface colloidal suspension to allow the SERS enhancement for the detection of *Bt* samples.

5. OPTIMIZATION PROCEDURES FOR DETECTION OF VEGETATIVE CELLS AND ENDOSPORES OF *Bt* BY SERS

This chapter contains all the results obtained from the SERS experiments of samples suspensions at 5 h and 24 h of bacterial growth. The optimization procedures were performed using borohydride reduced-citrate capped NP with a small aggregation using Cl^- ions in pH range 5 to 7. The optimization allows a strong interaction between bacterial components and NP to obtain good SERS detection results. This technique is based in the interaction of the metal NP surface with the outer coating content of the cells.

5.1 Sample preparation

Bacterial samples were transferred to glass capillary tubes (0.9 x 90 mm) using sterile, disposable needles and syringes to obtain the Raman spectra. For SERS experiments, 200 μL of colloidal NP suspensions (as prepared) were mixed with 25 μL of bacterial suspension in a microcentrifuge tube and vigorously shaken in a mini vortex. Small amounts of mixtures were transferred to the capillary tubes and SERS spectra were obtained. To further increase Raman signals by stimulation of formation of hot spots on aggregation of NP, clustering was promoted [23] by the addition of 0.1, 0.3, 0.5 and 1.0 M NaCl to colloidal suspensions. To adjust the pH of the colloidal suspensions, small amounts of HCl and NaOH at concentrations of 0.01 or 0.1 M were added until obtaining the desired pH (1 to 11). Then, the mixtures were prepared for SERS experiments using the same parameters and procedure as described above and as illustrate Figure 24.

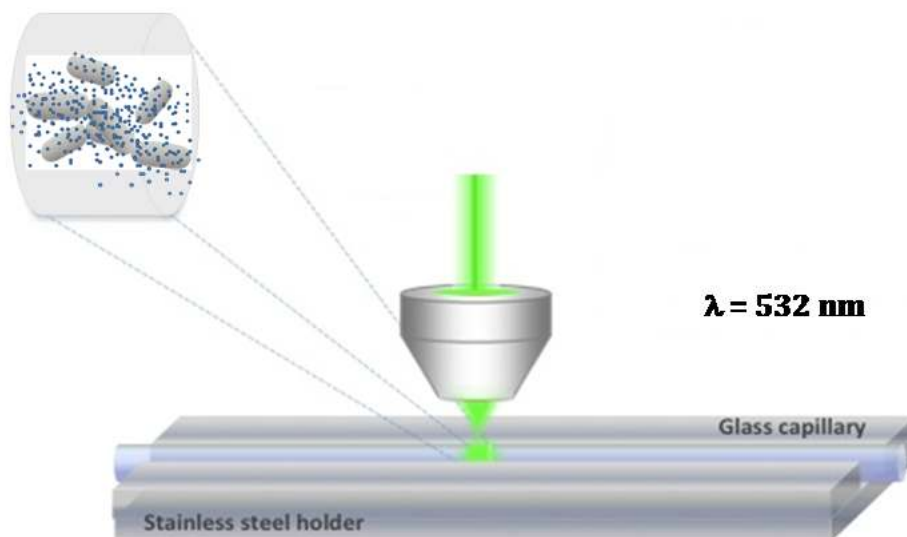


Figure 24. Experimental set up for bacterial identification by SERS using a laser excitation line of 532 nm with a 10x objective of radius spot of 25 μm and a glass capillary tube of 0.9 mm of inner diameter.

5.2 Results and discussion

5.2.1 Surface Enhanced Raman Spectroscopy (SERS) of *Bt*

Silver NP have a plasmon resonance band in the visible (VIS) region (400-700 nm) of the electromagnetic spectrum with excellent match with laser lines located at 514.5 and 488 nm and solid-state diode laser at 532 nm [55]. However, using excitation lines located at 633 and 785 nm will be far away from the transverse plasmon band of the silver nanoparticles prepared for this research. This fact will have a small contribution to the electromagnetic SERS effect. Therefore, the use of NIR laser sources was not necessary for their poor contribution in the electromagnetic effect. In order to have contributions of both electromagnetic and chemical effect a 532 nm laser and changes to the NP surfaces charges were performed. The biological samples show a high fluorescence that should be quenched before obtaining the SERS spectra to obtain good SERS

results. As mentioned in previous literature, the fluorescence of bacteria is “especially strong with 532-nm excitation, but some photobleaching is required even for near-infrared (NIR) excitation” [26]. In this study, 10 to 50 s of exposure time were used to minimize the fluorescence problems of the biological samples. SERS has been used as a more successful technique in the detection of this biosample compared with RS. This technique is based in the interaction of the metal NP surface with the outer coating content of the cells [40,57]. The affinity of the *Bt* biomolecular content to the Ag-NP was improved resulting in enhancement of the signal to noise ratio of the SERS spectra obtained with a significant decrease in fluorescence observed in the Raman spectra of this bacillus sample. The volume and concentration of the NP colloidal suspensions, the sample amount and concentration of the biological system under study, aggregation induction effects of the colloidal NP, and modifications of the charge of the layer of NP were the parameters that had to be optimized to obtain reproducible SERS signals. The SERS results of the optimal control of those parameters for 5 h and 24 h of *Bt* samples dealing with Ag-NP reduced by borohydride-citrate capped are discussed in details in the next sections.

5.2.2 Parameters to be optimized in the SERS experiments

Volume ratio of bacterial solutions to NP suspensions, activation of “hot spots”, aggregation effects and surface charge modifications of NP are the most important optimizing parameters to promote a better interaction of NP to bacterial cell wall or biological molecule to obtain a good SERS detection, characterization and identification. Effects of pH on nanoparticles or biological samples [4,7,11-13], aggregation induction effects of nanoparticles to biosamples [10] and volume ratio bacteria: NP [4,11,12] are some significant previous studies focused on detection and differentiation by statistical analysis of different bacteria strains and biological

molecules. Despite all reported studies, there are not complete studies until now with a simple detailed optimized procedure to differentiate between the vegetative cells or endospores of the same bacillus bacteria such as *Bt*. This has already been accomplished using IR spectroscopy. The results showed minimal differences between the vegetative cells and endospores spectra [14]. Spores and vegetative cells of *Bacillus globiggi* were discriminated by PCA with minimal spectral differences. However, the SERS results show fluorescence that suppress the chemical information obtained and the reliability of the sample identification [49]. Studies on improving the SERS detection of *Bacillus thuringiensis* using Ag NP reduced by hydroxylamine and borohydride capped with sodium citrate for a 15 h of bacterial growth sample was reported by our group in response to achieve a highly spectral quality SERS results [58]. The best optimization results were obtained when a slight aggregation of the NP as well as surface charge modification to a more acidic ambient was induced using small-size borohydride-reduced NP in the form of metallic suspensions aimed at increasing the Ag NP-Bt interactions [6]. Particularly, this study is focused on the use of two samples of the same bacterial strain, vegetative cells and endospores, to optimize the parameters of volume ratio of nanoparticles to bacteria, aggregation and surface charge modifications of NP until obtain good SERS results.

5.2.2.1 Volume ratio experiments

The volume ratio (VR) experiments include the concentration and amount of the NP colloidal suspensions to bacterial sample solution. The main objective in the optimization of this parameter is to increase the signal-to-noise ratio (S/N) of the SERS spectra and reduce the fluorescence from the analyte. Very weak Raman signals or strong background scattering is obtained when low and high concentrations of the biosample in the mixture are used [49].

Figure 25 shows the different cases that would happen, for instance, if a high concentration of NP suspension solution is being compared to the amount of bacteria (Figure 25a), a poor SERS effect is produced. If a low concentration of NP with respect to the amount of bacteria (Figure 25b) a poor SERS effect is also produced. In order to have a good SERS signal one must have a good proportion between NP concentration and the amount of bacteria (Figure 25c). In this study, the optimal volume or bacterial dilution with NaCl 0.1 M of a bacterial pellet obtained after centrifugation and washing procedure of 4 and 2 mL of 5 h and 24 h, respectively, of bacterial growth sample was determined. This was obtained varying the concentration of bacteria as evidenced through OD₆₀₀ measurements. For these SERS experiments, 200 μL of colloidal NP suspensions (as prepared) were mixed with 25 μL of bacterial suspension in a microcentrifuge tube and vigorously shaken in a mini vortex. The intensity of the peak at 730 cm⁻¹ (tentatively assigned as the glycosidic ring of NAG and NAM) was monitored in the SERS spectra to obtain the maximum peak and the best SERS signal detection (Figure 26). This intense sharp band was selected because represent bacterial content commonly found in the cell wall of Gram-positive bacteria. Results obtained from the optimization on the bacterial suspension dilution indicates that the bacterial sample obtained at 24 h of bacterial growth should be used in an OD₆₀₀ of 1; it corresponds to an amount of 2x10⁵ bacterial cells per μL. This measurement indicates the bacterial density in the sample. The 5 h bacterial sample was also diluted until reaching an OD₆₀₀ of 1 and the results were successfully obtained. Then, 25 μL of this bacterial sample was used in the SERS mixture, with 200 μL of NP at 10⁻⁴ M of Ag, corresponding to about 2x10⁴ bacterial cells/μL. The amount of bacteria illuminated under the laser spot for SERS experiments were in the range of approximately 30-40 bacteria.

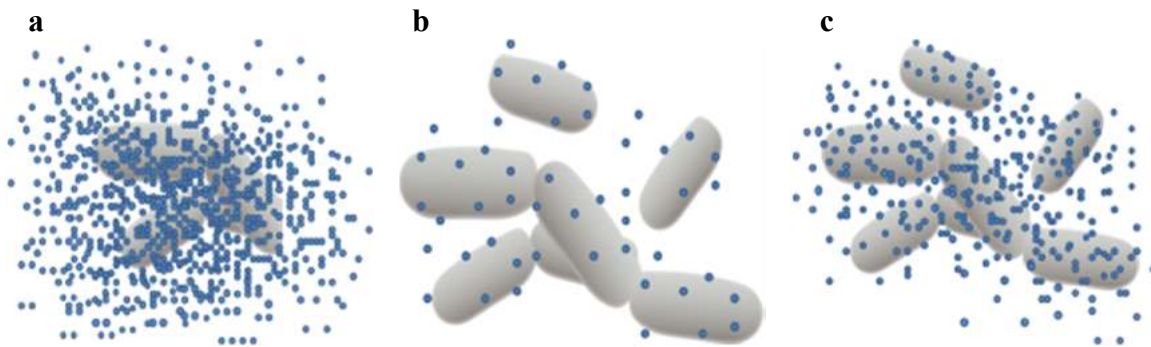
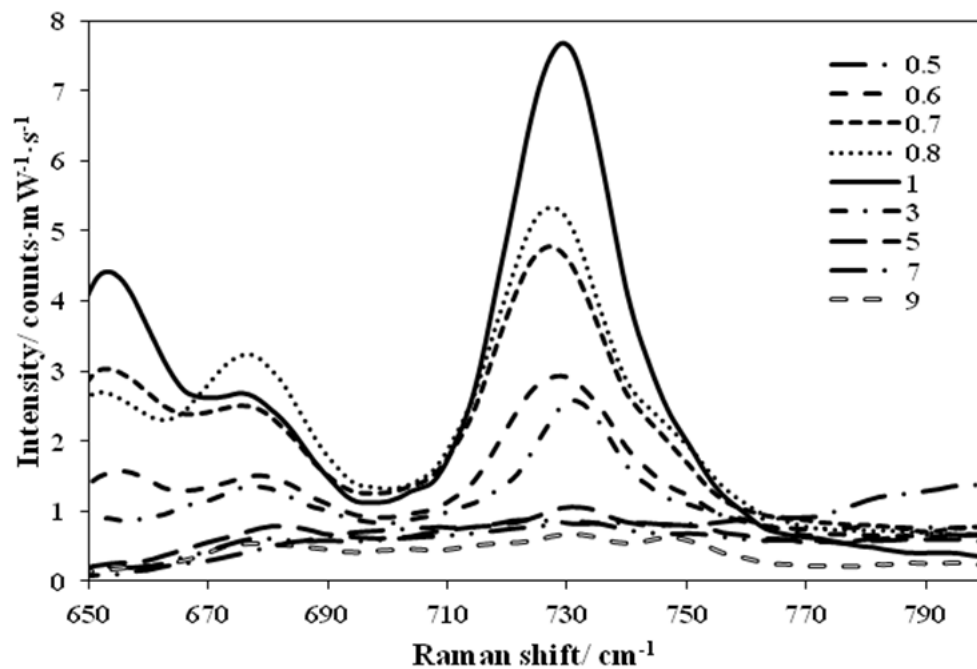


Figure 25. Principal cases can be involved in the volume ratio of colloidal NP suspension to bacterial sample in SERS. To obtain a maximum signal-to-noise ratio is important to optimize the colloid volume and the bacterial sample concentration. From these cases can be observed **(a, b)** high concentration of NP and bacteria, respectively and **(c)** good proportion of NP and bacteria.

a



b

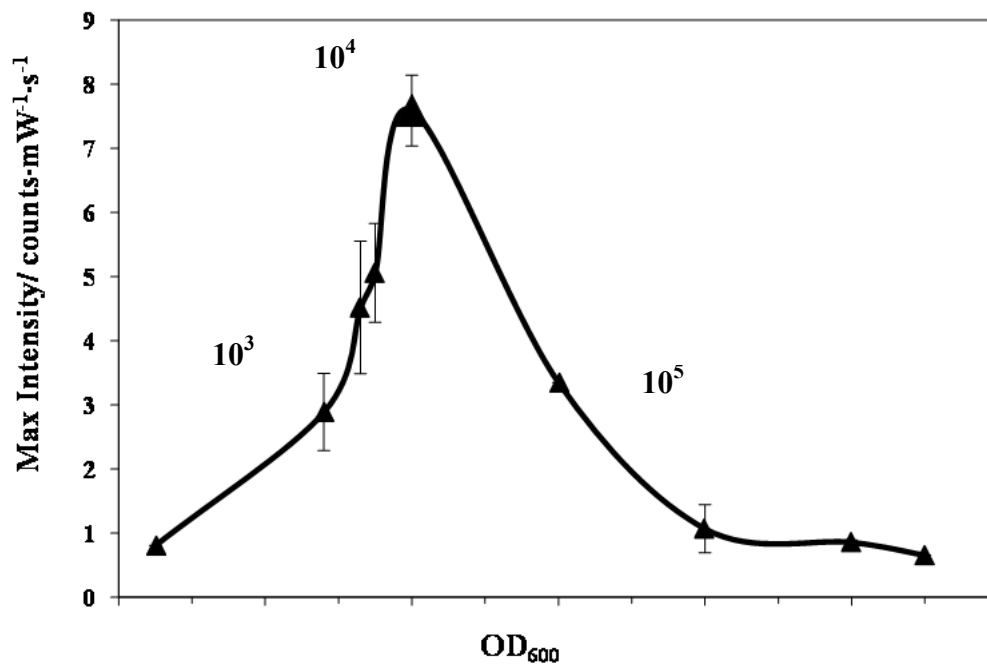


Figure 26. (a) SERS spectra range of Bt sample at 24 h of bacterial growth at different bacterial concentrations suspended in NaCl 0.1 M. **(b)** The results obtained were used for the optimization until achieve a maximum intensity in the 730 cm⁻¹ peak indicating an increasing in the scattered radiation collected and decreasing contributions from interferences at 10⁴ bacterial cells. Higher (10⁵ bacterial cells) or lower concentrations (10³ bacterial cells) resulted in a decrease of the SERS signal intensity.

5.2.2.2 Inducing agglomeration of NP

The effective binding to Raman active sites (“hot spots”) involved in the signal enhancement depends on the time required to obtain the effective binding of the analyte and metallic NP, and the type and strength of the adsorbate-substrate bond [49]. This binding dynamics of the colloidal suspension to the bacterial sample can be promoted by the addition of a salt thus increasing the ionic strength [31]. The distribution of NP on the cell wall depends on the concentration of the aggregation agent. The aggregation of the colloidal particles affects the size distribution of the colloidal particles and consequently, a decrease in the surface area, and the local field enhancement (Figure 27).

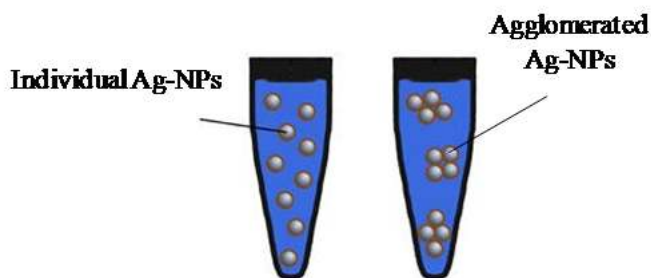


Figure 27. Effect observed when the agglomeration of nanoparticles is induced by the addition of a salt increasing in ionic strength.

A low concentration of the aggregation agent activates the “hot spots” on the NP surface increasing the SERS detection. Very high concentrations cause a high agglomeration of the Ag NP promoting a limited and non-uniform binding to the bacterial cell wall causing a decrease of the close contact of the small NP to the analyte and as a result a decrease of the SERS signal as shown in the spectra (Figure 29a and Figure 29b). To achieve the best agglomeration effect, 25 μL of various concentrations of NaCl, such as 0.1, 0.3, 0.5 and 1.0 M, were added to the mixture of bacterial suspension and colloidal NP. Aggregation was confirmed by the values of

hydrodynamic radii (Table 4) of the colloidal suspension and with the changes in colors of the mixtures (Figure 28). For bacterial samples of growth at 24 h, in which bacterial content is mainly due to the presence of endospores, the aggregating agent at a concentration of 0.1 M allows for a slight aggregation of the NP promoting a small increase in affinity of the bacterial sample and producing the activation of “hot spots” on the NP surface. At 0.3 M NaCl the NP are slightly aggregated, as the HR measurements shows and the color of the mixture becomes darker. From the TEM images (Figure 30), the slight aggregation effect can be observed on the bacterial sample, and the results in SERS signals (Figure 29) compare with different concentrations of the aggregating agent. Higher concentrations of NaCl, such as 0.5 and 1.0 M, resulted in a very high nanoparticles aggregation as obtained from the HR measurements; the gray color mixture is evidencing the oxidation of the NP by a decrease of the plasmon band (Figure 20) of the nanoparticles [50]. From the TEM images can be observed the highly aggregation effect to the bacterial sample and the results in SERS signal of bacterial growth is highly decreased compared with lower concentrations of the aggregating agent. The 730 cm^{-1} peak intensity graph for 5 and 24 h of bacterial growth sample shows a higher intensity in the spectra obtained when the aggregation effect is promoted by the NaCl at 0.1 M (Figure 29c). This result indicates that the activation of hot spots effect obtained by this NaCl concentration, in which the bacterial sample is resuspended, is enough to obtain good SERS results. For bacterial samples at 5 h, the bacterial content is mainly composed of vegetative cells; no significant difference was found for NaCl influences by the aggregation effect of nanoparticles at different concentrations of the aggregating salt. The color of biological sample and nanoparticles mixtures at different concentrations of NaCl did not show significant differences in color while the aggregation was promoted. In the TEM images for this sample, it can be observed the minimal differences in

affinity of nanoparticles to bacterial cell wall when the concentration of the aggregating agent is increasing to promote agglomeration of nanoparticles. The HR measurements and the SERS spectra of the bacterial sample and nanoparticles mixture at different concentrations of the aggregating salt are in agreement with the results observed with the 730 cm^{-1} peak intensity graph.

In conclusion, as our previous study already reported for a different hour-growth sample published [50], the SERS results also shows that the lower concentration of NaCl in which *Bt* was already suspended (0.1 M) can have an influence on the activation of “hot spots” on NP, inducing a closer, more effective interaction with biological samples and consequently increasing SERS signals for a bacterial sample with vegetative cells or endospores mainly. For convenience in the experiments procedures, both bacterial samples were resuspended in NaCl 0.1 M to promote the activation of “hot spots” in the nanoparticles observed when those are mixed and, at same time it is used as a solvent to preserve the bacterial sample refrigerated until the experiments were performed. This salt inhibits bacterial growth at a concentration that preserves the bacteria alive.

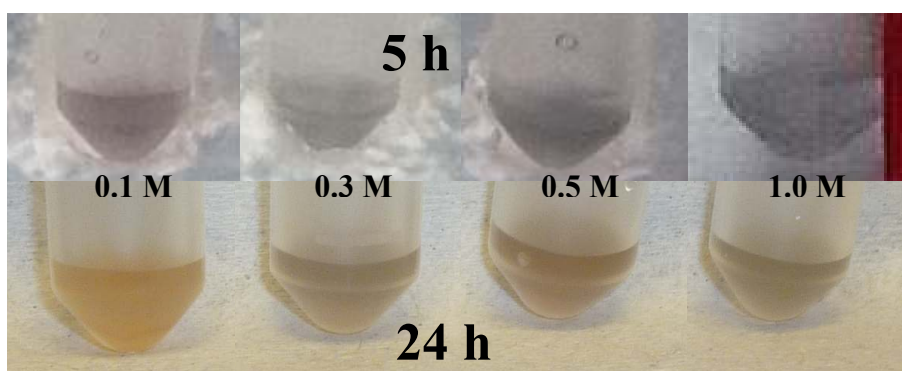
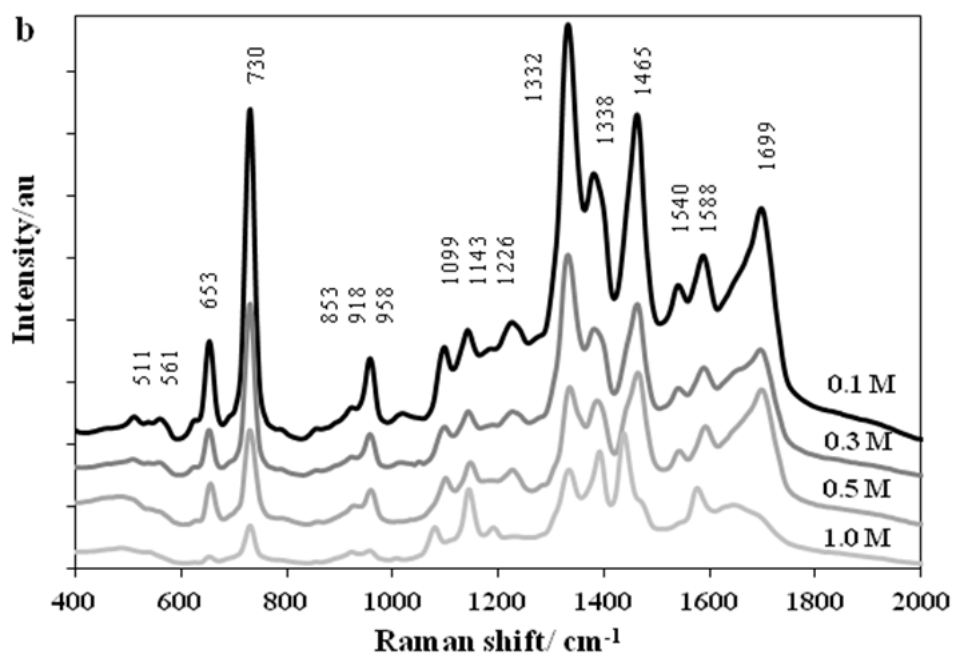
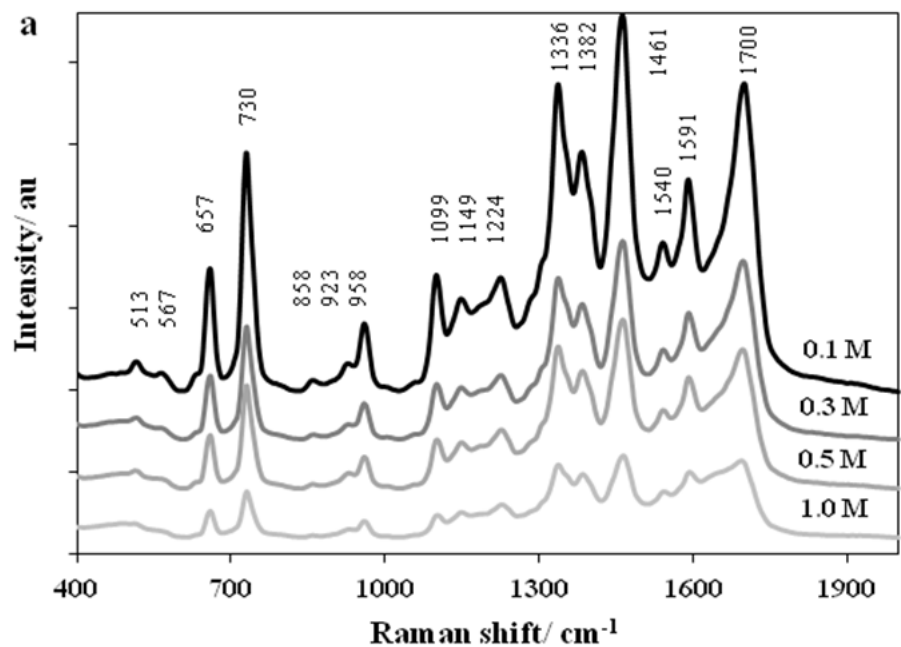


Figure 28. Changes in colors observed due to aggregation induced by adding different concentrations of NaCl to the mixtures of colloidal suspension and bacterial solution for 5 and 24 h of bacterial growth (above for 5 h and below for 24 h of bacterial growth).



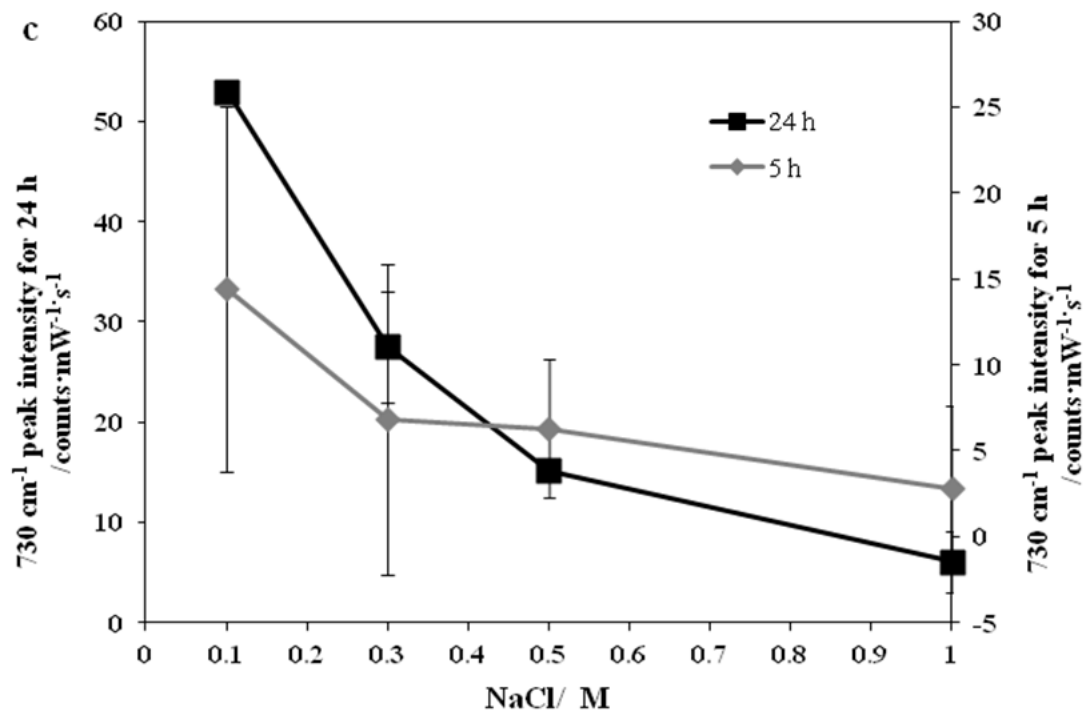
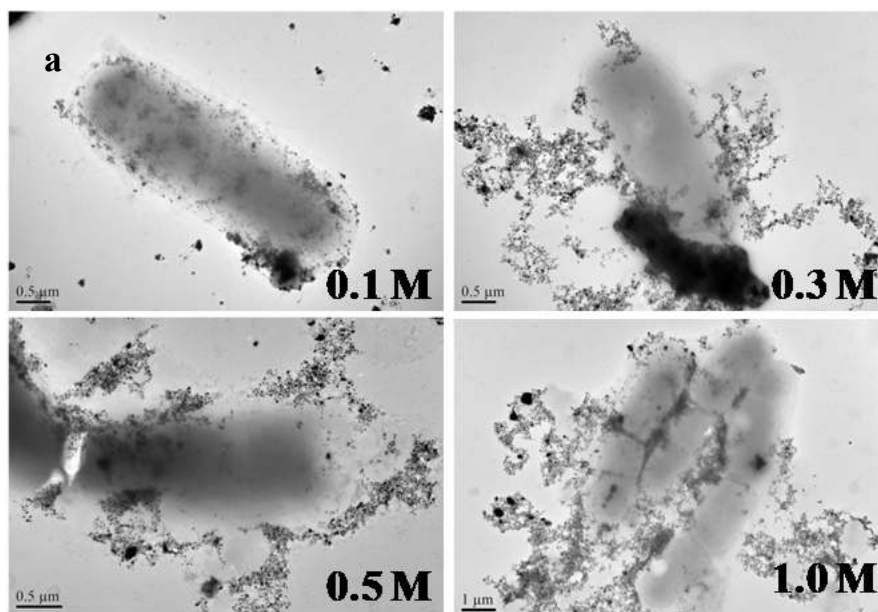


Figure 29. SERS results for the aggregation effect using different concentration of NaCl in mixtures of colloidal suspension and bacterial solution for (a) 5 (right axis) and (b) 24 h of bacterial growth (left axis); (c) aggregation promoted to nanoparticles using low concentration of this aggregation agent resulted in good SERS signals as shows the 730 cm^{-1} peak intensity graph for the spectra of 5 and 24 h of bacterial growth.



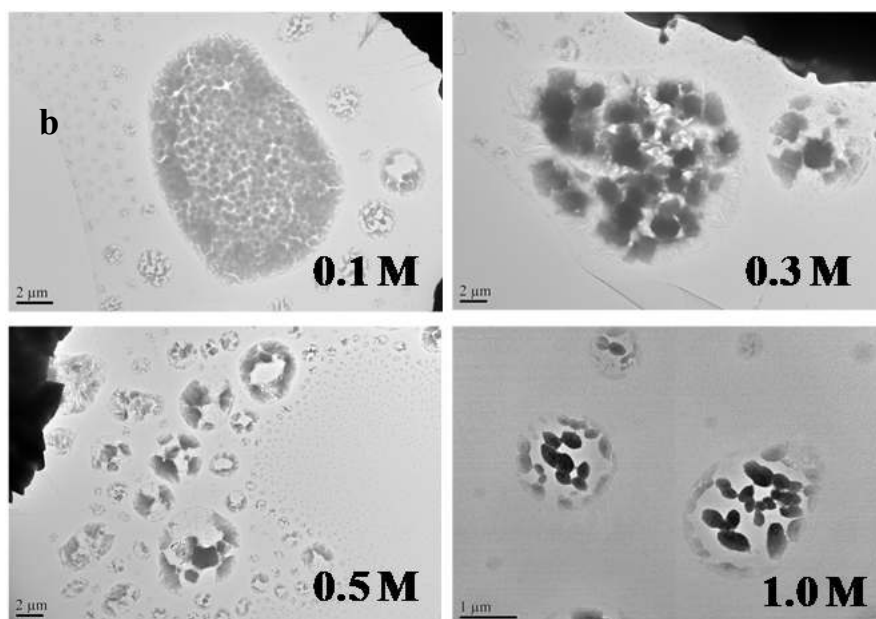


Figure 30. TEM images of the mixtures colloidal suspension and bacterial solution using different concentrations of the aggregating agent for **(a)** 5 and **(b)** 24 h. As can be clearly observed, lower concentrations of the aggregating agent resulted in an increasing of the affinity nanoparticles to bacterial cell wall. Higher concentrations resulted in a high agglomeration of the NP and a decrease in the close contact of the small NP to the analyte.

All these results indicate that the agglomeration induced with the use of NaCl 0.1 M is enough to obtain an optimal activation of “hot spots” of Ag NP promoting a better interaction with the bacterial cell wall and to obtain a best SERS results. As explained before, the aggregation effect promoted by adding different salt concentrations in the vegetative cells sample results cannot show significant aggregation influence. However, the results of endospores samples showed that a higher concentration of NaCl aggregates too much the NP limiting the contact bacteria required to obtain the desired SERS effect.

5.2.2.3 Surface charge modification of the nanoparticles

To optimize the adsorption of *Bt* on the SERS active substrate, the surface chemistry of Ag-NP can be altered by adjusting the pH of the sols and thus promoting the affinity of the

nanoparticles to the bacterial cell wall [18,33,16,25]. Biochemical content in the bacterial cell wall is dominated by negatively charged compounds. From those the interaction with nanoparticles are mostly through thiol (-SH), amino (-NH₃⁺) and carboxyl (-COO⁻) groups. Thus, strong electrostatic interactions dominate binding of NP with the bacterial cell wall content [38].

These surface charge modifications can be obtained by a reduction of the charge on the colloid by the addition of a neutral adsorbate, such as HCl and NaOH, until desired pH values are obtained at approximately 3, 5, 7 and 9. The z-potential measurements indicates that more acidic pH values with respect of the initial value of pH = 9 allows that the slight negatively charged induced by the citrate capping agent becomes less negative with the H⁺ ions added [59]. While the pH varies, the effect observed is based on the formation of a double-charge layer; these changes to the charge layer have influences in the behavior of the particles in the solution [16,58] (Figure 31).

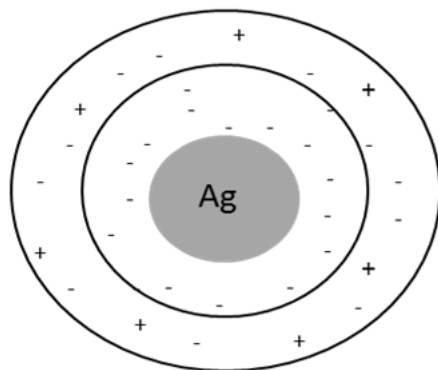


Figure 31. Effect observed on the formation of a double-charge layer to the slight negatively charged induced by the citrate capping agent, it becomes slightly more positive with the H⁺ ions added.

The explanation of this effect was already published [58], briefly colloidal suspension at very low and high pH values are very unstable. It becomes in precipitation by charge neutralization and by oxidation, respectively. Both resulted in a decrease of the plasmon band of

the nanoparticles and in the SERS signal [39]. To achieve the best surface charge modification effect, the pH of the sols was modified adding small amounts of HCl and NaOH to obtain different pH values. 200 μL of this colloidal suspension at each pH was added to the mixture with 25 μL of bacterial suspension. Small aggregation was confirmed by the values of hydrodynamic radii at more acidic pH values than the initial pH value (HR: nm) (Table 5) of the colloidal suspension and with the changes in colors of the mixtures for samples at 5 and 24 h of bacterial growth (Figure 33a and Figure 33b). Using pH value at 3, the nanoparticles are slightly aggregated but are precipitated as shown in a gray color of the mixture resulting in a poor affinity of the NP to the bacterial cell wall as shows the TEM images (Figure 35). The SERS signals obtained at pH 3 for the bacterial sample at 5 and 24 h of bacterial growth is lower than the others at higher pH values (Figure 34a and Figure 34b). At pH values of 5 to 7 the nanoparticles are also very slightly aggregated as the HR measurements show; the color of the mixture becomes in a particular color due to a promotion in the interaction of NP-bacterial cell wall as it can be observed from the TEM images. These pH range, 5 to 7, increase the affinity of NP to the bacterial sample resulting in a better SERS signals as shows the SERS results in Figure 34a and Figure 34b. The initial pH value of the colloidal suspension promotes a good interaction to the bacterial cell wall content but not sufficient to have a better influence to obtain an enhance SERS results. The negative charges obtained from the citrate capping agent in the colloidal suspension restrict the strength interaction between the NP and the bacterial cell wall. Therefore, it is important the change in surface charge of the NP to a less negative one. This can be explained by z-potential measurements: as pH decrease the surface charge of the NP becomes in a less negative one in which the interaction NP-bacterial cell wall is favored and consequently it results in an increasing of the SERS signal (Figure 32).

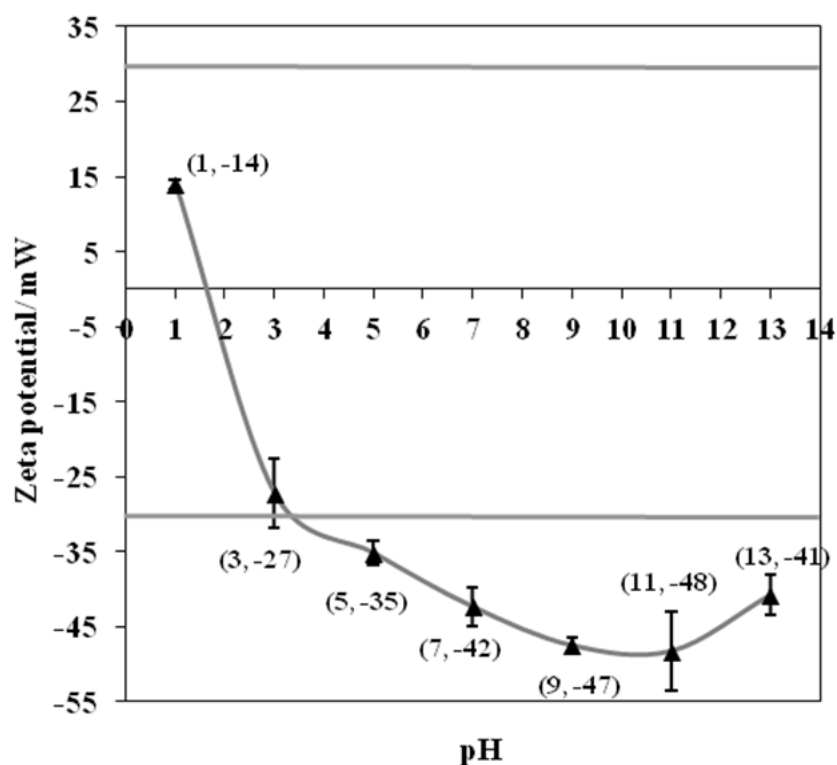


Figure 32: Zeta potential measurements of silver nanoparticles as a function of pH [59].

All of these results indicated that a less negative surface charge modification is helpful to induce an optimal interaction with the bacterial cell wall and to obtain a best SERS results. The results indicate that the range of pH in which a better interaction of the *Bt* bacterial components is promoted is 5 to 7. This is showed on the SERS results for the 730 cm^{-1} peak intensity graph for the spectra of 5 and 24 h of bacterial growth (Figure 34c). The pH of the nanoparticles from synthesis (above 7) also presents good results of bacterial components to nanoparticles interaction, but a less negative charge induce (-35 to -42 mV for pH 5 and 7, respectively) to the nanoparticles by pH changes promotes a better interaction resulting in good SERS results.

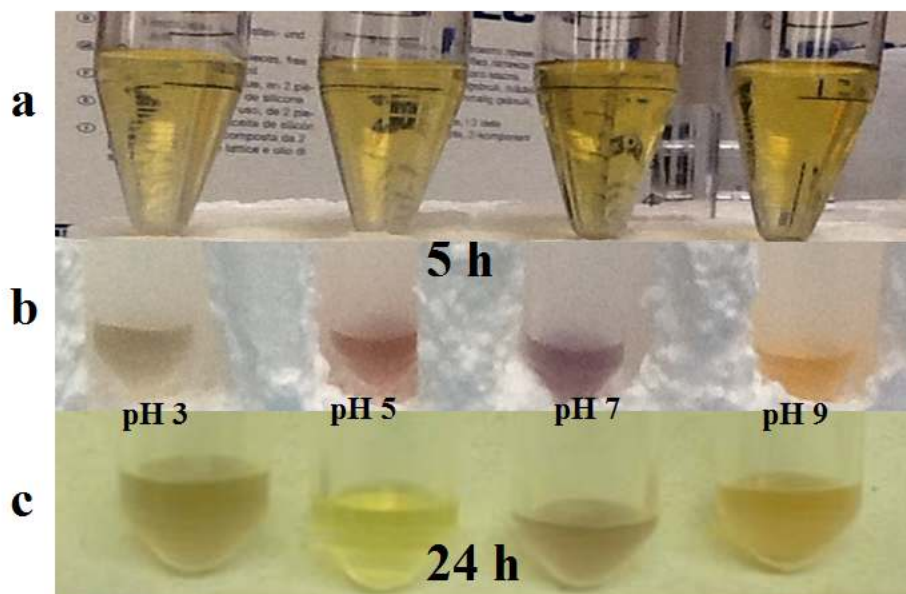
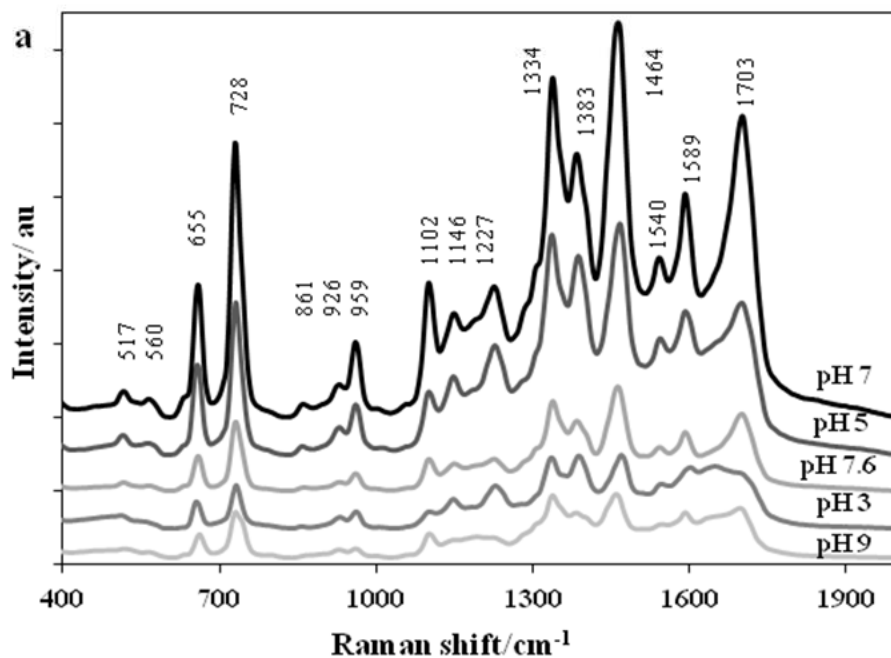


Figure 33. (a) Changes in colors observed due to surface charge modification induced by adjusting the pH of the sols. The colloidal suspension mixtures at different pH values (3, 5, 7 and 9) with the bacterial solution for (b) 5 and (c) 24 h of bacterial growth.



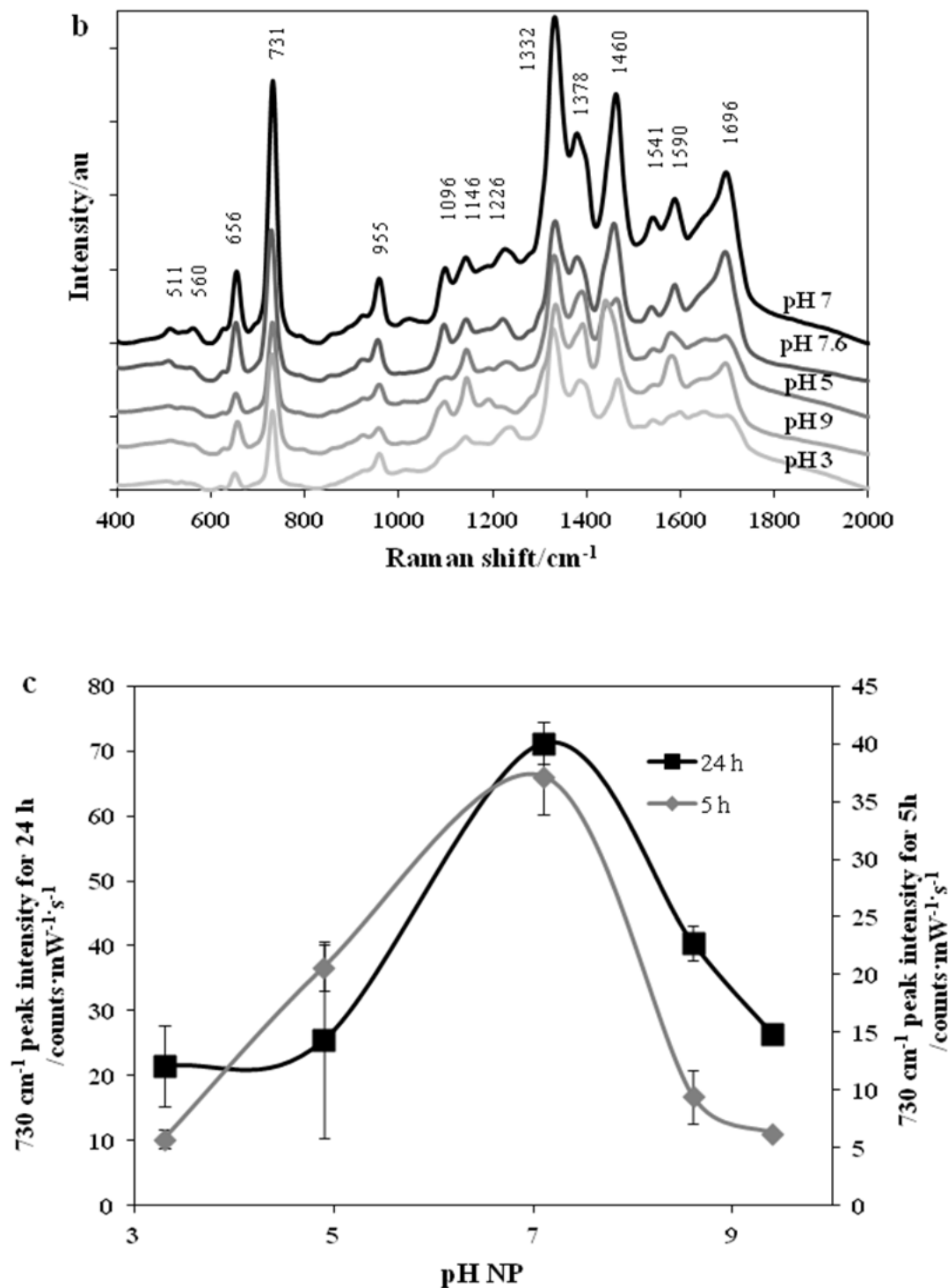


Figure 34. SERS results for the surface charge modification to the NP in mixtures of colloidal suspension and bacterial solution for (a) 5 (right axis) and (b) 24 (left axis) h of bacterial growth. (c) The interaction of the NP to bacterial cell wall promoted by modifications to the surface charge of the NP resulted better in a range to 5 to 7 in which the charge of the NP is turned to a slightly positive one in good agreement to a best interaction, it is showed on the SERS results for the 730 cm^{-1} peak intensity graph for the spectra of 5 and 24 h of bacterial growth.

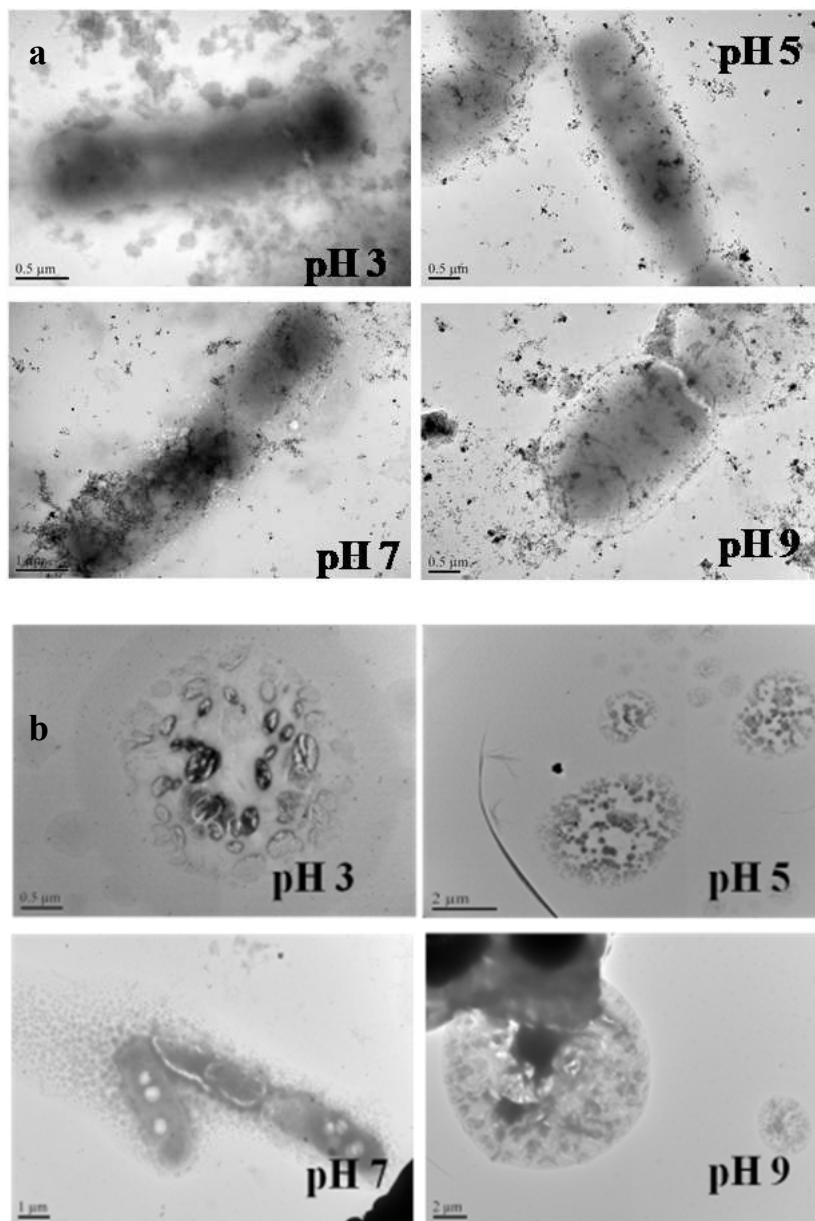


Figure 35. TEM images of the mixtures colloidal suspension and bacterial solution with modifications to the surface charge of the NP for **(a)** 5 and **(b)** 24 h of bacterial growth sample. As can be clearly observed, pH in range 5 to 7 resulted in an increasing the affinity of nanoparticles to bacterial cell wall. Lower pH value (~3) resulted in a high oxidation and precipitation of the nanoparticles and a decrease in the close contact of the small NP to the analyte.

5.2.3 Bacterial cells analyzed by SERS

It is an important fact to know an approximate quantity of the bacterial cells analyzed in this study for applications focused on detection of microorganisms. The SERS active substrates of Ag-NP citrate capped-reduced by borohydride when were used for *Bt* bacteria detection could detect cells in a range of as few as 30 to 40 bacterial cells in bacterial samples of vegetative cells and endospores. Table 5 shows the bacterial cells quantity: in the range mixed with NP in a volume ratio bacteria: NP of 0.125, under the laser spot of a 10x objective using a capillary tube of 0.9 mm of internal diameter for the SERS analysis. The cells in 500 μ L of bacterial solution obtained from the optimization parameter and bacterial bulk solution for NR experiment. These results were calculated from the initial bacterial concentration of 10^8 cfu/mL and the bacterial dilutions required obtaining good SERS spectra following the optimization procedure established to detect and identify bacterial samples of *Bt*.

Surface enhancement factor (SEF) of 10^3 and 10^4 were obtained from the intensity of vibrational signatures for 24 and 5 h of bacterial growth sample, respectively under well controlled conditions. These results were obtained using Raman analysis of the bacterial samples for a bulk solution and a SERS analysis with an optimized solution with NP. The magnitude of this factor indicates that the enhancement in the Raman scattering, due to the presence of suspended metallic colloidal nanoparticles or a roughened metal surface, can be explained by a poor contribution of the electromagnetic field enhancement. It is based on the interaction of the surface plasmon discontinuous metallic surface and the analyte.

Table 5. An approximately bacterial cells number analyzed in this study.

5 h	24 h	Bacterial sample
1.9E+04	2.2E+04	<i>Bt</i> in NP mixture
34	39	SERS
307	353	Raman diluted
4418	4418	Raman bulk

5.2.4 Amino acids SERS experiments

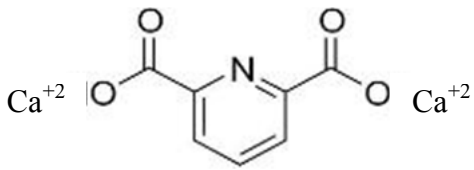
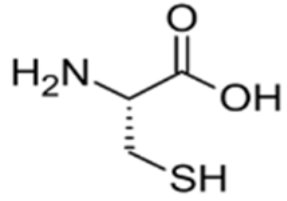
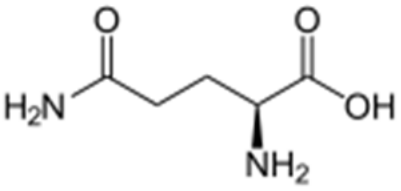
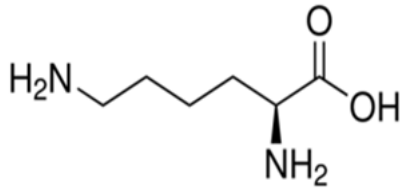
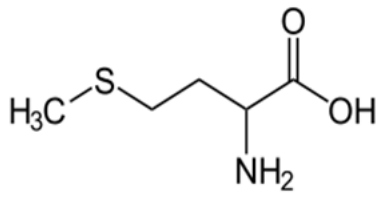
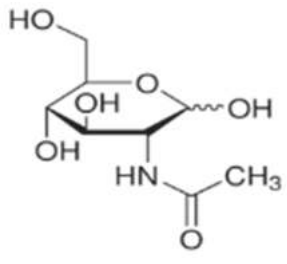
In order to assign properly the vibrational bands of the bacterial content in the SERS results, some selected amino acids present in vegetative cells and endospores were analyzed individually by SERS. The SERS active substrates of Ag-NP citrate capped-reduced by borohydride were used to evaluate the SERS spectra of the biocomponents.

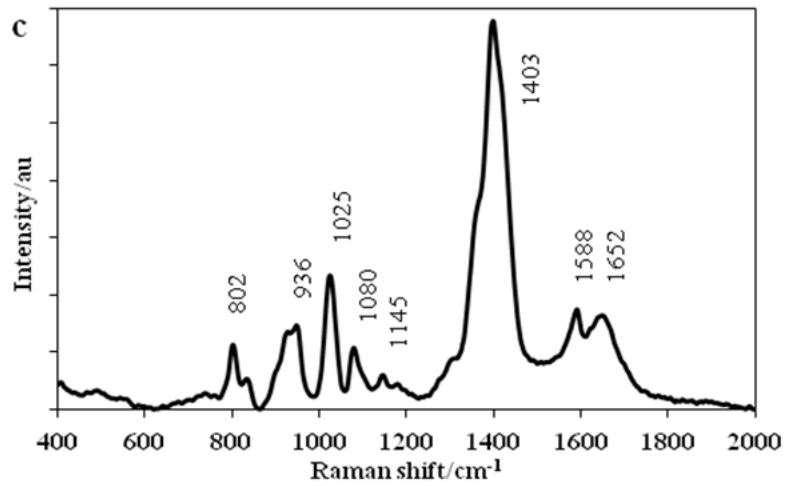
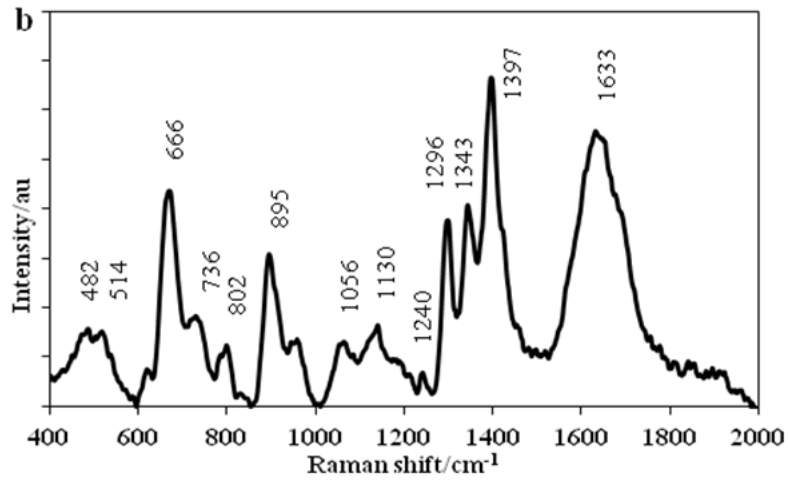
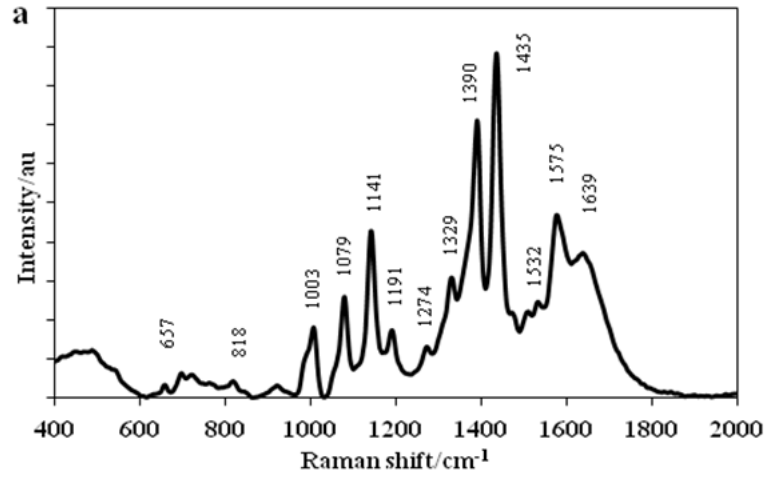
The NAG protein contained in the peptidoglycan layer was the component individually analyzed for vegetative cells sample. For the endospores sample, the dipicolinic complex with calcium (Ca^{+2} -DPA) and some small acid-soluble spore proteins (SASP) present in *Bt* sample such as lysine, glutamic acid, methionine and cystein [60] were the representative samples individually analyzed by SERS. The chemical structures of those aminoacids are shown in Table 6. All of those bacterial components contain Raman active groups that can be identify by SERS. The SERS results of some of these biomolecules were already published with the vibrational bands assigned [61], but the interaction with the NP used in this experiment has to be optimized to achieve a better affinity at certain conditions due to the variability of pH-dependent ionizable groups in the biomolecules. Optimization parameters such as volume ratio biomolecule to NP, aggregation of NP and modifications to the surface charge of the NP were analyzed until a better interaction between a biomolecule and NP was obtained. The analyte bound to the substrate depends on the presence of the protonated and deprotonated structure and coordination site, which is critically dependent on pH of the medium [59,62]. Therefore, the pKa values of the

biomolecules have to be taken into account to induce the electrostatic interaction of certain groups of the molecule with the charge induced in the NP at several pH values. To achieve this, the surface charge of the NP was modified in a range from 3 to 11 of pH values to induce the interaction of a functional group to the SERS substrate. The SERS results were shown in Figure 36.

The vibrational signatures observed in the SERS results were tentatively assigned and described in Table 7 following previous literature values. It also contains, at the bottom of each vibrational bands assigned, the pH of the biomolecules solution and nanoparticles used for the mixture in SERS experiments. The results allow the properly assignment of the vibrational bands of the biomolecules present in *Bt* bacterial content indicating that the carboxyl, amino and thiols groups interacts with the Raman active sites in the metal substrate. Some of this aminoacids are contained in the inner side of the bacteria cell wall but some functional groups contained in this aminoacids could interact with the Ag-NP in a similar way than others that contain the group. This can help in the analysis of the bacterial content by SERS. Although these results are from pure biomolecules sample and the interaction with the NP is not exactly the same as is in the bacterial content mixture, the results can be used to confirm the content of the biological sample and the assignment of bands obtained from SERS experiments. The presence of certain peaks observed in the SERS results of this biomolecules and the lack of certain of those vibrational bands in the SERS spectra of *Bt* samples does not indicates that the molecule is not contented in the bacterial sample. For this, we have to takes into account that the results observed in the SERS spectra indicate the interaction with certain functional groups that were oriented in a particular way observed by SERS effect, the concentration of the sample, the presence of the protonated and deprotonated specific functional groups, among others.

Table 6. Chemical structures of the aminoacids analyzed by SERS, is included the final concentration of detection and the pKa and pI values used in the experiments.

<p>a</p>  <p>calcium dipicolinate complex 0.3 mM pKa: 2.16, 4.76 pI: 2.87</p>	<p>b</p>  <p>L-cysteine 1.0 mM pKa: 1.96, 8.18 pI: 5.07</p>
<p>c</p>  <p>L-glutamic acid 1.0 mM pKa: 2.19, 4.25, 9.67 pI: 3.22</p>	<p>d</p>  <p>L-lysine 1.0 mM pKa: 2.18, 8.95, 10.53 pI: 9.74</p>
<p>e</p>  <p>Methionine 10.0 mM pKa: 2.28, 9.21 pI: 5.74</p>	<p>f</p>  <p>NAG 0.08 mM</p>



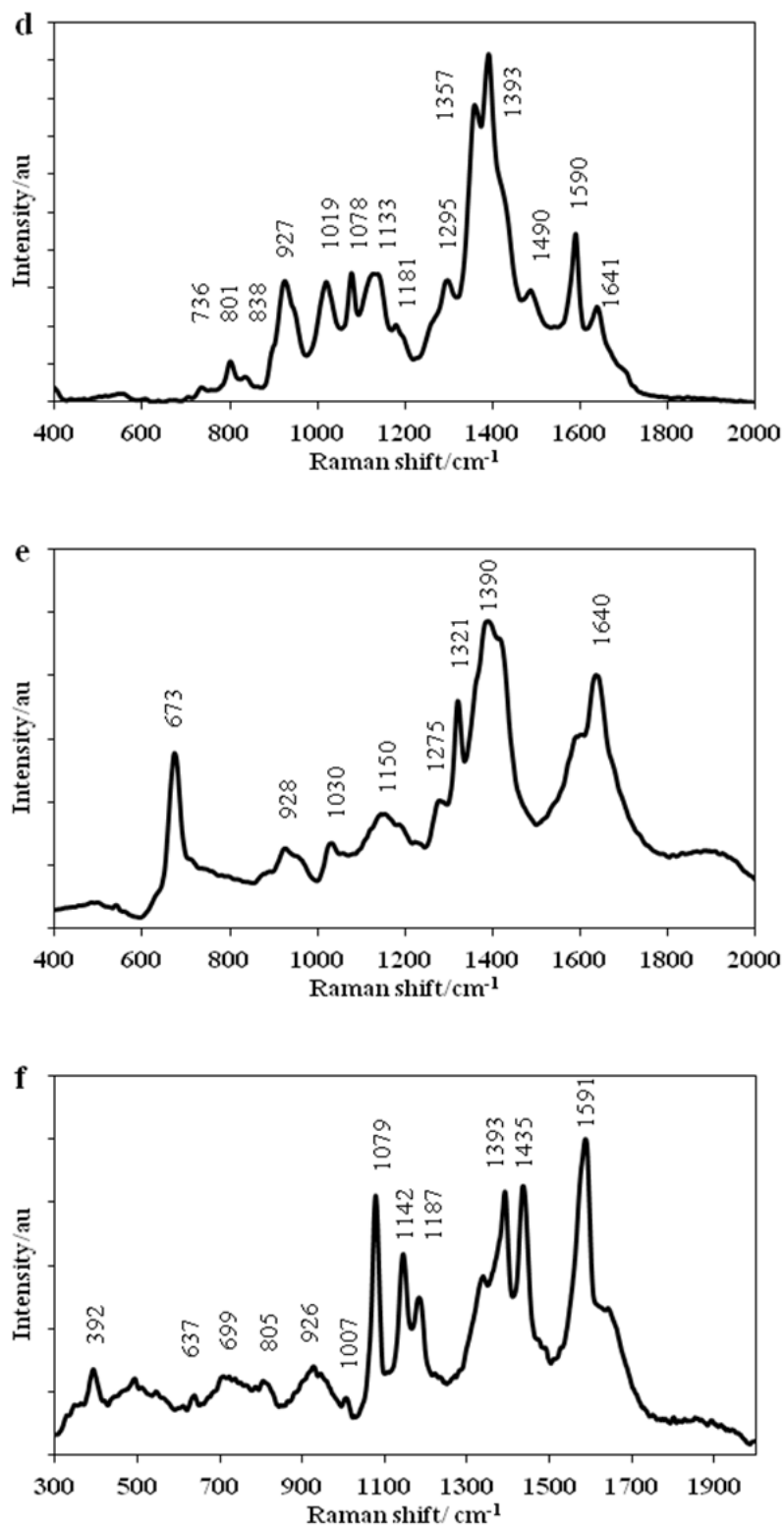


Figure 36. SERS of aminoacids such as (a) calcium dipicolinate complex, (b) L-lysine, (c) L-glutamic acid, (d) L-cysteine, (e) methionine and (f) NAG using 532 nm, 10x objective, 10s, 47.5 mW.

Table 7. SERS vibrational assignments of selected components analyzed present in vegetative cells samples and endospores samples of *Bt*. [30,63-65,49]

Vibrational band	CaDPA 0.3 mM	Vibrational band	L-cysteine 1.0 mM	Vibrational band	L-glutamic acid 1.0 mM
C-C ring bend	657	C-C skeletal str	482	C-C str	802
C-H out of plane	818	S-S str	514	CCN str, COO ⁻ str	936
C-O-C assym str (cyclic)	925	C-S str	666	CH ₂ w, C-N str	1025
Sym ring breathing	1003	C-OH tw	736	C-N str	1080
Trig ring breathing	1079	C-OO- bending	802	C-C str, NH ₂ tw	1145
C-H bend	1141 1191	C-C skeletal str C-COOH str	895	CH ₃ sym def, COO ⁻ sym def	1403
C-C ring mode	1274	C-N str/amino terminal group	1056	NH ₂ sc, COO ⁻ antisym def	1588
C-O str	1329	C-C str NH ₂ tw	1130	NH ₂ antisym def	1652
COO- str sym	1390	CH ₂ tw, r	1240		
C-C ring str C-C bend sym	1435	CH ₂ tw, def	1296		
Ring str	1532	C-H def, COO- sym str	1343		
COO- str assym	1575	CH ₃ sym def, COO ⁻ sym str	1397		
COO- asym str	1639	NH ₂ def, COO ⁻ antisym str	1633		
pH solution / pH NP	pH 2.87 / Np pH 9		pH 5.02 / Np pH 3		pH 3.22 / Np pH 9

Vibrational band	L-lysine 1.0 mM	Vibrational band	Methionine 10 mM	Vibrational band	NAG 0.08 mM
C-OH tw	736	C-S stretch	673		392
C-OO- bending	801	C-C stretch/COOH stretch	928	COO- wagg	637
C-C skeletal str, C- COOH str	838 927	C-N stretch/amino terminal group	1030	Glycosidic ring	699
C-C str, C-N str	1019	C-C stretching/NH ₂ tw/NH ³⁺ wagg	1150	COO- bend	805
C-N str	1078	C-N-H bend (Amide III vib)	1275	C-C str/CCN str/COO- str	926
C-C str, COO- sym str, NH ₂ tw	1133 1181	C-HH def/COO- sym stretch	1321	C-C str/ Sym ring breathing	1007
CH ₂ tw	1295	CH ₃ sym def/COO- sym def/CNH ³⁺ str	1390	C-C str/C-O str	1079
C-H def, COO- sym str	1357 1393	NH ₂ sc/NH ₂ antisym def	1640	C-C str/ NH ₂ tw	1142
C-H ₂ def	1490			C-N-C antisym str amine II	1187
NH ₂ sc, COO ⁻ antisym def	1590			COO- sym str/C-N str	1393
NH ₂ antisym def	1641			C-H & CH ₃ def	1435
				COOH str	1591
	pH 9 / Np pH 9		pH 5 / Np pH 7		pH 3 / Np pH 3

5.2.5 Conclusion

The results presented demonstrate that SERS spectra obtained with Ag-NP reduced by borohydride capped by citrate were successfully used to spectroscopically characterize *Bt*. The use of colloidal suspensions of metallic NP is favorable to enhance the SERS detection of large biological samples compared to the small size of the nanoparticles. It is due by the electrostatic interactions that dominate the interaction of the NP and bacterial content can occur around the entire biological sample and not on one side as is the case of the Raman vibrational enhancement produced by solid metallic surfaces. The small borohydride nanoparticles used with a slightly activated “hot spots” and pH surface modifications of the NP to more acidic pH values than the pH of nanoparticles synthesis preparation (pH 9) resulted in good SERS substrates for *Bt* detection. High concentrations of NaCl, as 1.0 M, results in a nanoparticles oxidation and a decrease in the SERS signal. Bacterial samples suspended in low concentrations of NaCl (0.1 M) and modifications of the borohydride nanoparticles surface in a range of 5 to 7 pH values can improve SERS detection of *Bt*. A summary of these results is presented in Table 8. As shown in this work, surface modifications of NP with pH changes results in more reliable spectral information of *Bt* because neat Raman spectra with the modified NP were obtained at all pH values. Raman spectra obtained from NP aggregated with NaCl presented several peaks that interfere with the bacterial identification. Results of SERS spectra of experiments with bacteria in contact with NP at different pH values differ significantly from one another in some biomolecules and bacteria, depending on the conditions imposed to the interacting microorganisms and NP systems. An improved interaction, as judged from higher intensity SERS signals, was obtained for NP with slightly positive charge surface was in contact with this Gram-positive bacteria (*Bt*) containing the negatively charged groups of the teichoic acids

transverse in peptidoglycan layer and the carboxylic groups in the dipicolinic complex of the exosporium layer of endospores, among other Raman active groups. The results suggested that high signal enhancements from the bacterial cell wall and endospores components of *Bt* can be obtained by tailoring the conditions of SERS experiments. Surface enhancement factor (SEF) of 10^3 and 10^4 were obtained from the intensity of vibrational signatures for vegetative cells and endospores samples under well-controlled conditions, respectively.

In order to assign properly the vibrational bands of the bacterial content in the SERS results, some selected aminoacids present in vegetative cells and endospores were analyzed individually by SERS using as SERS active substrates the Ag-NP citrate capped-reduced by borohydride.

Table 8. Summary of the optimization parameters obtained from the simple protocol established for SERS detection of vegetative cells and endospores of *Bt*.

Optimization parameter		Result	Observation
VR: bacteria/NP	0.125	OD ₆₀₀ : ~ 1 10 ⁴ cells/mL	↑ S/N of the SERS spectra, ↓ fluorescence from the analyte
Agglomeration effect	+ NaCl	0.1 M	activation of “hot spots” on NP & solvent to preserve the bacterial sample
Modifications to the surface charge NP	+ H	pH 5-7	optimal interaction with the bacterial cell wall content

6. APPLICATIONS IN DETECTION OF *Bt* SAMPLES: MONITORING, DISCRIMINATION AND BIOAEROSOL DETECTION

This chapter contains details on the applications of optimized SERS detection of vegetative cells and endospores of *Bt*. The discrimination between samples at different growth stages in suspension and the monitoring the grown process of the bacterial life cycle was achieved using PCA, PLS and PLS-DA. The detection of *Bt* endospores as aerosol particles using rough metal surfaces in colloidal suspension and as solid substrates is discussed as one of the challenges and the end goal of this research.

6.1 Methodology for data analysis

SERS spectra obtained were analyzed using OPUS™ software (Bruker Optics, Billerica, MA). Baseline correction was applied to allow a proper tentative assignment of vibrational bands. Spectra were normalized for intensity, laser power and acquisition time ($\text{counts}\cdot\text{mW}^{-1}\cdot\text{s}^{-1}$) and the averages are shown for each case. Peak areas were calculated using OPUS™ software, and distinctive peaks with areas correlated to bacterial growth were identified. The discriminant information of samples was obtained through multivariate analysis using MatLab version 7.6.0.324 R2008a (The Mathworks, Natick, MA) with PLS Toolbox version 6.3 (Eigenvector Technologies, Wenatchee, WA). PCA is a multivariate analysis tool that is widely used for data reduction, exploration and visualization. It consists in linear combinations of the original variables into new variables known as principal components (PC). PC are calculated in such a way that the first component captures most of the variance in the original data set and each

additional component captures remaining sources of variation until all variation is captured. Each PC is described by two variables; scores and loadings. The scores is a measure of the relation between samples in the data set in terms of that specific PC. The loadings describe the contribution of each variable to that PC. A plot of the scores of PC against other PCs provides information of how similar or different are the samples in a data set. A loadings plot for a PC will provide information of the source of the variation captured by that PC. PCA was used to observe the spectral similarities and/or differences of the SERS spectra of bacteria at different stages of the growth using a spectral range of 400-2000 cm^{-1} . In PLS the variation among the samples captured by PCA (x block) is linearly correlated to information provided (y block). In this case the information in y is growth time. The linear regression model is used to predict the stage of new samples.

Discriminant analysis was achieved through partial least squares discriminant analysis (PLS-DA). For this analysis the information captured by PCA is fitted in a linear regression (PLS) where the information in “y” is group composition. The outcome of the analysis is a model of whether a sample is member of a group (1) or not (0). It was used to discriminate between vegetative cells and endospores of *Bt*. The model can be used to predict content of new samples.

Due to the complexity of the data, preprocessing algorithms were applied to remove variation within the data that does not pertain to the analytical information. The data obtained was preprocessed in the spectral range in the region 300-2000 cm^{-1} using first derivative in polynomial order of 2 and multiplicative scatter correction or spectral mean centering. This preprocessing is used to make sure that the data analysis takes in consideration the spectral differences emphasizing the variability of the data defining small spectral changes in the

bacterial sample decreasing the baseline shifts and, influences on intensity of the spectra due to the sample concentration and, respectively.

6.2 Monitoring and discrimination of bacterial samples

6.2.1.1 Spectral differences between vegetative cells and endospores

The spectra of the sample containing mainly vegetative cells were obtained from the sample at 5 h of bacterial growth and a sample containing mainly endospores from the sample collected at 24 h of bacterial growth. The surface charge of nanoparticles were slightly modified at pH 7 and bacterial sample diluted in NaCl 0.1 M as the results of the optimization parameters explained before indicating a better interaction bacterial sample-nanoparticles. The SERS spectra of these bacterial suspension solutions are shown in Figure 37. The vibrational bands were assigned according literature values and are listed in Table 9. The spectral differences between the vegetative cells and endospores cannot be clearly observed to the naked eye but the PCA clearly demonstrates that there are differences between the groups.

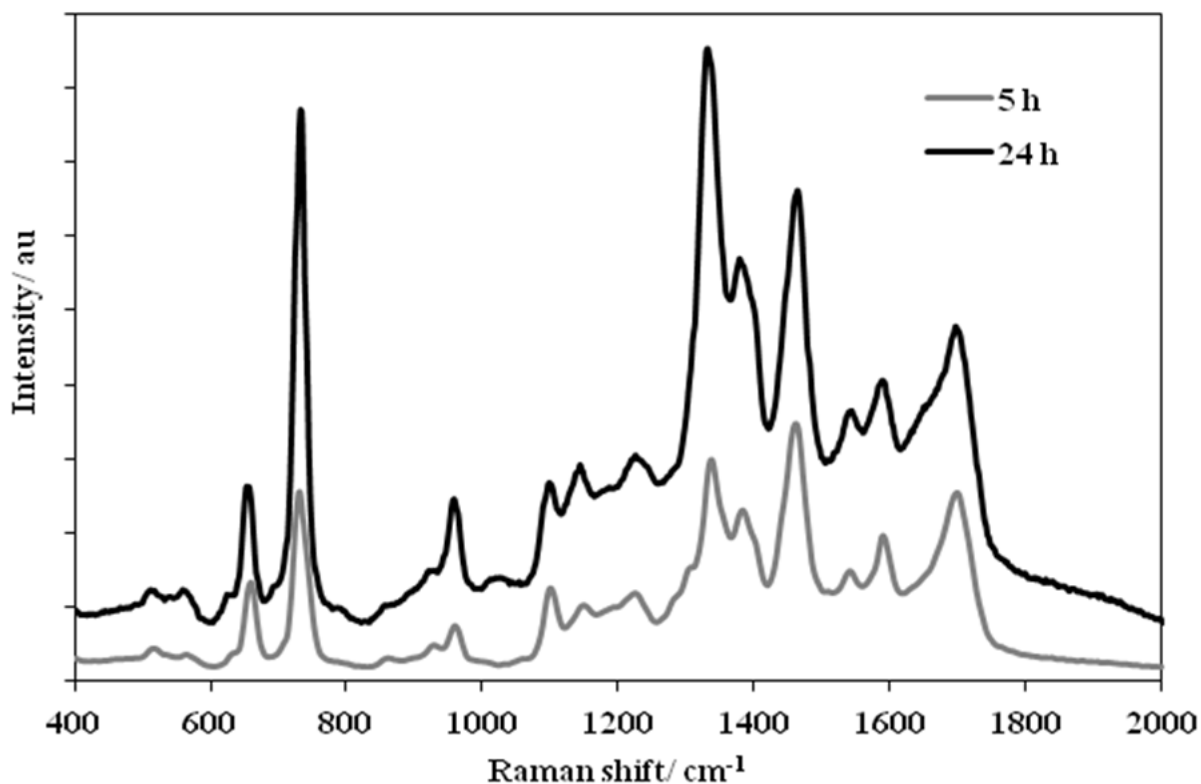


Figure 37. SERS of vegetative cells (5 h) and endospores (24 h) of *Bt* sample solutions using the optimization procedure discussed previously.

Table 9. Tentative assignment for vibrational bands of vegetative cells and endospores samples of suspension solution of *Bt* [40,66,29]

Vibration mode	5 h	24 h
	Raman shift / cm^{-1}	
S-S stretching of cysteine	516	514
C-C skeletal of carbohydrates	566	562
		1049
C-S stretching of cysteine		637
N-H deformation of amide II	659	657
glycosidic ring of NAG and NAM	730	732
C=C deformation of tyrosine	857	
	923	
	960	959
carbohydrates	1052	
C-N and C-C stretching	1100	1098
C-H in plane bending		1017

=C-C= of lipids or C-N aromatic in proteins	1148	1143
amide III	1226	1224
		1276
C-NH ₂ stretching of amide II	1337	1332
COO ⁻ stretching	1383	1380
C-H deformation of lipids	1463	1463
	1543	1541
C=C ring stretching of lipids	1591	1589
amide I	1700	1700

The results from the PCA are summarized in Figure 38. The scores plot of PC1 vs. PC2 (Figure 38a) obtained from the analysis shows that the first two PC describes the greatest source of variation within the data with 95% confidence level. The identified spectral features could be attributed to specific vegetative cells and endospores chemical components presents in the sample. The loadings plot (Figure 38b) can be used to identify regions that present the main spectral differences in the samples. The band assignments of the areas with the variation captured by PC1 are detailed below (Table 10).

Table 10. Band assignment of the areas with the variation captured by PC1 for vegetative cells and endospores *Bt* samples

Spectral region / cm ⁻¹	Band assignment of the area
~700	N-H def of amide II & glycosidic ring of NAG and NAM
~1080-1100	C-N & C-C str
~1300	C-NH ₂ str amide II & COO ⁻ str
~1460	C-H def
~1600	ring vib & N-H ₂ assym def

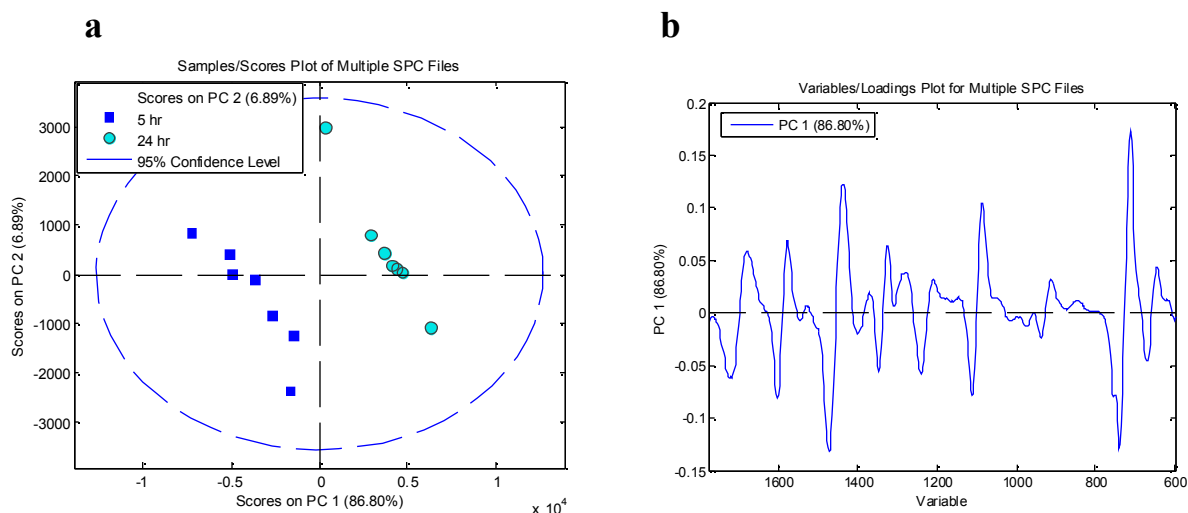


Figure 38. (a) The PCA scores plot allowed a comparison between the vegetative cells and endospores SERS spectra. **(b)** Loadings plot presenting the spectral regions contributing to the spectral differences between samples.

Figure 39 shows the PLSDA based model for discrimination of vegetative cells from endospores. The samples are grouped by a 0-1 scale where zero (0) means that the sample is not part of the predicted group (in this case vegetative cells) and which samples are part of the group. The variation in the samples can be considered expected and normal because the spectra of microorganism were collected from a growing media and pure samples cannot be assured. However, the model was able to completely discriminate between the two stages.

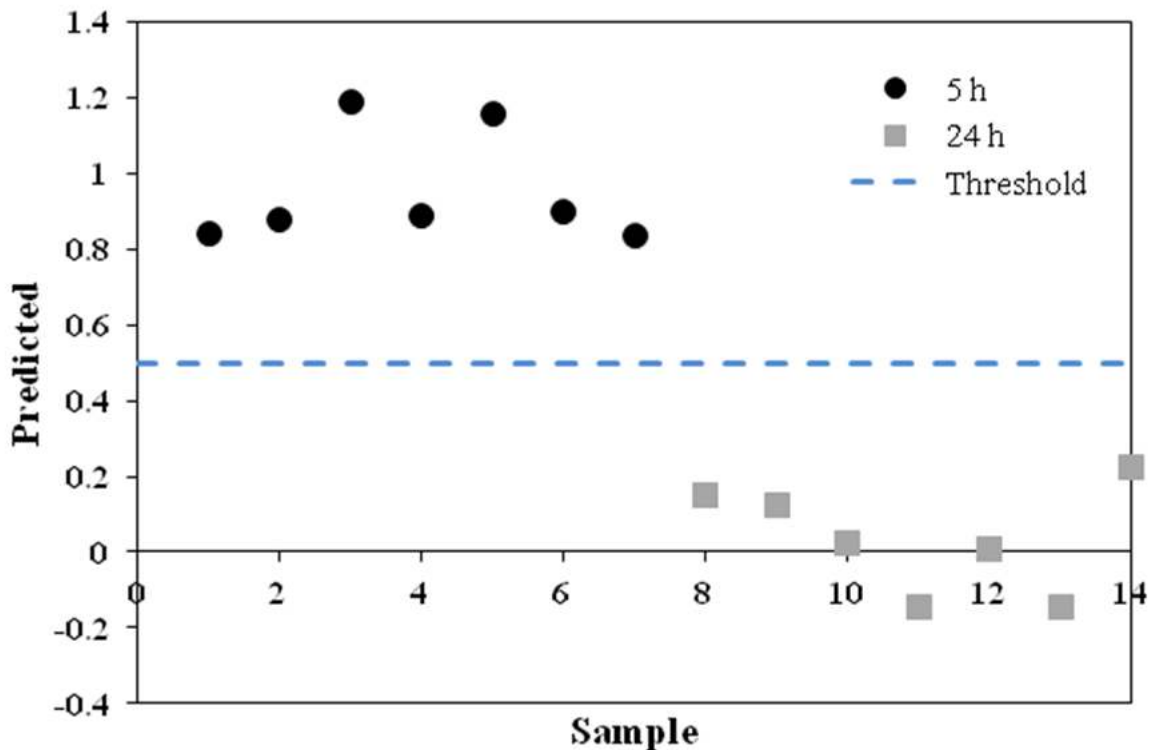


Figure 39. PLS-based discriminant analysis of *Bt* samples at two different bacterial content. A positive value (~ 1) implies presence of vegetative cells and zero value (~ 0) implies not considered vegetative cells samples (suggesting in this case the endospores.)

6.2.1.2 SERS assisted monitoring of the *Bt* growth stages

Several random samples were analyzed by SERS while *Bt* was grown following the optimization parameters explained before that result in better interaction bacterial sample-NP. The bacterial growth of *Bt* was monitored for 24 h. The sample collection and preparation for SERS analysis was the same as explained in the experimental section. The results obtained showed an increase of specific peaks with assigned vibrational modes related to content more commonly found in the endospore formation. These results from the SERS spectra of *Bt* at times show differences in bacterial content related to the growth stages. The average of SERS spectra at each h collected sample is shown in Figure 40a. The peak area of several spectral regions was

analyzed using the *B* integration method (Figure 40 inside at left) in OPUS software and the most important results are presented in Figure 40b and Figure 40c.

Table 11. Spectral regions analyzed in SERS spectra of the samples at different growth stages.

Spectral region/ cm^{-1}		Raman shift/ cm^{-1}		Assignment band
468.3-810.9	495.25-530.42	a	514	S-S str cysteine in spore coat
	542.14-577.32	b	566	C-C carbohydrate proteins
	635.94-679.91	c	637 657	C-S str cysteine spore coat N-H amide II
	679.91-764.91	d	730	glycosidic ring NAM & NAG
980.1-1320.6	1081.48-1113.72	e		C-C & C-N str
	1116.65-1160.62	f	1148	=C-C= lipids & C-N arom proteins
	1198.72-1254.42	g	1226	N-H amide II
	1315.97-1385.8	h	1337	C-NH ₂ str amide II
	1362.87-1398.04	i	1380	COO⁻ str CaDPA
1661.1-1489.8	1518.22-1559.26	j	1543	C-H def lipids
	1573.91-1609.09	h	1589	C=C ring str

Several spectral regions were analyzed accordingly with the assigned peaks which refer to different sample content, but three regions had a special behavior according with the expected results of the bacterial growth content in a PLS analysis using multiplicative scatter correction for data preprocessing. The three general regions with the greatest differences referent to bacterial hour growth identified by OPUS are: 468.3-810.9, 980.1-1320.6 and 1661.1-1489.8, and in each range several peaks were analyzed as presented in Table 11. Figure 40 has the spectral regions highlighted and the bands identified as explained in Table 11).

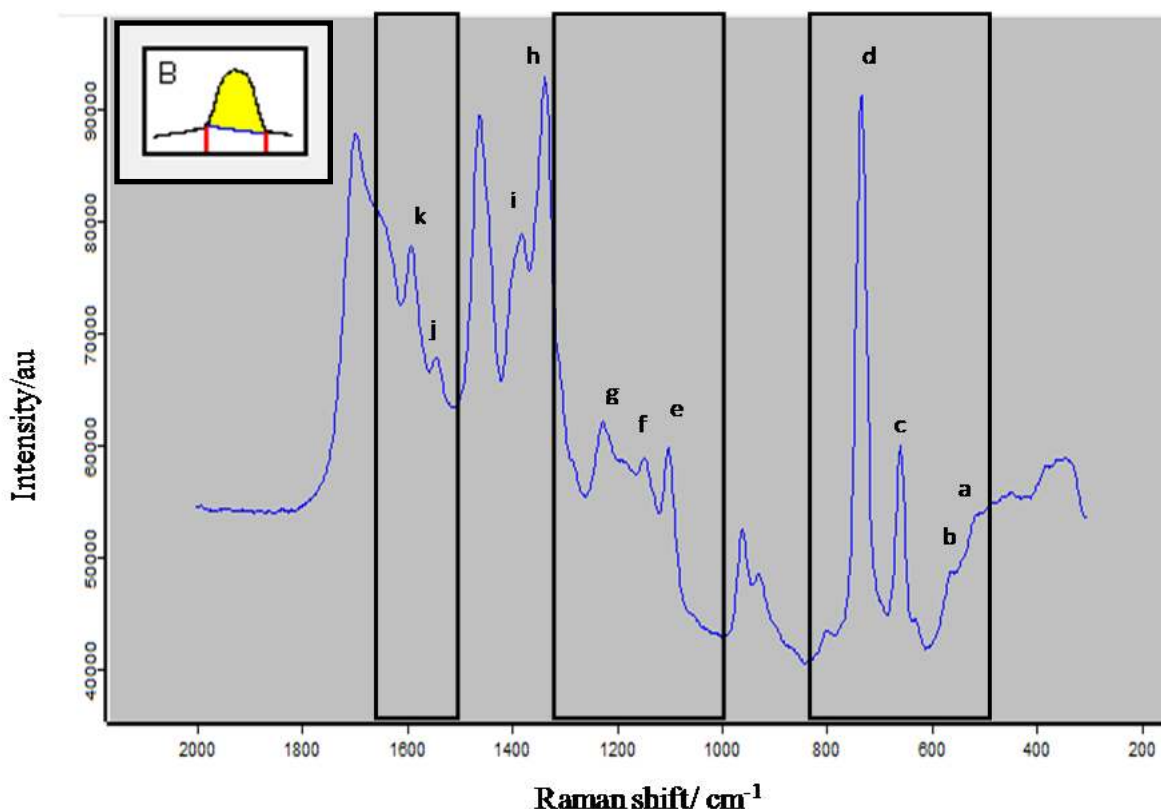
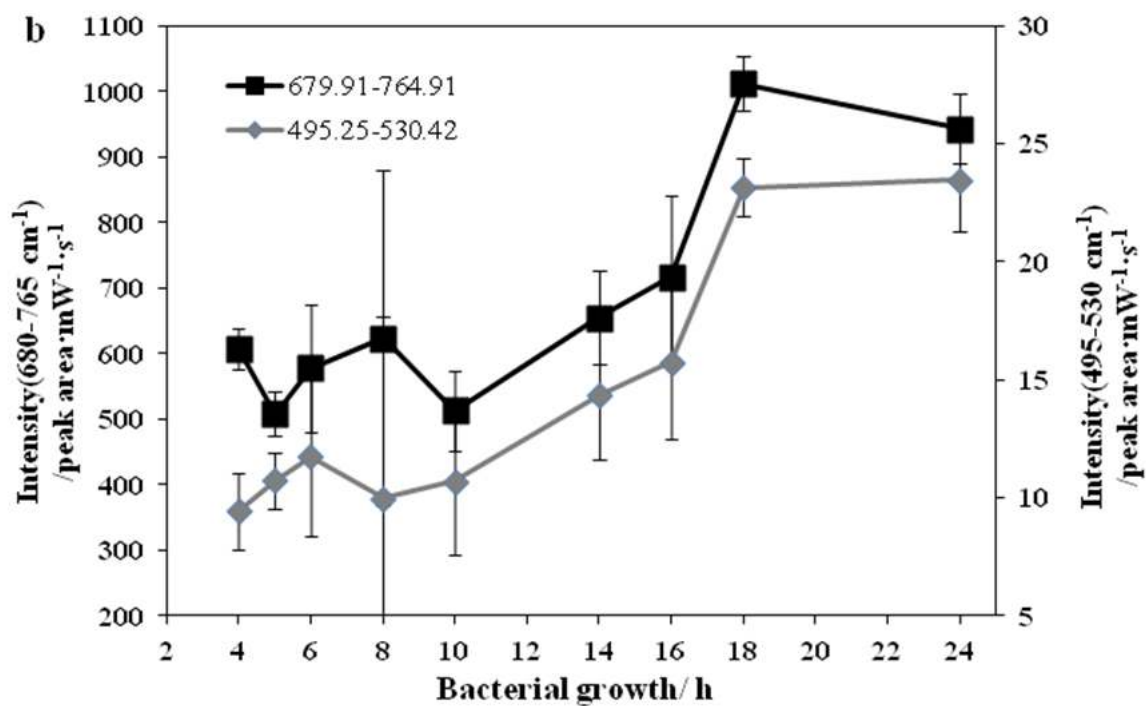
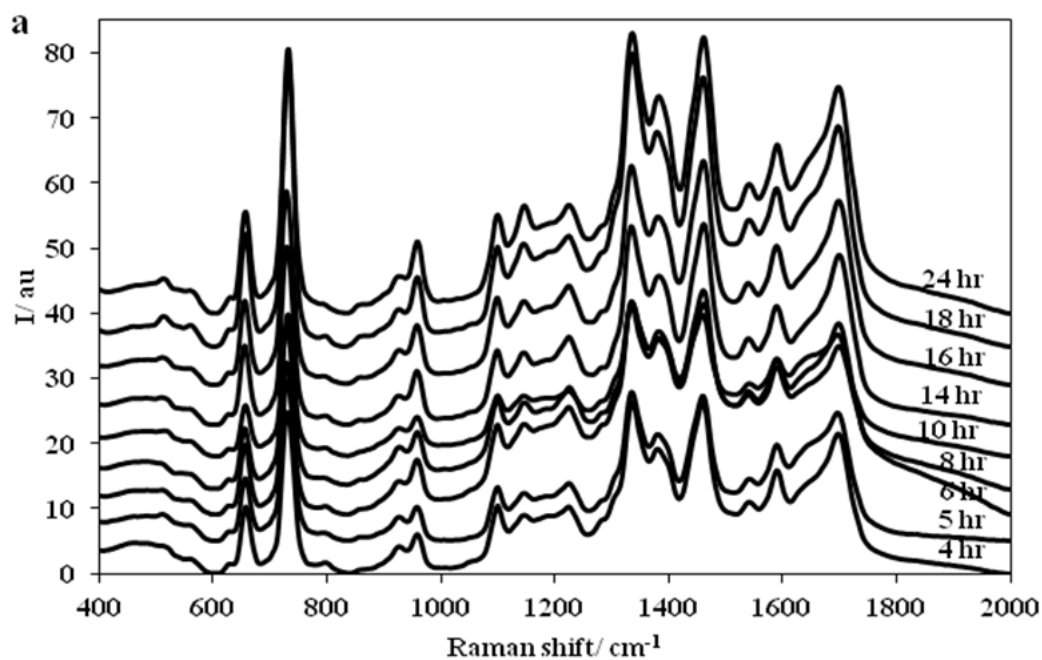


Figure 40. Example of a SERS spectrum of *Bt* to show the regions in which the peaks area were analyzed according Table 10.

All the regions presented show an increasing of the peak area while *Bt* is growing (Figure 41b and Figure 41c). This is in agreement with the expected results because the exosporium content area is increasing while the endospores are forming from vegetative cells. Those results clearly show that the bacterial content changes while *Bt* cells are growing. This is also in agreement with the results presented by Kahraman [57], where is well explained that the changes in bacterial SERS spectra during the growth of bacterial cells are evidence of changes in the biomolecular composition of the cell surface structure. This information could be obtained from SERS results and the optimized parameters worked in this research.



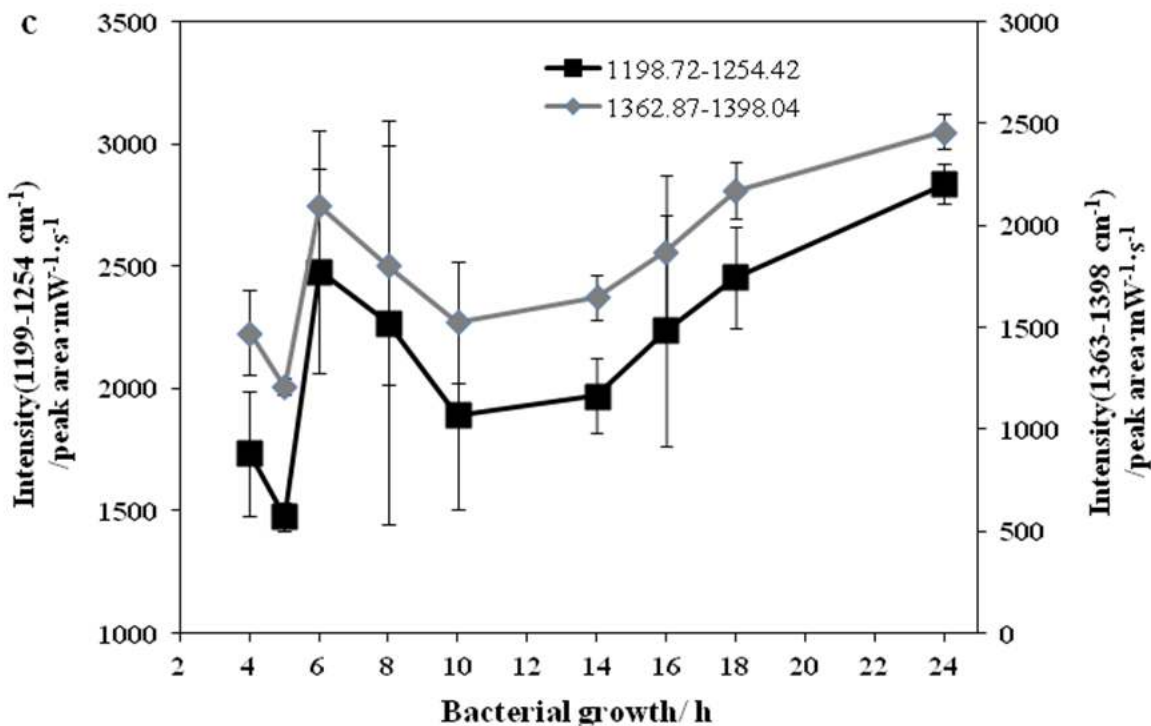


Figure 41. SERS results of *Bt* at different growth stages: (a) SERS spectra of *Bt* at different h of bacterial growth. As can be seen while *Bt* grows. (b, c) The peak area of several spectral regions presents an increasing behavior.

Spectroscopic data at various stages (h) of bacterial growth was used to build a PLS predictive model to estimate the bacterial growth time based on spectroscopic information. The lineal regression model using PLS was calculated with the SIM-PLS algorithm using a preprocessing data of first derivative and mean center. As can be observed in Table 12, 6 leverages for variables were enough to capture 98.81% the variance in the data.

The linear calibration was obtained using cross-validation leave one out method (A technique for assessing how the results of a statistical analysis will generalize to an independent data set. It is mainly used in settings where the goal is prediction, and one wants to estimate how accurately a predictive model will perform in practice. One round of cross-validation involves partitioning a sample of data into complementary subsets, performing the analysis on one subset,

and validating the analysis on the other subset. To reduce variability, multiple rounds of cross-validation are performed using different partitions, and the validation results are averaged over the rounds). The model for PLS regression (Figure 42) for the data indicates in the value of root mean square error for cross-validation that the model can predict the hour of bacterial growth in ± 1.6 h approximately with a correlation coefficient for cross-validation of 0.98 in a 95% of confidence level. This variability can be attributed by the mixture of bacterial content in most of the bacterial growth stages.

Table 12. Sum squared captured information from PLS analysis

Percent Variance Captured by Regression Model

Comp	-----X-Block-----		-----Y-Block-----	
	This	Total	This	Total
1	88.82	88.82	17.62	17.62
2	4.42	93.24	53.57	71.19
3	3.89	97.12	18.48	89.67
4	0.60	97.72	5.23	94.90
5	0.48	98.20	1.69	96.59
6	0.61	98.81	0.83	97.42

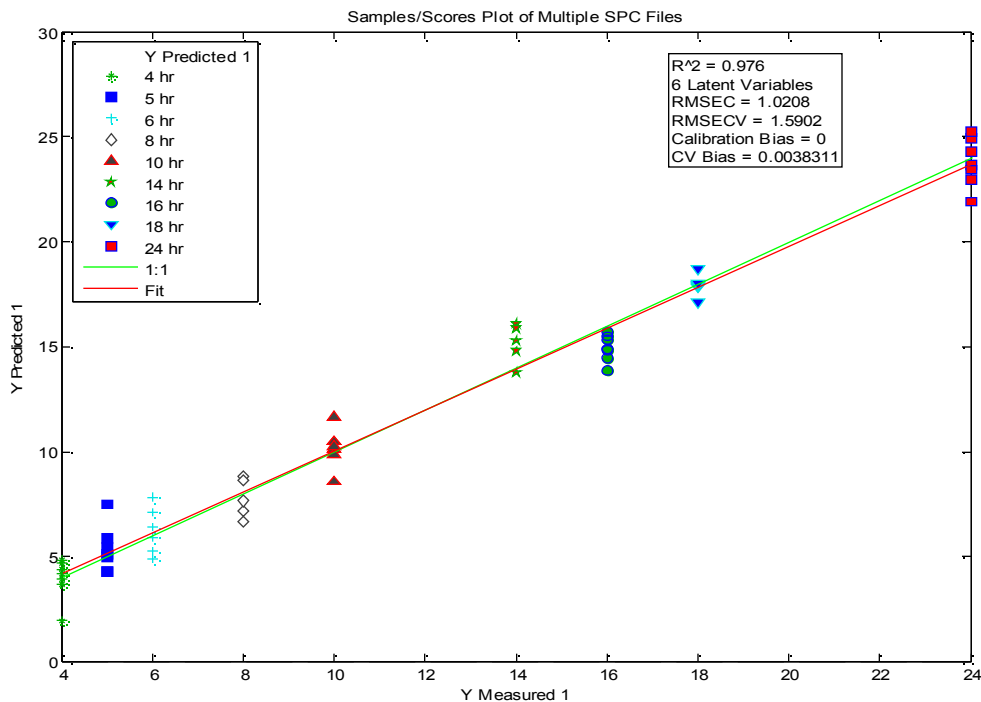


Figure 42. PLS regression of time in the growth of *Bt*. Spectra was preprocessed with first derivate and mean centering. With 6 variables the error is estimated in 1.59 h (RMSECV) and the correlation is 0.98.

Figure 42 shows a plot of the scores values per sample for LV2 (PC2). This figure shows tree different groups of bacterial content. The first group is around 4 to 6 h of bacterial growth; the bacterial content at these hours is mainly composed of vegetative cells. From 6 to 16 h of bacterial growth; initially the vegetative cells are reproduced almost in a maximum growth, when the bacteria are in nutritional deficiency as environmental stress begins to produces intracellular protein crystals toxic. At these times of bacterial growth a combination of vegetative cells, toxic crystals and internal endospores creates the bacterial samples content in a mixture of them with great variability in content. Finally, the formation of the endospores as a defense mechanism can be observed after 18 h of bacterial growth.

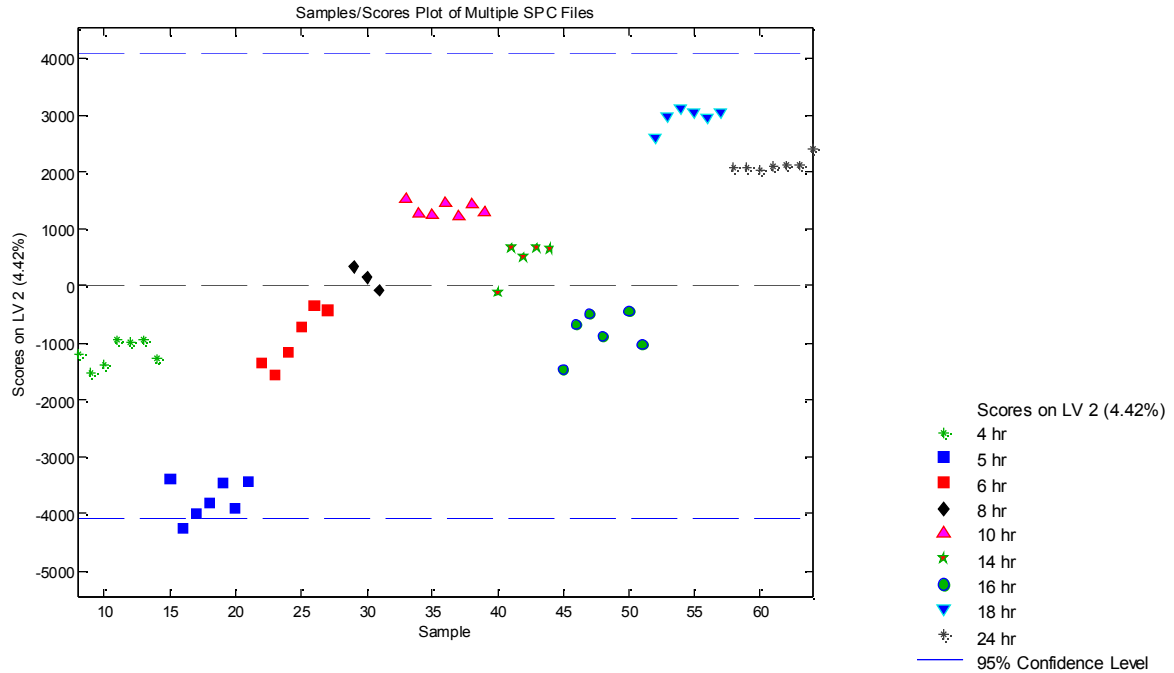


Figure 43. Scores plot per sample showing three stages during the growth of *Bt*.

6.3 Bioaerosol detection of *Bt* endospores

6.3.1 Materials and instrumentation for bioaerosol generation

The biological samples used to generate the bioaerosol follows the same sample preparation of biological growth, washing, centrifugation and dilution procedure until obtaining two different concentrations of bacteria cells/ μL . The concentrations used of the bacterial content in NaCl 0.1 M were at the optimal dilution to obtain an OD_{600} at ~ 1 and a lower one at 0.5. The bioaerosol of *Bt* was generated using a Broadband Ultrasonic Generator by controlling pressure with an ultrasonic nozzle and Model 11 and a Virtually Pulse Free Syringe Pump 55-2111. A Broadband Ultrasonic Generator was used to provide the necessary energy to operate an ultrasonic atomizing nozzle. The syringe pump coupled with a pressure adjuster was used to adjust the pressure of the air stream of bacteria in order to have an optimized bioaerosol mist. In

this case, 125 μL of bacterial sample was aerosolized to fall on 1000 μL of nanoparticles at a distance of 7.5 cm with a pump rate 50 mL/h, 1.5 atm of air pressure and 0.10 W of broadband speed.

6.3.1.1 SERS for detection of endospores of *Bt* as bioaerosol particles

The outstanding detection results with the endospores biological sample in aqueous suspensions were extrapolated to the detection of bacterial sample as aerosol particles. The aerosol detection has been reported using several methods of bioaerosol sampling. Sengupta *et al.*, [30] identified the spectral region of interest, and the concentrations of microorganisms and colloid particles needed to maximize the Raman signal. The aerosolized microorganisms were impacted and transferred to a colloidal suspension of silver nanoparticles to obtain reproducible Raman spectra. The results presented SERS spectra of two samples of aerosolized ML4100 *E. coli* and PAO1 *Pseudomonas aeruginosa* compared to the spectra of non-aerosolized sample. The samples were aerosolized to a borohydride NP suspension solution as shows Figure 44. The parameters used to acquire the spectra in real-time were using a laser line of 514 nm, < 250 mW, 60-120 s and 50-100 μL of analyte in a bacterial concentration of 10^7 - 10^8 cfu/mL. However, the results showed high spectral fluorescence that limits the chemical information observed in spectra. Based on this study, we have constructed an experimental set up for aerosol generation to detect and identify endospores of *Bt* by SERS.

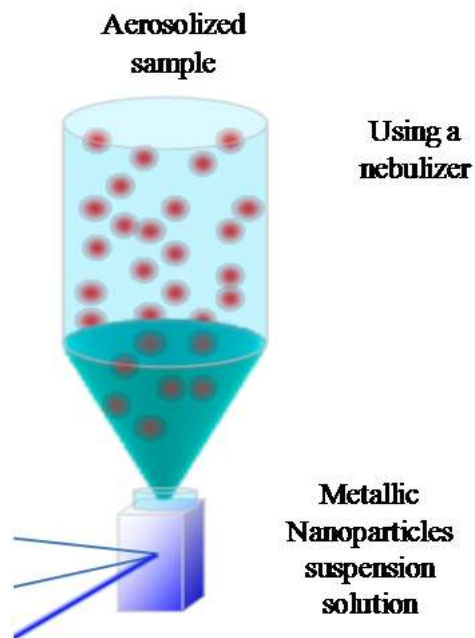


Figure 44. Experimental set up system for SERS experiments to aerosolized samples used by Sengupta [30] in the bioaerosol experiments published.

6.3.1.1.1 Using colloidal suspension solution

Results already discussed in previous chapters include bacterial solution in suspension as analyte. It is important to note that all of the optimization parameters explained before helps to achieve the big challenge detection using bioaerosol *Bt* particles. The experiment was performed following the results obtained in optimization parameters experiments according to the volume ratio bacteria: NP, aggregation effects and surface charge modification to the nanoparticles. The volume ratio bacteria: NP was increased using 1 mL as a total volume of NP. The mixture bacteria aerosolized: NP was analyzed using the same procedure used with the bacterial sample suspension as detailed in experimental section and previous literature reported from our group [58]. Bioaerosol detection of *Bt* was obtained using the experimental setup showed in Figure 45

to generate the aerosolized sample. The bacterial sample solution was aerosolized falling to the nanoparticles at a distance of 7.5 cm from the nebulizer.



Figure 45. Experimental setup used to aerosolize the bacterial sample to the nanoparticles for SERS experiments. The parameters used were 50 mL/h, 1.5 atm at 0.10 of broadband speed.

The mixture of aerosolized bacterial solution in NP was analyzed using the same procedure explained for sample preparation for SERS analysis. The SERS spectrum could be obtained and it is shown in Figure 46b. The vibrational bands observed correspond to the same observed using the optimized procedure for bacterial suspension sample. The results obtained were in agreement as expected. The color change observed of the NP on optimization experiments using bacterial suspension solution directly mixed as shown in Figure 46a and in the SERS spectra can be observed the vibrational bands corresponding to the bacterial content aerosolized. SERS results presented on Figure 46b were obtained using two different bacterial concentrations. The bacterial concentration used were at $OD_{600} \sim 1$, the optimal concentration to

obtain the best interaction and good SERS results, and a lower bacteria concentration ($OD_{600} \sim 0.5$). As can be clearly observed, the SERS spectrum of the optimal bacterial to NP concentration of the aerosolized bacterial sample is comparable to the obtained in the sample suspension solution directly mixed. The vibrational bands can be tentatively assigned as shown in Table 13. Results are in good agreement to previously reported detection of aerosolized bacterial samples.

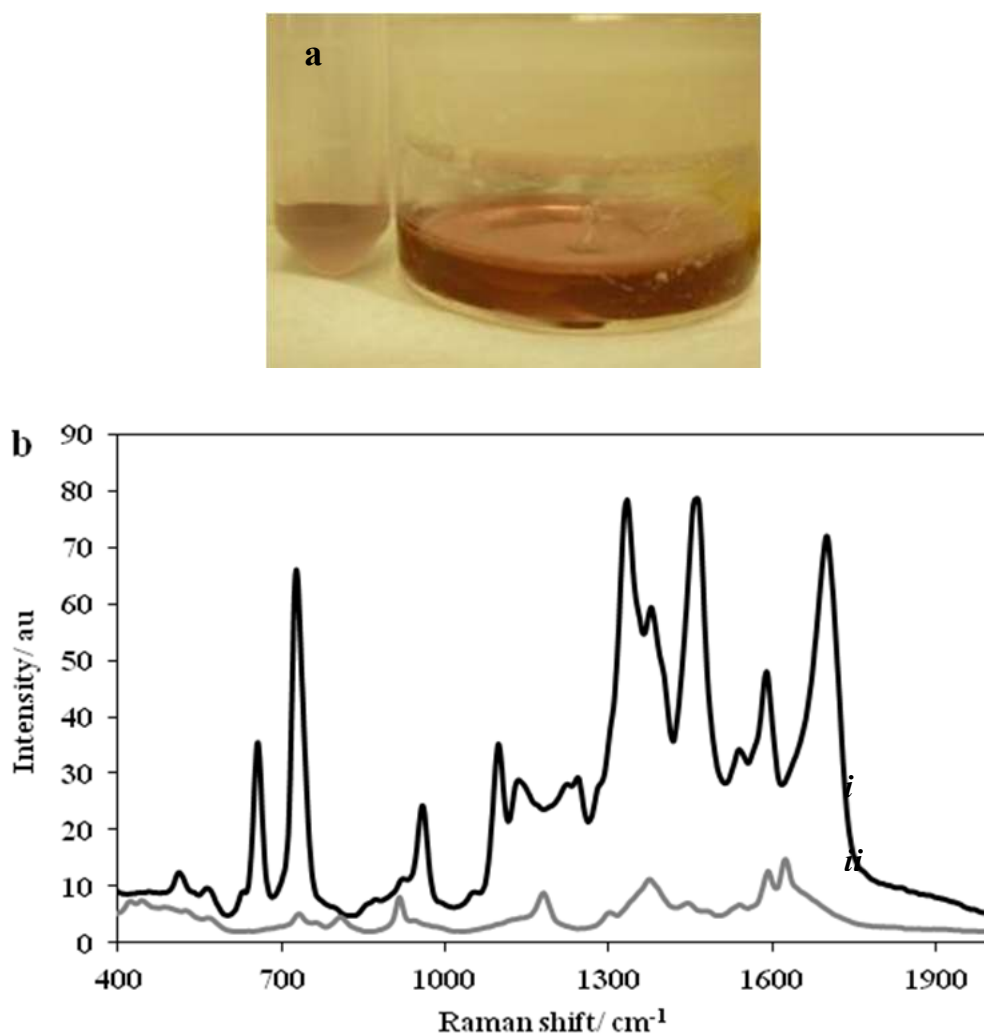


Figure 46. Results obtained from the bioaerosol experiments: **(a)** the change in color of the nanoparticles and bacteria mixture (bacterial sample suspension non aerosolized at left and aerosolized at right) and **(b)** the SERS results obtained from the aerosolized bacterial sample at two different concentrations (*i* OD_{600} at 1 and *ii* 0.5).

Table 13. Tentatively Raman band assignments of the SERS spectra obtained from the mixture of aerosolized bacterial sample solution of endospores (24 h of bacterial growth) at different bacteria concentration.

Vibration mode	24 h	24 h
	aerosolized OD 1	aerosolized OD 0.5
	Raman shift / cm^{-1}	
S-S stretching of cysteine	514	
C-C skeletal of carbohydrates	567	570
	1049	
C-S stretching of cysteine	637	
N-H deformation of amide II	656	
glycosidic ring of NAG and NAM	729	730
C=C deformation of tyrosine		808
		918
	957	
C-N and C-C stretching	1097	
C-H in plane bending	1017	
=C-C= of lipids or C-N aromatic in proteins	1136	1180
amide III	1224	
	1244	
C-NH ₂ stretching of amide II	1334	1302
COO ⁻ stretching	1379	1374
C-H deformation of lipids	1461	
	1539	
C=C ring stretching of lipids	1591	1594
amide I	1700	1626

6.3.1.1.2 Using a solid substrate

The solid substrates are commonly used as metal rough surfaces to obtain the enhanced effect for the detection and identification by SERS of several samples including biological components [37,67,51,68]. The successful SERS results from previous literature focused on detection and identification of biological components using solid substrates have captured our attention. The SERS results using Ag-NP as colloidal suspension solution were used to be compared with the results using *Bt* endospores aerosolized sample in solid substrate. The

substrate was obtained from UPRM colleagues, Raymond Vélez and Jenifier Olavarría, which worked under the supervision of Dr. M. De Jesús. They are currently using this solid substrate for agriculture, biomedical and environmental applications.

6.3.1.1.2.1 Preparation of the Ag/PDMS polymer solid substrate

Polydimethyl siloxane (PDMS) is used as the polymer substrate due to the simple preparation process, facile adaptation to glass surfaces, and excellent dielectric properties required for achieving a good resonance plasmon upon irradiating the metalized surface. PDMS slabs were fabricated by thoroughly mixing Sylgard® 184 curing agent and Sylgard® 184 elastomer base (both from Ellsworth Adhesive Company) in a 1:10 ratio. The reaction mixture was degassed for 15 minutes, poured onto a previously cleaned glass slide, and dried at 85°C for an hour. Afterwards, the polymer substrate was placed in a vacuum chamber where it was allowed to reach full mechanical strength (about 24 h) prior to depositing the desired metal. Then, the thin film (approximately 20 nm) of Ag (Sigma-Aldrich, 99.9999%) was deposited on the polymer substrate using a physical vapor deposition (PVD) apparatus (Edwards A306 Automatic Evaporator) under pressure ($\sim 10^{-6}$ tor). The deposition rate was set to 1.0 (+1) kÅ/s, and the thickness of the deposition was monitored using an integrated quartz sensor (similar to those used on analytical balances). The metalized polymer nanocomposite (MPN) was stored under vacuum until the moment of use. SERS activity of the fabricated MPN was confirmed with reference standard solutions ($\sim 10^{-4}$ M) of rhodamine 6G (R6G, Sigma-Aldrich) and p-aminobenzoic acid (PABA, Sgima-Aldrich).

6.3.1.1.2.2 SERS results of *Bt* endospores detection using a Ag/PDMS

solid substrate

The solid substrate was located behind the nebulizer following the same experimental method for aerosolized sample with NP suspension solution experiments as shows Figure 44. The bacterial sample aerosolized ($OD_{600} \sim 0.5$) to the solid substrate could be observed from the Raman microscopy, as shown in Figure 47a, this bioaerosol was spread 1" x 1" to the solid substrate (Figure 47b) and the SERS spectrum was collected. The solid substrate with 10s of bioaerosol exposure was analyzed at 0.77 mW using a 532 nm laser line and a 10x objective. The neat solid substrate and it with the bacterial solvent solution did not show any anomalous band that can mask the vibrational band of the bacterial sample in the SERS analysis. The vibrational bands obtained from the analyzed bacterial sample aerosolized at two different concentrations are presented in Figure 48. The bands assignment of the bacterial content observed are tentatively described in Table 14.

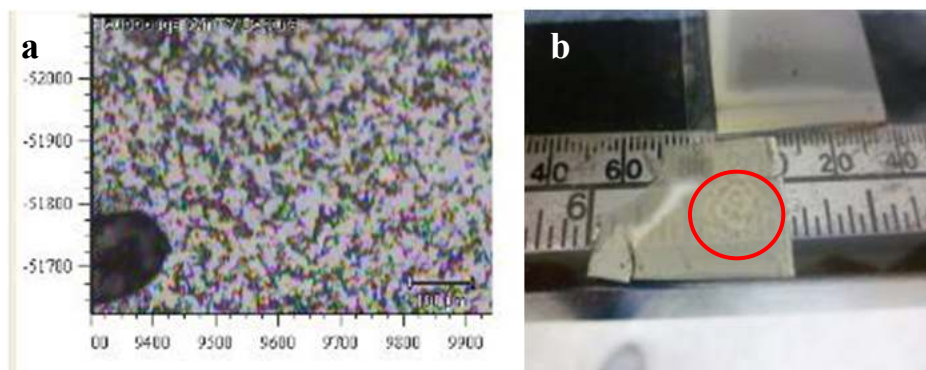


Figure 47. (a) View of the bacterial sample aerosolized to the solid substrate from Raman microscopy using a 10x objective. (b) The bacterial sample was spread 1" x 1" to the solid substrate using the same experimental parameters of NP suspension solution experiments to generate the aerosol.

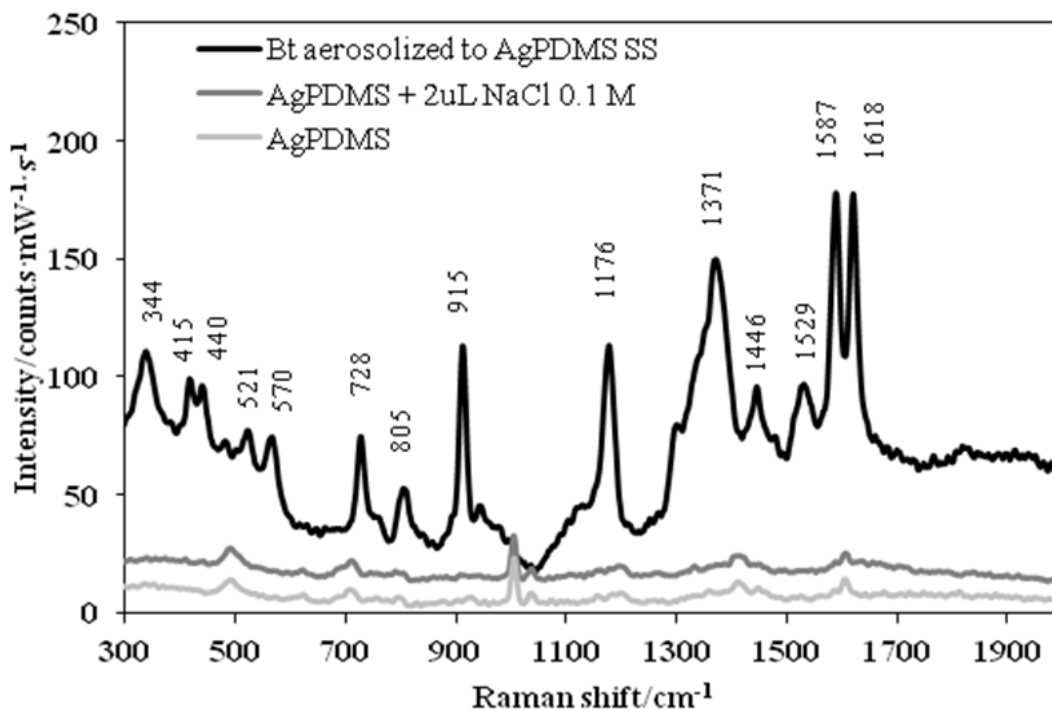


Figure 48. SERS spectra of endospores of *Bt* aerosolized for 10s to the Ag/PDMS solid substrate, it shows a good SERS detection and identification of the vibrational band assigned to bacterial content.

Table 14. Tentative Raman band assignments of the SERS spectra obtained from aerosolized bacterial sample solution of *Bt* endospores (24 h of bacterial growth) to the Ag/PDMS solid substrate.

Raman shift/cm ⁻¹	Tentative assigned bands of endospores of <i>Bt</i>
415, 440	carbohydrates
521	S-S stretching of cysteine in spore coat
570	C-C skeletal of carbohydrates
728	glycosidic ring of NAG and NAM
805	tyrosine “exposed”
915	COC str
1176	aromatic amino acids in proteins
1371	C-H bend (protein)
1446	C-H deformation of lipids
1529	Guanine, Adenine ring str
1587	C=C ring stretching of lipids
1618	amide I

6.4 Conclusion

Our optimization protocol was able to discriminate between 5 h and 24 h of bacterial growth which samples contains mainly vegetative cells and endospores, respectively by PCA and PLS-DA. Also, it was able to distinguish bacterial growth by stages (h) showing an increasing behavior of certain important peaks and a PLS analysis allowed a predictive model to estimate the bacterial growth time based on spectroscopic information. This clearly demonstrates that the bacterial content changes while *Bt* cells grow. Applications focused on the bacterial samples detection by generating an aerosol were the biggest challenge in this research. The results showed that the optimization was successfully used to observe and assign the characteristic peaks of aerosolized *Bt* endospores. In those experiments, metal rough surfaces in colloidal suspension and as solid substrate were used to enhance the Raman effect for SERS experiments. Both of them allowed a good interaction to the bacterial sample, the results obtained shows vibrational signal enhancement with identifiable bacterial components. The colloidal suspension NP solution allows activation of the Raman active sites (“hot spots”) and modifications to the surface charge to obtain effective interaction bacteria: NP although a volume ratio bacteria: NP has to be controlled to obtained good SERS results. The colloidal NP can be distributed close to the bacterial cell wall around all the bacterial structure allowing high kinetic rates, but low detection sensitivity due to a high degree of dispersion within the sensing volume. This effect allows a vibrational enhancement and good SERS results due to the interaction promoted. However, less bacterial cells can be used for SERS experiments using solid surface substrates but the interaction bacteria: NP is limited to one side of the bacteria close to the NP in the surface. It is according with the effects explained by Kahraman *et al* [69] about the method based on the “convective assembly” to cover the bacterial wall with silver colloidal nanoparticles. The

optimization parameters such as agglomeration of NP, activation of the Raman active sites and modifications to the surface charge of the NP to enhance the affinity of the biomolecular content to the NP cannot be controlled, after the NP preparation or in the same time of mixture with bacterial sample, to improve the signal to noise of the SERS spectra.

7. RESEARCH CONTRIBUTIONS

In this research, a simple protocol was developed to detect bacterial components of vegetative cells and endospores of *Bacillus thuringiensis* in suspension solutions and as bioaerosol particles by SERS. The optimization procedures dealing with volume ratio bacteria: NP, activation of the Raman active sites, agglomeration of NP, and modifications to the surface charge of NP allows a great SERS signals for identification of the bacterial samples immediately.

In this study, the bacterial range detection of 10^3 to 10^4 was important because this range is considered pathogenic concentrations. As demonstrated in this research work, SERS can be used as a quick method for liquid bacterial detection in suspension and for bioaerosol particles with great interest on standoff detection. The bacterial range detection of 10^4 is important because this range is considered a pathogenic concentration. Inglesby and colleagues have published a series of academic articles related to anthrax [65]. Accordingly, a study indicating the toxicity of anthrax conveys the following information: "... the Center for Disease Control (CDC) estimates that inhalation of 10,000 anthracis endospores or 100 nanograms will be lethal to 50% of an exposed population (LD50)" [70].

These results can be used to build biosensors constructed as an alternative method for early warning in cases of biological threats or environmental monitoring in cases of higher presence of bacteria in air or water.

REFERENCES

1. Madigan MT, Brock TD (2009) Brock biology of microorganisms. Pearson/Benjamin Cummings, San Francisco, CA
2. Manahan SE (1993) Fundamentals of environmental chemistry / Stanley E. Manahan. Lewis Publishers, Boca Raton, [Fla.]
3. Yan F, Vo-Dinh T (2007) Surface-enhanced Raman scattering detection of chemical and biological agents using a portable Raman integrated tunable sensor. *Sensors and Actuators B-Chemical* 121 (1):61-66. doi:10.1016/j.snb.2006.09.032
4. Kiefer W (2007) Recent Advances in linear and nonlinear Raman spectroscopy I. *Journal of Raman Spectroscopy* 38 (12):1538-1553. doi:10.1002/jrs.1902
5. Kiefer W (2008) Recent advances in linear and nonlinear Raman spectroscopy II. *Journal of Raman Spectroscopy* 39 (12):1710-1725. doi:10.1002/jrs.2171
6. Pacheco-Londono LC, Ortiz-Rivera W, Primera-Pedrozo OM, Hernandez-Rivera SP (2009) Vibrational spectroscopy standoff detection of explosives. *Analytical and Bioanalytical Chemistry* 395 (2):323-335. doi:10.1007/s00216-009-2954-y
7. Wallin S, Pettersson A, Ostmark H, Hobro A (2009) Laser-based standoff detection of explosives: a critical review. *Analytical and Bioanalytical Chemistry* 395 (2):259-274. doi:10.1007/s00216-009-2844-3
8. Simard JR, Roy G, Mathieu P, Laroche V, McFee J, Ho J (2004) Standoff sensing of bioaerosols using intensified range-gated spectral analysis of laser-induced fluorescence. *IEEE Transactions on Geoscience and Remote Sensing* 42 (4):865-874. doi:10.1109/tgrs.2003.823285
9. Félix-Rivera H, Hernández-Rivera S (2012) Raman Spectroscopy Techniques for the Detection of Biological Samples in Suspensions and as Aerosol Particles: A Review. *Sensing and Imaging: An International Journal* 13 (1):1-25. doi:10.1007/s11220-011-0067-0
10. Smith E, Dent G (2005) *Modern Raman Spectroscopy - A Practical Approach*. J. Wiley & Sons, Ltd., Hoboken, NJ
11. Premasiri WR, Moir DT, Klempner MS, Krieger N, Jones G, Ziegler LD (2005) Characterization of the Surface Enhanced Raman Scattering (SERS) of bacteria. *Journal of Physical Chemistry B* 109 (1):312-320. doi:10.1021/jp040442n
12. Lee PC, Meisel D (1982) Adsorption and surface-enhanced Raman of dyes on silver and gold sols. *The Journal of Physical Chemistry* 86 (17):3391-3395. doi:10.1021/j100214a025
13. Tortora GJ, Funke BR, Case CL (2010) *Microbiology: an introduction*. Pearson Benjamin Cummings, San Francisco, CA
14. Vilas-Boas GT, Peruca APS, Arantes OMN (2007) Biology and taxonomy of *Bacillus cereus*, *Bacillus anthracis*, and *Bacillus thuringiensis*. *Canadian Journal of Microbiology*, vol 53. Canadian Science Publishing,
15. Choudhury B, Leoff C, Saile E, Wilkins P, Quinn CP, Kannenberg EL, Carlson RW (2006) The Structure of the Major Cell Wall Polysaccharide of *Bacillus anthracis* Is Species-specific. *Journal of Biological Chemistry* 281 (38):27932-27941. doi:10.1074/jbc.M605768200

16. Kahraman M, Yazici MM, Sahin F, Bayrak OF, Culha M (2007) Reproducible surface-enhanced Raman scattering spectra of bacteria on aggregated silver nanoparticles. *Applied Spectroscopy* 61 (5):479-485
17. Wang YL, Lee K, Irudayaraj J (2010) Silver Nanosphere SERS Probes for Sensitive Identification of Pathogens. *Journal of Physical Chemistry C* 114 (39):16122-16128. doi:10.1021/jp1015406
18. Sengupta A, Laucks ML, Davis EJ (2005) Surface-enhanced Raman spectroscopy of bacteria and pollen. *Applied Spectroscopy* 59 (8):1016-1023
19. Esposito AP, Talley CE, Huser T, Hollars CW, Schaldach CM, Lane SM (2003) Analysis of single bacterial spores by micro-Raman spectroscopy. *Applied Spectroscopy* 57 (7):868-871
20. Tripathi A, Jabbour RE, Guicheteau JA, Christesen SD, Emge DK, Fountain AW, Bottiger JR, Emmons ED, Snyder AP (2009) Bioaerosol Analysis with Raman Chemical Imaging Microspectroscopy. *Analytical Chemistry* 81 (16):6981-6990. doi:10.1021/ac901074c
21. Rösch P, Harz M, Peschke K-D, Ronneberger O, Burkhardt H, Schüle A, Schmauz G, Lankers M, Hofer S, Thiele H, Motzkus H-W, Popp J (2006) On-Line Monitoring and Identification of Bioaerosols. *Analytical Chemistry*, vol 78.
22. Carmona P (1980) Vibrational-spectra and structure of crystalline dipicolinic acid and calcium dipicolinate trihydrate. *Spectrochimica Acta Part a-Molecular and Biomolecular Spectroscopy* 36 (7):705-712
23. Kolomenskii AA, Jerebtsov SN, Opatrny T, Schuessler HA, Scully MO (2003) Spontaneous Raman spectra of dipicolinic acid in microcrystalline form. *Journal of Modern Optics* 50 (15-17):2369-2374. doi:10.1080/0950034032000120803
24. Chan J, Fore S, Wachsmann-Hogiu S, Huser T (2008) Raman spectroscopy and microscopy of individual cells and cellular components. *Laser & Photonics Reviews* 2 (5):325-349. doi:10.1002/lpor.200810012
25. Kazanci M, Schulte JP, Douglas C, Fratzl P, Pink D, Smith-Palmer T (2009) Tuning the Surface-Enhanced Raman Scattering Effect to Different Molecular Groups by Switching the Silver Colloid Solution pH. *Applied Spectroscopy* 63 (2):214-223
26. Guicheteau J, Christesen S, Emge D, Tripathi A (2010) Bacterial mixture identification using Raman and surface-enhanced Raman chemical imaging. *Journal of Raman Spectroscopy* 41 (12):1342-1347. doi:10.1002/jrs.2601
27. Efrima S, Zeiri L (2009) Understanding SERS of bacteria. *Journal of Raman Spectroscopy* 40 (3):277-288. doi:10.1002/jrs.2121
28. Jarvis RM, Law N, Shadi LT, O'Brien P, Lloyd JR, Goodacre R (2008) Surface-enhanced Raman scattering from intracellular and extracellular bacterial locations. *Analytical Chemistry* 80 (17):6741-6746. doi:10.1021/ac800838v
29. Chalmers JL, Griffiths PR (eds) (2002) *Handbook of Vibrational Spectroscopy*, vol I. Theory and Instrumentation. John Wiley & Sons Ltd, Chichester
30. Sengupta A, Laucks ML, Dildine N, Drapala E, Davis EJ (2005) Bioaerosol characterization by surface-enhanced Raman spectroscopy (SERS). *Journal of Aerosol Science* 36 (5-6):651-664. doi:10.1016/j.jaerosci.2004.11.001

31. Ayora MJ, Ballesteros L, Perez R, Ruperez A, Laserna JJ (1997) Detection of atmospheric contaminants in aerosols by surface-enhanced Raman spectrometry. *Analytica Chimica Acta* 355 (1):15-21
32. Griffiths WD, Decosemo GAL (1994) THE ASSESSMENT OF BIOAEROSOLS - A CRITICAL-REVIEW. *Journal of Aerosol Science* 25 (8):1425-1458
33. Sengupta A, Mujacic M, Davis EJ (2006) Detection of bacteria by surface-enhanced Raman spectroscopy. *Analytical and Bioanalytical Chemistry* 386 (5):1379-1386. doi:10.1007/s00216-006-0711-z
34. Daniels JK, Caldwell TP, Christensen KA, Chumanov G (2006) Monitoring the kinetics of *Bacillus subtilis* endospore germination via surface-enhanced Raman scattering spectroscopy. *Analytical Chemistry* 78 (5):1724-1729. doi:10.1021/ac052009v
35. Sengupta A, Brar N, Davis EJ (2007) Bioaerosol detection and characterization by surface-enhanced Raman spectroscopy. *Journal of Colloid and Interface Science* 309 (1):36-43. doi:10.1016/j.jcis.2007.02.015
36. Schweiger G (1990) Raman-Scattering on Single Aerosol-Particles and on Flowing Aerosols - A Review. *Journal of Aerosol Science* 21 (4):483-509
37. Yan F, Wabuyele MB, Griffin GD, Vass AA, Vo-Dinh T (2005) Surface-enhanced Raman scattering, detection of chemical and biological agent simulants. *Ieee Sensors Journal* 5 (4):665-670. doi:10.1109/jsen.2005.850993
38. Knauer M, Ivleva NP, Niessner R, Haisch C (2010) Optimized Surface-enhanced Raman Scattering (SERS) Colloids for the Characterization of Microorganisms. *Analytical Sciences* 26 (7):761-766
39. Alvarez-Puebla RnA, Arceo E, Goulet PJG, Garrido JnJ, Aroca RF (2005) Role of Nanoparticle Surface Charge in Surface-Enhanced Raman Scattering. *The Journal of Physical Chemistry B* 109 (9):3787-3792. doi:10.1021/jp045015o
40. Guicheteau J, Argue L, Emge D, Hyre A, Jacobson M, Christesen S (2008) *Bacillus* spore classification via surface-enhanced Raman spectroscopy and principal component analysis. *Applied Spectroscopy* 62 (3):267-272
41. Vehring R, Aardahl CL, Schweiger G, Davis EJ (1998) The characterization of fine particles originating from an uncharged aerosol: Size dependence and detection limits for Raman analysis. *Journal of Aerosol Science* 29 (9):1045-1061
42. Kahraman M, Yazici MM, Sahin F, Culha M (2007) Experimental parameters influencing surface-enhanced Raman scattering of bacteria. *Journal of Biomedical Optics* 12 (5):054015. doi:10.1117/1.2798640
43. Harz A, Rosch P, Popp J (2009) Vibrational Spectroscopy-A Powerful Tool for the Rapid Identification of Microbial Cells at the Single-Cell Level. *Cytometry Part A* 75A (2):104-113. doi:10.1002/cyto.a.20682
44. Xie C, Mace J, Dinno MA, Li YQ, Tang W, Newton RJ, Gemperline PJ (2005) Identification of single bacterial cells in aqueous solution using confocal laser tweezers Raman spectroscopy. *Analytical Chemistry* 77 (14):4390-4397. doi:10.1021/ac0504971
45. Schmid U, Rosch P, Krause M, Harz M, Popp J, Baumann K (2009) Gaussian mixture discriminant analysis for the single-cell differentiation of bacteria using micro-Raman

- spectroscopy. *Chemometrics and Intelligent Laboratory Systems* 96 (2):159-171. doi:10.1016/j.chemolab.2009.01.008
46. Jarvis RM, Brooker A, Goodacre R (2004) Surface-enhanced Raman spectroscopy for bacterial discrimination utilizing a scanning electron microscope with a Raman spectroscopy interface. *Analytical Chemistry* 76 (17):5198-5202. doi:10.1021/ac049663f
47. Luna-Pineda T, Soto-Feliciano K, De La Cruz-Montoya E, Londono LCP, Rios-Velazquez C, Hernandez-Rivera SP (2007) Spectroscopic characterization of biological agents using FTIR, Normal Raman and surface enhanced Raman scattering. Paper presented at the Proceedings of SPIE - The International Society for Optical Engineering,
48. Guicheteau J, Christesen S, Emge D, Tripathi A (2010) Bacterial mixture identification using Raman and surface-enhanced Raman chemical imaging. *Journal of Raman Spectroscopy* 41 (12):1632-1637. doi:10.1002/jrs.2601
49. Guicheteau J (2006) Principal component analysis of bacteria using surface-enhanced Raman spectroscopy. *Proceedings of SPIE--the international society for optical engineering* 6218 (1):62180-62181
50. Bechtel DB, Bulla LA (1976) Electron microscope study of sporulation and parasporal crystal formation in *Bacillus thuringiensis*. *Journal of Bacteriology* 127:1472-1481
51. Cheng HW, Luo WQ, Wen GL, Huan SY, Shen GL, Yu RQ (2010) Surface-enhanced Raman scattering based detection of bacterial biomarker and potential surface reaction species. *Analyst* 135 (11):2993-3001. doi:10.1039/c0an00421a
52. Bandyopadhyay P, Mukhopadhyay S (2002) Kinetics of oxidation of hydroxylamine by [ethylenebis(biguanide)]silver(III) in aqueous media. *Polyhedron* 21 (19):1893-1898
53. Leopold N, Lendl B (2003) A new method for fast preparation of highly surface-enhanced Raman scattering (SERS) active silver colloids at room temperature by reduction of silver nitrate with hydroxylamine hydrochloride. *Journal of Physical Chemistry B* 107 (24):5723-5727. doi:10.1021/jp027460u
54. Keir R, Sadler D, Smith WE (2002) Preparation of Stable, Reproducible Silver Colloids for use as Surface-Enhanced Resonance Raman Scattering Substrates. *Applied Spectroscopy* 56:551-559
55. Primera-Pedrozo OM, Jerez-Rozo JI, De la Cruz-Montoya E, Luna-Pineda T, Pacheco-Londono LC, Hernandez-Rivera SP (2008) Nanotechnology-based detection of explosives and biological agents simulants. *Ieee Sensors Journal* 8 (5-6):963-973. doi:10.1109/jsen.2008.923936
56. Yaffe NR, Blanch EW (2008) Effects and anomalies that can occur in SERS spectra of biological molecules when using a wide range of aggregating agents for hydroxylamine-reduced and citrate-reduced silver colloids. *Vibrational Spectroscopy* 48 (2):196-201
57. Kahraman M, Kesero, lu K, ulha M (2011) On Sample Preparation for Surface-Enhanced Raman Scattering (SERS) of Bacteria and the Source of Spectral Features of the Spectra. *Applied Spectroscopy* 65:500-506
58. Félix-Rivera H, González R, Rodríguez G, Primera-Pedrozo OM, Ríos-Velázquez C, Hernández-Rivera SP (2011) Improving SERS Detection of *Bacillus thuringiensis* using Silver Nanoparticles Reduced with Hydroxylamine and with Citrate Capped Borohydride. *International Journal of Spectroscopy* 2011. doi:10.1155/2011/989504

59. Primera-Pedrozo OM, Rodriguez GDM, Castellanos J, Felix-Rivera H, Resto O, Hernandez-Rivera SP (2012) Increasing surface enhanced Raman spectroscopy effect of RNA and DNA components by changing the pH of silver colloidal suspensions. *Spectrochimica Acta Part A: Molecular and Biomolecular Spectroscopy* 87 (0):77-85
60. Cucchi A, Sanchez de Rivas C (1998) SASP (Small, Acid-Soluble Spore Proteins) and Spore Properties in *Bacillus thuringiensis israelensis* and *Bacillus sphaericus*. *Current Microbiology* 36 (4):220-225. doi:10.1007/s002849900298
61. Guicheteau J, Argue L, Hyre A, Jacobson M, Christesen SD (2006) Raman and surface-enhanced Raman spectroscopy of amino acids and nucleotide bases for target bacterial vibrational mode identification.
62. Papadopoulou E, Bell SEJ (2011) Label-Free Detection of Single-Base Mismatches in DNA by Surface-Enhanced Raman Spectroscopy. *Angewandte Chemie International Edition* 50 (39):9058-9061. doi:10.1002/anie.201102776
63. Cheng H-W, Huan S-Y, Wu H-L, Shen G-L, Yu R-Q (2009) Surface-Enhanced Raman Spectroscopic Detection of a Bacteria Biomarker Using Gold Nanoparticle Immobilized Substrates. *Analytical Chemistry* 81 (24):9902-9912. doi:10.1021/ac9014275
64. Stöckel S, Meisel S, Böhme R, Elschner M, Rösch P, Popp J (2009) Effect of supplementary manganese on the sporulation of *Bacillus endospores* analysed by Raman spectroscopy. *Journal of Raman Spectroscopy* 40 (11):1469-1477. doi:10.1002/jrs.2292
65. Farquharson S, Gift AD, Maksymiuk P, Inscore FE (2004) Rapid Dipicolinic Acid Extraction from *Bacillus* Spores Detected by Surface-Enhanced Raman Spectroscopy. *Appl. Spectrosc.* 58 (3):351-354
66. De Gelder J, Scheldeman P, Leus K, Heyndrickx M, Vandenabeele P, Moens L, De Vos P (2007) Raman spectroscopic study of bacterial endospores. *Analytical and Bioanalytical Chemistry* 389 (7-8):2143-2151. doi:10.1007/s00216-007-1616-1
67. Zhang XY, Young MA, Lyandres O, Van Duyne RP (2005) Rapid detection of an anthrax biomarker by surface-enhanced Raman spectroscopy. *Journal of the American Chemical Society* 127 (12):4484-4489. doi:10.1021/ja0436623b0b
68. Dhawan A, Du Y, Yan F, Gerhold MD, Misra V, Vo-Dinh T (2010) Methodologies for Developing Surface-Enhanced Raman Scattering (SERS) Substrates for Detection of Chemical and Biological Molecules. *Ieee Sensors Journal* 10 (3):608-616. doi:10.1109/jsen.2009.2038634
69. Kahraman M, Zamaleeva AI, Fakhrullin RF, Culha M (2009) Layer-by-layer coating of bacteria with noble metal nanoparticles for surface-enhanced Raman scattering. *Analytical and Bioanalytical Chemistry* 395 (8):2559-2567. doi:10.1007/s00216-009-3159-0
70. Inglesby TV (2002) Anthrax as a biological weapon, 2002: Updated recommendations for management (vol 287, pg 2236, 2002). *JAMA (Chicago, Ill.)* 288 (15):1849-1849